THESIS

TRANSCRIPTOME AND ELEMENTAL ANALYSIS OF THE SELENIUM HYPERACCUMULATOR *STANLEYA PINNATA* AND NON-ACCUMULATOR *STANLEYA ELATA*

Submitted by

Jiameng Wang

Department of Biology

In partial fulfillment of the requirements

For the Degree of Master of Science

Colorado State University

Fort Collins, Colorado

Spring 2015

Master's Committee:

Advisor: Elizabeth Pilon-Smits

Daniel Sloan
Laurie Stargell

ABSTRACT

TRANSCRIPTOME AND ELEMENTAL ANALYSIS OF THE SELENIUM HYPERACCUMULATOR *STANLEYA PINNATA* AND NON-ACCUMULATOR *STANLEYA ELATA*

The element selenium (Se) naturally occurs in soil and water in various forms. Selenium is an essential micronutrient for mammals and many other organisms, who incorporate Se into specific selenoproteins. Selenium is not known to be a nutrient for higher plants. It can even be damaging as an oxidant, or if it is non-specifically substituted for sulfur (S) in proteins due to the chemical similarity of Se to S. It is therefore curious that certain plant species are able to accumulate high concentrations of Se without detrimental effects. These plants are known as Se hyperaccumulators. Previous studies have implicated that Se hyperaccumulators may take up more Se by upregulating the gene expression of sulfate transporters; they may also possess transporters with increased specificity for selenate relative to sulfate. Hyperaccumulator species are Se hypertolerant as well; several studies have found evidence that their sulfate assimilation pathway is upregulated, converting inorganic selenate to organic forms, which can be further methylated and thus excluded from nonspecific incorporation into proteins. These methylated end products are often sequestered in epidermal tissues as a further possible tolerance mechanism, and perhaps also to deter herbivory. As an additional tolerance mechanism, hyperaccumulator plants may have an enhanced abilities to scavenge the free radicals generated by Se and to recycle misfolded Se-containing proteins. Selenium hyperaccumulators are not only

intrinsically interesting to study for their Se accumulation and tolerance mechanisms, but also because they may harbor applicable Se accumulation and tolerance genes that may be cloned into more economically viable species for a variety of applicable uses, ranging from remediating sites polluted with Se to fortifying crops in areas where soils are low in Se.

The goal of this study was to gain better insight into which genes are responsible for the transport and metabolism of Se in hyperaccumulators, and which genes are involved in the signaling cascade leading to Se hyperaccumulation and hypertolerance in the hyperaccumulator *Stanleya pinnata*. To answer these questions, the transcriptomes of *S. pinnata* and a non-accumulating relative, *Stanleya elata*, both grown with or without selenate, were analyzed for root and shoot gene expression differences.

The introduction chapter of this thesis presents a review of Se hyperaccumulation, beginning with a summary of the history and properties of Se, followed by a closer look at the uptake and metabolism of Se through sulfate transporters and assimilation pathways. The known mechanisms for tolerance and accumulation in hyperaccumulators are reviewed, as well as some proposed mechanisms requiring more definitive experimental evidence.

The second chapter presents the methods and findings of a transcriptome-wide comparison between *S. pinnata* and *S. elata*. Plants were grown in triplicate on 0 or 20 μM selenate, and harvested for elemental analysis and Illumina RNA-seq. The two species did not differ in biomass production, regardless of Se treatment, but the Se levels in both species were significantly different (*S. pinnata* accumulated more Se than *S. elata*), and also significantly increased with Se supply. A total of 205,543 reads were assembled, yielding 19,572 annotated genes that showed detectable expression levels in both Stanleya species. Statistical comparison of the transcriptome libraries showed that gene expression was affected by Se relatively more in

the root of *S. elata* and in the shoot of *S. pinnata*. Genes involved in sulfate transport (particularly sulfate transporter (*Sultr)1;2, Sultr2;1, Sultr3;1, Sultr3;4*) and assimilation (particularly ATP sulfurylase (*Atps)2,* APS reductase (*Apr)3*), and in oxidative stress resistance (glutathione-related genes, peroxidases) were among the most differentially expressed between *S. pinnata* and *S. elata*, with many showing constitutively elevated expression in *S. pinnata*. Since earlier studies found that the application of defense hormones to plants affected their ability to accumulate or tolerate Se, defense hormone- and other defense-related genes were also investigated in this study. It was found that genes involved in defense hormone biosynthesis and signaling (*Lox, Acx, Pal, Ics, Ein, Jar, Tga*) were more expressed in *S. pinnata*, as were hormone-induced defense genes, including *Pr* and *Pdf*. Several upstream signaling genes reported to upregulate defense hormone genes were also more expressed in *S. pinnata* than *S. elata*, and might initiate these Se responses. In conclusion, Se hyperaccumulation in *S. pinnata* appears to be mediated by constitutively upregulated hormone-regulated defense systems, which may mediate elevated sulfate/selenate uptake and assimilation, as well as elevated antioxidant capacity. This concerted action likely contributes to Se hyperaccumulation and hypertolerance.

Lastly, some preliminary findings are presented on the effects of varying Se and S concentrations on Se and S uptake in *S. elata*, and compared with previous data from *S. pinnata* grown in similar conditions. To determine if either species showed selective uptake, the concentrations and enrichment ratios of Se over S were determined for *S. elata* and *S. pinnata*. *S. pinnata* was notably more enriched in Se compared to S, relative to its growth substrate and relative to *S. elata*, especially under conditions of increased S supply. The selenate uptake system in S. pinnata was much less inhibited by sulfate. These results indicate that the Se hyperaccumulator *S. pinnata* has a transporter with increased specificity for selenate relative to

sulfate. The identity and properties of this transporter will be an interesting topic for further study.

ACKNOWLEDGEMENTS

Thanks to my advisor, Lianne, whose guidance made all of this possible, and who taught me to take things one step at a time. Many thanks to Wen Zhou for tirelessly providing data and recalculations, Jennifer for guidance, and Jonathan Harris and Eric Patterson for their willingness to help on software troubleshooting. Also, I would like to thank Patrick Edger for assembling the transcriptome. I would like to thank my committee members Daniel Sloan and Laurie Stargell for their meaningful discussions. Finally, I would like to acknowledge and thank the Stavros Family Fund of Colorado State University, and the Colorado Mountain Club Foundation Fellowship for funding our research.

DEDICATION

I dedicate this to Anarin; and to Bubbles, my orange cat

TABLE OF CONTENTS

CHAPTER 1:

INTRODUCTION TO SELENIUM, SELENIUM METABOLISM, AND SELENIUM HYPERACCUMULATION IN PLANTS

Selenium (Se) is the 34th element of the periodic table. It was discovered in 1817 by Jöns Jacob Berzelius, who originally mistook it for tellurium (Te) and later named it selenium, after the Greek goddess of the moon. Like Te, it is similar to sulfur (S). Selenium has the property of converting light energy to electron flow energy, which makes it useful in photocopiers and photovoltaic cells (Wilber, 1980; McFarlane & McFarlane, 1987). Selenium is mainly present in soils in the most oxidized form of selenate, SeO_4^{2-}. In aquatic environments, Se mainly occurs in the more reduced form of selenite, SeO_3^{2-} (Gattow and Heinrich 1964; Geering et al., 1968). The elemental form, Se^0 also exists, as well as many organic forms (Wilber 1980). Selenium is an important trace element required for many animals, bacteria and archaea, and certain algae. Due to the chemical similarities of Se to S, Se can be assimilated non-specifically through the S pathway to selenocysteine (SeCys) and selenomethionine (SeMet) (Kohrle et al., 2000; Sors et al., 2005). In mammals, SeCys is specifically incorporated into the active site of selenoproteins, which have various redox functions including reactive oxygen species (ROS) detoxification and thyroid hormone signaling (Xu et al., 2007; Shchedrina et al., 2010). In addition, many prokaryotes have selenoproteins (Zhang et al., 2005). In some algae, such as *Chlamydomonas reinhardtii*, selenoproteins have been found to function in ROS detoxification (Novoselov et al., 2002). However, to date no selenoproteins have been found in higher plants or fungi, and it has been proposed that these clades may have lost essential Se metabolism (Lobanov et al., 2009). Nevertheless, non-specific incorporation of Se into S-containing amino acids (SeCys, SeMet)

does occur in plants. The non-specific incorporation of SeCys into proteins may be detrimental: the larger atomic radii of Se in amino acids disrupts disulfide bridges and may cause protein misfolding with subsequent loss of activity (Hondal et al., 2012).

Se toxicity and deficiency as a nutrient

The window between Se toxicity and deficiency is very narrow, and both are problems worldwide. In the western United States and parts of northern and southern China, high concentrations of Se found in carbonaceous shale have weathered into soil used for agriculture or rangelands. In the livestock industry, toxicity is a "hidden" economic factor, causing an estimated 5% in mortality and another 9% in indirect losses due to nutritional imbalances (Mortimer et al., 1978). Se pollution can also magnify through the food chain; for example, contaminated runoff from coal mines are known to cause deformities in char fry (*Salvelinus malma*) (McDonald et al., 2010). Although essential at low levels (recommended daily intake 55-75 µg for humans), an intake in excess of 4-6 mg Se per day leads to selenosis. The symptoms range from hair loss to gastrointestinal disorders, to granulomatous lung disease (Diskin et al 1979; Yang and Xia 1995). Selenium deficiency can affect individuals with poor nutrient absorption or diets inadequate in Se, which may lead to Kashin-beck disease. Insufficient intake of less than 20 µg Se per day may lead to Keshan cardiomyopathy, and the risk is much higher in patients infected with the Coxsackie virus (Yang and Xia 1995). In HIV+ patients, Se deficiency is positively correlated with higher mortality rates (Baum et al., 1997). The health cost of dietary Se imbalances are staggering: around a billion people worldwide have been estimated to be Se deficient (Lyons et al., 2003).

Selenium accumulation in plants

Although plants do not require Se, certain plant species found on seleniferous soil have developed the ability to accumulate high levels of Se in their tissues without significant detrimental effects. Selenium hyperaccumulators are defined as species accumulating >1000 mg Se/kg^{-1} dry weight (DW), with some like *Astragalus bisulcatus* reported to have up to 15,000 mg Se/kg^{-1} DW. Secondary accumulators can accumulate >100 mg Se/kg^{-1} DW (Galeas et al., 2007; Cappa et al., 2014). The majority of plants are non-accumulators, and generally sensitive to Se concentrations >100 mg Se/kg^{-1} DW. Since Se and S are so similar, hyperaccumulators may be hypothesized to have greater Se uptake through sulfate transporters (SULTR) as well as a higher rate of S/Se assimilation, since hyperaccumulator species contain very high levels of organic Se forms (Freeman et al., 2006). Also, hyperaccumulators may possess transporters with enhanced specificity for Se over S, since hyperaccumulators tend to enrich themselves with selenate relative to sulfate, compared to the growth substrate, and their selenate uptake is less inhibited compared to non-hyperaccumulators when increasing amounts of sulfate are supplied (Harris et al., 2014).

Se and S uptake and transport

In the model species *Arabidopsis thaliana*, sulfate (and thus, selenate) is imported from the rhizosphere into the root symplast by the high-affinity sulfate-H^+ symporters SULTR1;2 and SULTR1;1 (El Kassis et al., 2007). Among these, SULTR1;2 is the major transporter. SULTR1;1 is expressed at much lower levels and only under conditions of S starvation; it may have lower specificity for selenate than sulfate (Takahashi et al., 2000). The SULTR transporters have 12 transmembrane-spanning domains with the N- and C- termini located in the cytoplasm. Helices 1 and 2 are conserved, and may function as the catalytic site, since mutations in the

region severely affected transport activity (Leves et al., 2008). The C-terminal STAS domain is also essential for SULTR1;2 function, and thought to interact with Se/S assimilation enzymes to regulate uptake rates (Rouached et al., 2005; Shibagaki & Grossman, 2006, 2010). Sulfate/selenate can be stored in the root vacuoles and made available for translocation by vacuolar exporters SULTR4;1 and SULTR4;2; both are also present in shoots (Takahashi et al., 2011). Sulfate/selenate is transported from the root cortex to xylem parenchyma cells by low-affinity transporter SULTR2;1, which responds to S deficiency and is considered a major transporter for translocation from roots to growing leaves (Zayed et al., 1998; Liang & Yu 2010). This transport to xylem parenchyma can also occur through low affinity transporter SULTR2;2, which is activated through possible heterodimerization with SULTR3;5 (Kataoka et al., 2004). SULTR2;1 and the high-affinity SULTR1;3 may be present in phloem parenchyma and serve to remobilize sulfate/selenate from source to sink tissues, such as to developing seeds (Takahashi et al, 2011). Uptake of sulfate/selenate into leaf cells may involve SULTR1;2, and is followed by transport into the chloroplasts by SULTR3;1 (Cao et al., 2013), where the majority of S assimilation is thought to occur.

As SULTR activity is dependent on S status, it is conceivable that Se hyperaccumulators may constantly sense S starvation and therefore continuously transport S and Se into their tissues. A study showed that both nonaccumulators and hyperaccumulators in the *Astragalus* genus had high levels of *Sultr1*, *Sultr2*, and *Sultr4* gene expression, regardless of S deprivation or Se supply, and overall expression levels that were similar to those of non-accumulator *Astragalus* and other species under S deprivation (Cabannes et al., 2011). Selenium hyperaccumulators may have transporters with higher affinity for selenate over sulfate, in view of their high Se/S tissue ratio (White et al., 2004, 2007). In a study by Harris et al. (2014)

comparing hyperaccumulator *Stanleya pinnata* with non-hyperaccumulator *Brassica juncea*, Se accumulation decreased 10-fold in *B. juncea* with increasing sulfate supply, but only 2-3-fold in *S. pinnata*. Similarly, in a later study *S. pinnata* was enriched 5-fold with Se relative to S, compared to the growth medium, whereas *B. juncea* was only enriched up to 1.3-fold with Se over S (Schiavon et al., 2015). The mechanism by which Se hyperaccumulators discriminate between selenate and sulfate is not clear and should be an interesting topic to investigate.

Se and S assimilation and regulation

Once in the chloroplast, selenate/sulfate is activated into adenosine phosphosulfate/selenate (APS/APSe) by ATP sulfurylase (APS) in the first and rate-limiting step of Se/S assimilation (Fig 1.1) (Dilworth & Bandurski, 1977; Pilon-Smits et al., 1999). The APS/APSe may be reduced to sulfite/selenite by APS reductase (APR) in the chloroplast; this is also a rate-limiting step (Bick & Leustek, 1998). Alternatively, APS can be phosphorylated into phosphoadenosine phosphosulfate (PAPS) by adenosine phosphokinase (APK) in the cytosol, which is a starting point for producing sulfated metabolites like glucosinolates (Mugford et al., 2009). PAPS may also be converted to PAP, which is thought to be a signaling molecule that induces the expression of oxidative stress response genes (Bohrer et al., 2015, Hideki Takahashi, pers. comm.).

Sulfite/selenite can be reduced into selenide by sulfite reductase, and selenite may also be non-enzymatically reduced by glutathione (GSH) (Terry et al., 2000). Sulfide/selenide can then be coupled with O-acetylserine (OAS) through cysteine synthase to form (Se)Cys (Ng & Anderson 1978). Selenocysteine can be further utilized in various product pathways. For example, it may be incorporated into proteins, which is considered toxic. This toxicity may be avoided in Se hyperaccumulators by converting SeCys to Se-cystathionine by cystathionine

gamma synthase (CGS), or to methylselenocysteine (MeSeCys) through a methylation step mediated by SeCys methyltransferase (SMT) (Neuhierl & Bock, 1996; Van Huysen et al., 2003, Freeman et al., 2006; Cakir & Ari 2013). It is interesting to note that the hyperaccumulator *A. bisulcatus* had up to 17.5-times higher SMT activity than non-accumulator *A. drummondii* (Sors et al., 2009). Also, when *A. bisulcatus* SMT was cloned and overexpressed in *Arabidopsis* and *B. juncea*, this conferred both enhanced tolerance and accumulation of Se (LeDuc et al., 2004). Se(Cys) can also be used for glutathione (GSH) synthesis. GSH (Glu-Cys-Gly) is synthesized via a two-step process involving gamma-glutamylcysteine synthetase (ECS) and glutathione synthetase (GS) in the cytosol and chloroplast, and is an important reducing agent thought to alleviate oxidative stress (Pasternak et al., 2008).

In model species *A. thaliana*, sulfate assimilation is regulated by microRNA395, which is in turn regulated by transcription factor SULFUR LIMITATION 1 (SLIM1); both are strongly induced by S starvation (Kawashima et al., 2011). SLIM1 directly upregulates the levels of group 1 sulfate transporters (*Sultr1;1, Sultr1;2*) in roots. MicroRNA395 targets SULTR2;1 and three of the four ATP sulfurylase genes (*Aps1*, *Aps3*, *Aps4*). Under conditions of S deficiency, these regulatory factors are thought to result in increased transport of S into the plant and partitioning to growing leaves (Liang & Yu, 2010; Kawashima et al., 2011).

Se tolerance in hyperaccumulators and the role of antioxidants

Because selenate, and especially selenite, is toxic and inhibit plant growth (Hopper & Parker, 1999), hyperaccumulators may have greater rates of conversion from inorganic Se (which causes protein and lipid oxidation) to organic forms (Sors et al., 2009; Yatusevich 2010). In comparisons of the hyperaccumulator *S. pinnata* with related non-hyperaccumulators, higher expression levels of genes catalyzing the first two steps of S/Se assimilation were detected

through quantitative RT-PCR (*Aps1*, *Aps2*, and *Aps4*) and macroarray analysis (*Apr1*, *Apr2*, *Apr3*; *Aps1*, *Aps2*) (Freeman et al., 2010; Schiavon et al., 2015). This may explain why *S. pinnata* accumulates almost exclusively organic Se, whereas related non-hyperaccumulators accumulate relatively more inorganic Se (Freeman et al., 2006; Cappa et al., 2015).

While studies have found that low concentrations of selenate boosted the expression of antioxidant enzymes like glutathione peroxidase, with Se supplementation even being proposed as a growth promotant, concentrations $\geq$10 mg kg^{-1} Se caused chlorosis and inhibited growth in the non-accumulator *Lolium perenne* (Hartikainen et al., 2000). Hyperaccumulator *S. pinnata*, however, had much higher levels of leaf Se and yet accumulated less superoxide and hydrogen peroxide than non-hyperaccumulator *Stanleya albescens* (Freeman et al., 2010). This suggests that hyperaccumulators are able to avoid cellular damage, potentially by increasing the levels of antioxidants and associated enzymes, increasing conjugation of Se to metabolites for transport or storage, and increasing turnover of misfolded proteins due to Se incorporation (Neuhierl & Bock, 1996). When *S. pinnata* plants were treated with a proteasome inhibitor and challenged with 0, 40 then 80 μM selenate, a marked increase of ubiquitinated proteins was observed; in contrast, in *S. pinnata* not treated with the inhibitor, there was only a slight increase in ubiquitinated proteins. Furthermore, *S. pinnata* with inhibited proteasome function had a 60% increase of Se incorporated into protein, and almost one-fourth of these proteins were ubiquitinated. Together, these results indicate that *S. pinnata*, and possibly other hyperaccumulators, may selectively target selenoproteins for ubiquitin-mediated proteasome degradation (Sabbagh & Van Hoewyk, 2012).

Se tolerance, speciation, and localization in hyperaccumulators

Se hyperaccumulators may also have the ability to avoid the deleterious effects of protein incorporation by sequestering Se in the non-proteinaceous forms methylselenocysteine or methylselenomethionine (MeSeMet), or by removing Se altogether through volatilization as dimethyl selenide (DMSe) and dimethyl didiselenide (DMDSe) (Brown and Shrift 1981; Meija et al., 2002). The main form (90%) of Se in *S. pinnata* leaves was found to be methylSeCys, and the highest concentrations of Se were found in the epidermis and leaf margins (Freeman et al., 2006; Cappa et al., 2014). As mentioned earlier, *A. bisulcatus* may depend on SMT to convert SeCys to MeSeCys (a C-Se-C compound). It was indeed found that *A. bisulcatus* contained 91% of Se in C-Se-C form(s) in leaves, and in the leaf Se was mainly (98%) found in trichomes (Freeman et al., 2006; Barillas et al., 2012). *S. pinnata* also accumulated predominantly C-Se-C (shown to be 88% MeSeCys), not only leaves but also in seeds and flowers, suggesting a remobilization of this Se compound from leaf tissues to the reproductive organs (Quinn et al., 2011; Cappa et al., 2014). In contrast, the non-accumulators *S. elata* and *Stanleya albescens* had higher proportions of inorganic than organic Se forms. In *S. elata*, almost no Se was detected in the leaf when treated with selenate (Cappa et al., 2015). Of the small amount of Se found in the comparable non-hyperaccumulator *S. albescens*, ~70% was detected in the C-Se-C form, and consisted entirely of selenocystathionine (Freeman et al., 2010). Interestingly, the legume Se hyperaccumulator *A. bisulcatus* had >30% of Se in the elemental form (Se^0) in root nodules, which may be influenced by the activity of symbiotic rhizobacteria capable of reducing selenite to Se^0, and may serve as an additional mechanism of Se tolerance (Oremland et al., 2004; Barillas et al., 2012). Finally, Se hyperaccumulators may have greater rates of Se volatilization in the roots, given that species like *A. bisulcatus* have greater SMT activity, and because the non-

enzymatic production of volatile forms is largely driven by the amount of MeSeCys and MeSeMet available. A study by Feist & Parker (2001) found that the apparent amount of Se volatilized, calculated from the difference of the Se amount added to solution and lost through plants, was higher for *S. pinnata* than *B. juncea* regardless of Se and S treatment (Feist & Parker, 2001). Moreover, the rates of Se volatilization measured directly from *S. pinnata* (Freeman and Banuelos, 2011) were much higher than those reported in earlier studies for *B. juncea* (De Souza et al., 1998).

Ecological and practical aspects of Se hyperaccumulation

Selenium accumulation in organs with high fitness value or palatability may function as a defense against herbivory. When given a choice, prairie dogs (*Cynomys ludovicianus*) avoided eating *B. juncea* or *S. pinnata* plants with concentrations of Se as low as 38 mg kg^{-1} DW (Quinn et al., 2007. Similarly, aphids (*Myzus persicae*) avoided feeding on high-Se plants, and when given only the choice of feeding on leaves containing Se declined in population, already at leaf Se levels around 10 mg kg^{-1} (Hanson et al., 2004). Se hyperaccumulation may also function in elemental allelopathy: the high Se soils around hyperaccumulators may exclude non-tolerant plant neighbors: they inhibited the germination and growth of *A. thaliana* (El Mehdawi et al., 2011). The combined effects of elemental allelopathy and the continued buildup of Se in the soil from high-Se tissue likely make Se hyperaccumulation evolutionarily adaptive (El Mehdawi and Pilon-Smits, 2012).

Selenium (hyper)accumulation has several emerging uses. Naturally occurring Se often becomes a problem when it gets locally concentrated due to human activities such as mining, refining seleniferous fossil fuels or irrigation with Se-rich water. Selenium-accumulating plants may be used to clean up excess Se from soil, water and air, a process called phytoremediation.

Phytoremediation is 1000-fold less expensive than mechanical soil removal, according to soil cost evaluations (Cunningham & Ow 1996; Banuelos et al., 1997). Selenium containing plants may also be of nutritive value; for example, prickly pear (*Opuntia ficus-indica*) can accumulate up to 47 mg kg^{-1} Se and 111 mg kg^{-1} Se in its edible fruits and pads, respectively (Banuelos et al., 2011). Figure 1.2 summarizes the plant processes that affect Se mobility and chemical speciation.

Since hyperaccumulators are often slow growing and of little economic value (Salt et al., 1998), they have limited direct applicability for phytoremediation or biofortification. However, they could be a valuable tool to identify genes involved in Se accumulation and tolerance, which may be expressed in a more productive and economically viable species. Such genes may include Se transporters or enzymes involved in Se metabolism. Ideally, if a key signaling gene could be identified that triggers the entire hyperaccumulation syndrome, this would be a most promising candidate for genetic engineering. So far, very little is known about upstream processes that activate the extreme Se uptake and accumulation in hyperaccumulators, and their concomitant Se hypertolerance. However, there is evidence that the defense hormones jasmonic acid (JA), salicylic acid (SA) and ethylene facilitate Se accumulation and tolerance: their levels were higher in *S. pinnata* compared to non-hyperaccumulator *S. albescens*, and supplying them externally to Se-sensitive *Stanleya* and *Arabidopsis* taxa enhanced Se accumulation and tolerance (Tamaoki et al., 2008; Freeman et al., 2010). Since these hormones have been reported to sense S deficiency and upregulate the S/Se assimilation pathway, this may explain the elevated Se levels in the hyperaccumulator (Iqbal et al., 2013). However, upstream processes that cause the elevated hormone levels remain obscure. Defense-related genes known to be

upregulated by these hormones were also expressed at higher levels in *S. pinnata*; whether they play any role in Se hyperaccumulation remains to be investigated.

The goal of this project described in this thesis was to determine which genes play a role in Se hyperaccumulation in *S. pinnata*. The approach was to do a full transcriptome comparison between this hyperaccumulator and related non-hyperaccumulator *S. elata*. This non-accumulator species was found in recent studies to accumulate the least Se of all *Stanleya* species (Cappa et al., 2014, 2015). In addition to genes directly involved in taking up and metabolizing the Se, the RNA sequencing approach used allows the identification of novel genes that may act upstream in the perception of Se and the signaling cascade that leads to the upregulation of Se uptake and assimilation processes. The knowledge gained through this project may not only help develop plants with superior phytoremediation or biofortification properties, but is also intrinsically valuable as it gives insight into the mechanisms underlying the fascinating phenomenon of hyperaccumulation.

FIGURES

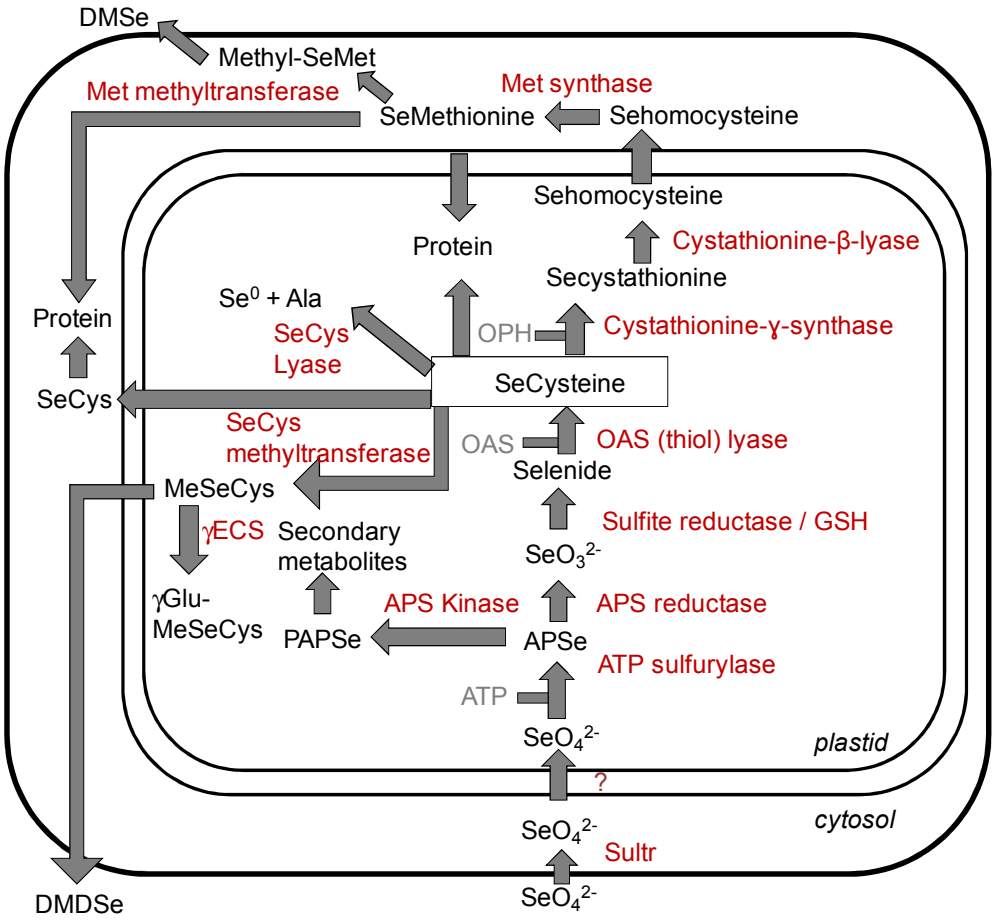

Figure 1.1 Proposed model for Se assimilation in plants, from Pilon-Smits (2015). Enzymes are shown in red, metabolites in black or gray. APSe: adenosine phosphoselenate; PAPSe: phospho-adenosine phosphoselenate; OAS: O-acetylserine; OPH: O-phosphohomoserine; SeCys: selenocysteine; (Se)Met: (seleno)methionine; Ala: alanine; MeSeCys: methyl-SeCys; gGlu-MeSeCys: g-glutamyl MeSeCys; gECS: g-glutamylcysteine synthetase; GSH: glutathione; DMSe: dimethylselenide; DMDSe: dimethyldiselenide.

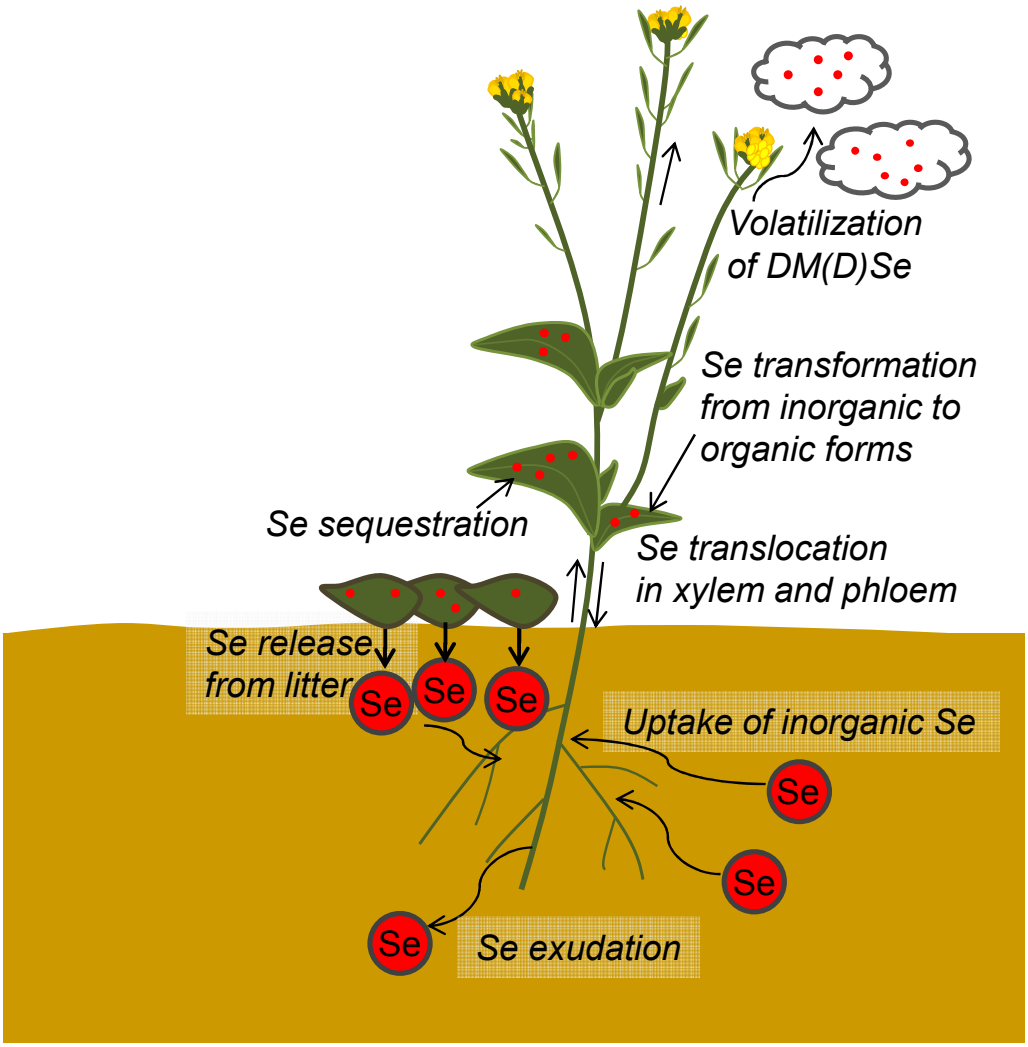

Figure 1.2 Plant effects on Se cycling and transformation, taken from Pilon-Smits (2015). Inorganic Se: selenate, selenite; organic Se: methylselenocysteine or selenocystathionine; volatile DM(D)Se: dimethyl(di)selenide. Se from accumulators may protect plants from pathogens and herbivores.

REFERENCES

Alford ER, Pilon-Smits EAH, Fakra SC, Paschke MW. 2012. Selenium hyperaccumulation by Astragalus (Fabaceae) does not inhibit root nodule symbiosis. *American Journal of Botany* 99: 1930-1941.

Banuelos GS, Ajwa HA, Terry N, Zayed A. 1997. Phytoremediation of selenium laden soils: A new technology. *Journal of Soil and Water Conservation* 52: 426-430.

Banuelos GS, Fakra SC, Walse SS, Marcus MA, Yang SI, Pickering IJ, Pilon-Smits EAH, Freeman JL. 2011. Selenium Accumulation, Distribution, and Speciation in Spineless Prickly Pear Cactus: A Drought- and Salt-Tolerant, Sele bznium-Enriched Nutraceutical Fruit Crop for Biofortified Foods. *Plant Physiology* 155: 315-327.

Barillas JRV, Quinn CF, Freeman JL, Lindblom SD, Fakra SC, Marcus MA, Gilligan TM, Alford ER, Wangeline AL, Pilon-Smits EAH. 2012. Seleium Distribution and Speciation in the Hyperaccumulator *Astragalus bisulcatus* and Associated Ecological Partners. *Plant Physiology* 159: 1834-1844.

Baum MK, ShorPosner G, Lai SH, Zhang GY, Fletcher MA, Sauberlich H, Page JB. 1997. High risk of HIV-related mortality is associated with selenium deficiency. *Journal of Acquired Immune Deficiency Syndromes and Human Retrovirology* 15: 370-374.

Bick JA, Leustek T. 1998. Plant sulfur metabolism - the reduction of sulfate to sulfite. *Current Opinion in Plant Biology* 1: 240-244.

Bohrer AS, Yoshimoto N, Sekiguchi A, Rykulski N, Saito K, Takahashi H. 2014. Alternative translational initiation of ATP sulfurylase underlying dual localization of sulfate assimilation pathways in plastids and cytosol in *Arabidopsis thaliana*. *Frontiers in Plant Science* 5.

Brown TA, Shrift A. 1981. Exclusion of Selenium from Proteins of Selenium-Tolerant Astragalus Species. *Plant Physiology* 67: 1051-1053.

Cabannes E, Buchner P, Broadley MR, Malcolm JH. 2011. A Comparison of Sulfate and Selenium Accumulation in Relation to the Expression of Sulfate Transporter Genes in Astragalus Species. *Plant Physiology* 157: 2227-2239.

Cakir O, Ari S. 2013. Cloning and molecular characterization of selenocysteine methyltransferase (AchSMT) cDNA from *Astragalus chrysochlorus*. *Plant Omics* 6: 100-106.

Cao MJ, Wang Z, Wirtz M, Hell R, Oliver DJ, Xiang CB. 2013. SULTR3;1 is a chloroplast

localized sulfate transporter in *Arabidopsis thaliana*. *Plant Journal* 73: 607-616.

Cappa JJ, Yetter C, Fakra S, Cappa PJ, DeTar R, Landes C, Pilon-Smits EAH, Simmons MP. 2015. Evolution of selenium hyperaccumulation in Stanleya (Brassicaceae) as inferred from phylogeny, physiology and X-ray microprobe analysis. *New Phytologist* 205: 583-595.

Cunningham SD, Ow D. 1996. Promises and prospects of phytoremediation. *Plant Physiology* 110: 715-719.

Mortimer PH, Culvenor CCJ, Smith LW, Frahn JL, Cockrum PA. 1978. Selenium toxicity economic loss. In Keeler, R. F.; Van Kampen, K. R.;James, L. F. (Eds.) *Effects of poisonous plants on livestock. Pg 3. New york*: Academic Press.

El Kassis E, Cathala N, Rouached H, Fourcroy P, Berthomieu P, Terry N, Davidian JC. 2007. Characterization of a selenate-resistant Arabidopsis mutant. Root growth as a potential target for selenate toxicity. *Plant Physiology* 143: 1231-1241.

El Mehdawi AF, Quinn CF, Pilon-Smits EAH. 2011. Effects of selenium hyperaccumulation on plant-plant interactions: Evidence for elemental allelopathy? *New Phytologist* 191: 120-131.

El Mehdawi AF, Pilon-Smits EAH. 2012. Ecological Aspects of Plant Selenium Hyperaccumulation. *Plant Biology* 14: 1-10.

Davis AM. 1972. Selenium accumulation in *Astragalus* species. *Agronomy Journal* 64: 751 754.

de Souza MP, Pilon-Smits EAH, Lytle CM, Hwang S, Tai JC, Honma TSU, Yeh L, Terry N. 1998. Rate-limiting steps in selenium volatilization by Brassica juncea. *Plant Physiology* 117: 1487-1494

Dilworth GL, Bandurski RS. 1977. Activation of selenate by adenosine 5-triphosphate sulphurylase from *Saccharomyces cerevisiae*. *Biochemical Journal* 163: 521–529.

Diskin CJ, Tomasso CL, Alper JC, Glaser ML, Fliegel SE. 1979. Long-term selenium exposure. *Archives of Internal Medicine* 139: 824-6.

Feist LJ, Parker DR. 2001. Ecotypic variation in selenium accumulation among populations of *Stanleya pinnata*. New Phytologist 149: 61-69.

Freeman JL, Zhang LH, Marcus MA, Fakra S, McGrath SP, Pilon-Smits EAH. 2006. Spatial imaging, speciation, and quantification of selenium in the hyperaccumulator plants *Astragalus bisulcatus* and *Stanleya pinnata*. *Plant Physiology* 142: 124-134.

Freeman JL, Tamaoki M, Stushnoff C, Quinn CF, Cappa JJ, Devonshire J, Fakra SC, Marcus

MA, McGrath SP, Hoewyk DV, Pilon-Smits EAH. 2010. Molecular Mechanisms of Selenium Tolerance and Hyperaccumulation in *Stanleya pinnata*. *Plant Physiology* 153: 1630-1652.

Freeman JL, Banuelos GS. 2011. Selection of salt and boron tolerant selenium hyperaccumulator *Stanleya pinnata* genotypes and characterization of Se phytoremediation from agricultural drainage sediments. *Environmental Science and Technology* 45: 9703-10.

Gattow G, Heinrich G. 1964. Thermochemistry of selenium. II. Conversions of crystalline selenium modifications. III. Conversion of amorphous selenium modifications. *Zeitschrift für anorganische und allgemeine Chemie* 331: 256–288.

Geering HR, Cary EE, Jones L HP, Allaway WH. 1968. Solubility and redox criteria for the possible forms of selenium in soils. *Soil Science Society of America Proceedings* 32: 35-40.

Hanson BR, Lindblom SD, Loeffler ML, Pilon-Smits EAH. 2004. Selenium protects plants from phloem-feeding aphids due to both deterrence and toxicity. *New Phytologist* 162: 655-662

Hartikainen H, Xue TL, Piironen V. 2000. Selenium as an anti-oxidant and pro-oxidant in ryegrass. *Plant and Soil* 225: 193-200.

Hondal RJ, Marino SM, Gladyshev VN. 2012. Selenocysteine in thio/disulfide-like exchange reactions. *Antioxidants and Redox Signaling* 18: 1675-1689.

Hopper JL, Parker DR. 1999. Plant availability of selenite and selenate as influenced by the competing ions phosphate and sulfate. *Plant and Soil* 210: 199-207.

Iqbal N, Masood A, Khan MIR, Asgher M, Fatma F, Khan NA. 2013. Cross-talk between sulfur assimilation and ethylene signaling in plants.Plant Signaling & Behavior 8: 104-112.

Kataoka T, Hayashi N, Yamaya T, Takahashi H. 2004. Root-to-shoot transport of sulfate in Arabidopsis. Evidence for the role of SULTR3;5 as a component of low-affinity sulfate transport system in the root vasculature. *Plant Physiology* 136: 4198-4204.

Kawashima CG, Matthewman CA, Huang S, Lee BR, Yoshimoto N, Koprivova A, Rubio Somoza I, Todesco M, Rathjen T, Saito K, Takahashi H, Dalmay T, Kopriva S. 2011. Interplay of SLIM1 and miR395 in the regulation of sulfate assimilation in Arabidopsis. *Plant Journal* 66: 863-76.

Kohrle J, Brigelius-Flohe R, Bock A, Gartner R, Meyer O, Flohe L. 2000. Selenium in biology: Facts and medical perspectives. *Biological Chemistry* 381: 849-864.

Leves FP, Tierney ML, Howitt SM. 2008. Polar residues in a conserved motif spanning

helices 1 and 2 are functionally important in the SulP transporter family. *The International Journal of Biochemistry & Cell Biology* 40: 2596-2605.

Liang G, Yu D. 2010. Reciprocal regulation among miR395, APS and SULTR2;1 in *Arabidopsis thaliana*. *Plant Signaling & Behavior* 5: 1257-1259.

Lobanov AV, Hatfield DL, Gladyshev VN. 2009. Eukaryotic selenoproteins and selenoproteomes. *Biochimica Biophysica Acta* 1790: 1424-1428.

Meija J, Montes-Bayón M, Le Duc DL, Terry N, Caruso JA. 2002. Simultaneous Monitoring of Volatile Selenium and Sulfur Species from Se Accumulating Plants (Wild Type and Genetically Modified) by GC/MS and GC/ICPMS Using Solid-Phase Microextraction for Sample Introduction. *Analytical Chemistry* 74: 5837-5844.

McFarlane HCE, McFarlane W. Sulfur, selenium, and tellurium. In: Mason J, editor. Multinuclear NMR. New York (NY): Plenum Press; 1987. p. 417-435.

McDonald B, Deb A, Elphick J, Davies M, Bustard D, Chapman P. 2010. Developmental toxicity of selenium to Dolly Varden char (*Salvelinus malma*). *Environmental Toxicology & Chemistry* 29: 2800-2805.

Neuhierl B, Bock A. 1996. On the mechanism of selenium tolerance in selenium-accumulating plants - Purification and characterization of a specific selenocysteine methyltransferase from cultured cells of Astragalus bisculatus. *European Journal of Biochemistry* 239: 235-238.

Ng BH, Anderson JW. 1978. Synthesis of selenocysteine by cysteine synthase from selenium accumulator and non-accumulator plants. *Phytochemistry* 17: 2069–2074.

Novoselov SV, Rao M, Onoshko NV, Zhi HJ, Kryukov GV, Xiang YB, Weeks DP, Hatfield DL, Gladyshev VN. 2002. Selenoproteins and selenocysteine insertion system in the model plant cell system, *Chlamydomonas reinhardtii*. *Embo Journal* 21: 3681-3693.

Oremland RS, Herbel MJ, Blum JS, Langley S, Bevveridge TJ, Ajayan PM, Sutto T, Ellis AV, Curran S. 2004. Structural and spectral features of selenium nanospheres produced by Se-respiring bacteria. *Applied and Environmental Microbiology* 70: 52-60.

Pasternak M, Lim B, Wirtz M, Hell R, Cobbett CS, Meye AJ. 2008. Restricting glutathione biosynthesis to the cytosol is sufficient for normal plant development. *Plant Journal* 53: 999-1012.

Pilon-Smits EAH, Hwang SB, Lytle CM, Zhu YL, Tai JC, Bravo RC, Leustek T, Terry N. 1999. Overexpression of ATP sulfurylase in *Brassica juncea* leads to increased selenate uptake, reduction and tolerance. *Plant Physiology* 119:123-132.

Pilon-Smits EAH. 2015. Selenium in plants. Progress in Botany (Luettge, U, Ed.) Springer

Verlag, Heidelberg, Germany, pp 93-107.

Quinn CF, Freeman JL, Galeas ML, Klamper EM, Pilon-Smits EAH. 2007. The role of selenium in protecting plants against prairie dog herbivory: implications for the evolution of selenium hyperaccumulation. *Oecologia* 155: 267-275.

Quinn CF, Prins CN, Freeman JL, Gross AM, Hantzis LJ, Renolds RJB, Yang SI, Covey PA, Banuelos GS, Pickering IJ, Fakra SC, Marcus MA, Arathi HS, Pilon-Smits EAH. 2011. Selenium accumulation in flowers and its effects on pollination. *New Phytologist* 192: 727-737.

Rascio N, Navari-Izzo F. 2011. Heavy metal hyperaccumulating plants: How and why do they do it? And what makes them so interesting? *Plant Science: International Journal of Experimental Plant Biology* 180: 169-181.

Rouached H, Berthomieu P, El Kassis E, Cathala N, Catherinot V, Labesse G, Davidian JC, Fourcroy P. 2005. Structural and functional analysis of the C-terminal STAS (sulfate transporter and anti-sigma antagonist) domain of the *Arabidopsis thaliana* sulfate transporter SULTR1.2. *Journal of Biological Chemistry* 280: 1597-15983.

Sabbagh M, Van Hoewyk D. 2012. Malformed selenoproteins are removed by the ubiquitin proteasome pathway in *Stanleya pinnata*. *Plant Cell Physiology* 53: 555-564.

Salt DE, Smith RD, Raskin I. 1998. Phytoremediation. *Annual Review of Plant Physiology & Plant Molecular* Biology 49: 643-68.

Shchedrina VA, Zhang Y, Labunskyy VM, Hatfield DL, Gladyshev VN. 2010. Structure Function Relations, Physiological Roles, and Evolution of Mammalian ER-Resident Selenoproteins. *Antioxidants & Redox Signaling* 12: 839-849.

Schiavon M, Pilon M, Malagoli M, Pilon-Smits EAH. 2015. Exploring the importance of sulfate transporters and ATP sulphurylases for selenium hyperaccumulation—a comparison of *Stanleya pinnata* and *Brassica juncea* (Brassicaceae). *Frontiers in Plant Science* 6: doi: 10.3389.

Shibagaki N, Grossman AR. 2006. The role of the STAS domain in the function and biogenesis of a sulfate transporter as probed by random mutagenesis. *Journal of Biological Chemistry* 281: 22964-22973.

Shibagaki N, Grossman AR. 2010. Binding of Cysteine Synthase to the STAS Domain of Sulfate Transporter and Its Regulatory Consequences. *Journal of Biological Chemistry* 285: 25094-25102.

Shrift A, Virupaksha TK. 1965. Seleno-amino acides in selenium-accumulating plants. *Biochimica Biophysica Acta* 100: 65-75.

Sors TG, Ellis DR, Salt DE. 2005. Selenium uptake, translocation, assimilation and metabolic fate in plants. *Photosynthesis Research* 86: 373-389.

Sors TG, Martin CP, Salt DE. 2009. Characterization of selenocysteine methyltransferases from Astragalus species with contrasting selenium accumulation capacity. *The Plant Journal* 59: 110-122.

Takahashi H, Watanabe-Takahashi A, Smith FW, Blake-Kalff M, Hawkesford MJ, Saito K. 2000. The roles of three functional sulphate transporters involved in uptake and translocation of sulphate in *Arabidopsis thaliana*. *Plant Journal* 23: 171-182.

Takahashi H, Kopriva S, Giordano M, Saito K, Hell R. 2011. Sulfur assimilation in photosynthetic organisms: molecular functions and regulations of transporters and assimilatory enzymes. *Annual Review of Plant Biology* 62: 157-84.

Terry N, Zayed AM, de Souza PM, Tarun AS. 2000. Selenium in higher plants. *Annual Review of Plant Physiology and Plant Molecular Biology* 51:401-432

Van Huysen T, Abdel-Ghany S, Hale KL, LeDuc D, Terry N, Pilon-Smits EAH. 2003. Overexpression of cystathionine-gamma-synthase enhances selenium volatilization in *Brassica juncea*. *Planta* 218: 71-78.

White PJ, Bowen HC, Parmaguru P, Fritz M, Spracklen WP, Spiby RE, Meacham MC, Mead A, Harriman M, Trueman LJ, Smith BM, Thomas B, Broadley MR. 2004. Interactions between selenium and sulphur nutrition in *Arabidopsis thaliana*. *Journal of Experimental Botany* 55: 1927-1937.

White PJ, Bowen HC, Marshall B, Broadley MR. 2007. Extraordinarily high leaf selenium to sulfur ratios define Se accumulator plants. *Annals of Botany* 100: 111-118.

Wilber C. 1980. Toxicology of Selenium. *Clinical Toxicology* 17: 171-230.

Xu XM, Carlson BA, Zhang Y, Mix H, Kryukov GV, Glass RS, Berry MJ, Gladyshev VN, Hatfield DL. 2007. New developments in selenium biochemistry: Selenocysteine biosynthesis in eukaryotes and archaea. *Biological Trace Element Research* 119: 234-241.

Yang GQ, Xia YM (1995) Studies on human dietary requirements and safe range of dietary intakes of selenium in China and their application in the prevention of related endemic diseases. *Biomedical and Environmental Sciences* 8:187-201.

Zayed A, Lytle CM, Terry N. 1998. Accumulation and volatilization of different chemical species of selenium by plants. *Planta* 206: 284-92.

Zhang Y, Formenko DE, Gladyshev VN. 2005. The microbial selenoproteome of the Sargasso Sea. *Genome Biology* 6: 1-17.

Zhu YL, Pilon-Smits EAH, Jouanin L, Terry N. 1999. Overexpression of Glutathion Synthetase in Indian Mustard Enhances Cadmium Accumulation and Tolerance. *Plant Physiology* 119: 73-79.

Zhu J, Wang N, Li S, Li L, b, Su H, Liu C. 2008. Distribution and transport of selenium in Yutangba, China: Impact of human activities. *Science of the Total Environment* 392: 252–261.

CHAPTER 2:

DIFFERENTIAL GENE EXPRESSION BETWEEN SELENIUM HYPERACCUMULATOR *STANLEYA PINNATA* AND NONACCUMULATOR *STANLEYA ELATA* (*BRASSICACEAE*) IN RESPONSE TO SELENIUM: A COMPARATIVE TRANSCRIPTOME ANALYSIS

SUMMARY

The goal of this study was to obtain better insight into the molecular mechanisms of selenium (Se) hyperaccumulation in *Stanleya pinnata*. Transcriptome-wide differences in root and shoot gene expression levels were investigated between *S. pinnata* and related nonaccumulator *Stanleya elata*, grown with or without 20 μM selenate. Genes involved in sulfate/selenate transport (*Sultr1;2*, *Sultr2;1*, *Sultr3;1, Sultr3;4*) and assimilation (*Atps2, Apr3*) or in oxidative stress resistance (glutathione-related genes, peroxidases) were among the most differentially expressed between species; many showed constitutively elevated expression in *S. pinnata*. Many genes involved in synthesis and signaling of defense hormones jasmonic acid (JA), salicylic acid (SA) and ethylene were also more highly expressed in *S. pinnata* (*Lox*, *Acx*, *Pal*, *Ics*, *Ein, Jar, Tga*), as were related defense genes (*Pr, Pdf*). JA accumulation has been reported to induce sulfur assimilatory and glutathione biosynthesis genes. Several upstream signaling genes reported to upregulate defense hormone genes were more expressed in *S. pinnata* than *S. elata*

Note: Several other people contributed to the work described in Chapter 2. Before the start of this thesis work, Jennifer Cappa (Biology Department, Colorado State University) grew and harvested the plants for fresh weight analysis and RNA sequencing and Patrick Edger (Division of Biological Sciences, University of Missouri) prepared the cDNA, assembled the transcriptomes, prepared the normalized contig RPKMs and annotated the contigs. During this thesis work, Wen Zhou helped with the statistical comparisons between treatments. Jiameng Wang collaborated with Jennifer Cappa and grew, harvested the plants for dry weight and elemental analysis. Jiameng Wang analyzed the data, produced the figures, and wrote the manuscript.

and might initiate these Se responses. Selenium hyperaccumulation in *S. pinnata* appears to be mediated by constitutively upregulated JA, SA and ethylene-mediated defense systems, resulting in elevated sulfate/selenate uptake and assimilation as well as elevated antioxidant capacity. The concerted action of increased likely contributes to Se hyperaccumulation and hypertolerance.

INTRODUCTION

The element selenium (Se) is chemically similar to sulfur (S) (Wilbur, 1980). Selenium exists mainly in inorganic forms in soils where it is present in the oxidized state SeO_4^{2-} (selenate), which can be assimilated into living organisms either intentionally or inadvertently through the sulfur (S) assimilation pathway (Geering et al., 1968). Selenium is an essential trace element for many animals and bacteria as well as certain algae, where it plays a role in antioxidant and hormone metabolism (Foster & Sumar, 1997). In higher plants, Se is not known to have any essential functions, although it is considered a beneficial element at low levels (Pilon-Smits et al., 2009). Most plants that are grown on high concentrations of Se show stunted growth and chlorosis due to oxidative damage, usually at tissue levels above 100 mg Se kg^{-1}, or 0.01%, dry weight (DW) (Van Hoewyk, 2013). Toxicity may also occur due to nonspecific replacement of S with Se in cysteine (Cys), and possibly methionine (Met) (Ng & Anderson, 1978; Van Hoewyk, 2013).

Certain members of the Fabaceae (*Astralagus* spp.), Asteraceae (*Symphyotrichum ericoides*, *Xylorhiza* spp., *Oonopsis* spp.,) and Brassicaceae (*Stanleya pinnata*) have evolved the ability to accumulate up to 1% of their DW in Se and are known as Se hyperaccumulators (Freeman et al., 2006). Such plant Se concentrations are toxic when ingested by animals and therefore appear to be a defense strategy against herbivores and pathogens (Hanson et al., 2004; Freeman et al., 2007, 2009). Selenium hyperaccumulators may be a source of genes that can be

used for incorporation into crop species for Se phytoremediation or biofortification—if the mechanisms by which they tolerate and accumulate Se can be elucidated (Banuelos et al., 1997, 2010). Based on research so far, Se hyperaccumulators appear to tolerate Se better through Se detoxification mechanisms, including reducing selenate to less toxic forms, volatilizing methylated selenocompounds, and storing Se in non-protein amino acids such as selenocystathionine and methylselenocysteine (MeSeCys), often in peripheral tissues (Brown & Shrift, 1981; Zayed et al., 1998; Meija et al., 2002; Freeman et al., 2006; Cakir & Ari, 2013). For example, the hyperaccumulator *S. pinnata* accumulates MeSeCys and selenocystathionine in vacuoles of leaf epidermal cells as opposed to the related non-hyperaccumulator *Brassica juncea*, where Se remains as selenate in the vasculature (Freeman et al., 2006, 2010). Studies also suggest that increased expression of genes in the glutathione, antioxidant, and proteasome pathways may play a role in the extreme Se tolerance of hyperaccumulators, by preventing toxic effects of free radicals and recycling malformed proteins (Freeman et al. 2010; Van Hoewyk 2013).

In view of the similarity of Se to S, sulfate assimilation genes may be hypothesized to be modified in hyperaccumulators. The genes may have higher expression levels and also the gene product may have altered kinetic properties. For example, root sulfate transporters may have enhanced specificity for Se, since uptake of selenate was much less inhibited by sulfate in *S. pinnata* as compared to *B. juncea* (Harris et al., 2014). The main portal for selenate and sulfate into plant roots is a high-affinity (group 1) sulfate transporter (SULTR). *Arabidopsis thaliana* SULTR1;2 mutants showed enhanced selenate tolerance and lower selenate to sulfate ratios compared to wild-type plants (El Kassis, 2007; Ohno et al., 2012). Freeman et al. (2010), using a macroarray approach, found constitutively high expression of sulfur metabolism genes, and

higher expression of genes involved in GSH synthesis in *S. pinnata* compared to the non-hyperaccumulator *Stanleya albescens*. Despite the higher leaf Se concentrations in *S. pinnata*, *S. albescens* grown in the same conditions formed more reactive oxygen species (ROS).

Hyperaccumulators also tend to have constitutively high expression of genes involved in defense hormone synthesis and response, including jasmonic acid (JA), salicylic acid (SA) and ethylene (Freeman et al., 2010). Further evidence for a positive effect of JA on Se accumulation is that applications of 10μM methyl jasmonate to *S. pinnata* and *S. albescens* lead to increased leaf Se levels (Freeman et al., 2010). Similar results were found for nonaccumulator *A. thaliana* accessions, where selenite tolerance and uptake correlated with increased expression of genes involved in the biosynthesis and responses to JA and ethylene (Tamaoki et al. 2008a). Moreover, mutants that have impaired expression of those same genes had lower total S levels as well as lower levels of the reduced S compound GSH, which scavenges ROS (Tamaoki et al. 2008a). The causal connection between the enhanced levels of S/Se assimilation, and defense hormones awaits further clarification. The possibility remains that a key regulatory gene is deregulated in *S. pinnata*, leading to constitutively enhanced levels of the defense hormones JA, SA, and/or ethylene, which in turn upregulate pathways involved in biotic stress defense, including S assimilation.

In this study we investigated the transcriptome-wide differences in gene expression levels between *S. pinnata* and the Se-sensitive, nonaccumulator *S. elata* (El Mehdawi et al., 2012; Cappa et al., 2014). In a phylogenetic analysis of the *Stanleya* genus by Cappa et al. (2015), the *S. pinnata* species complex was found to be the most derived clade, with *S. elata* as a sister species. These two species were grown in the presence or absence of Se and compared with respect to growth, Se and S accumulation and their root and shoot transcriptome. Our purpose

was to determine which genes play a direct role in the Se hyperaccumulator phenotype, as well as which genes function upstream of the signaling cascade in response to Se.

MATERIALS AND METHODS

Plant growth

Seeds of *S. pinnata* (Western Native Seed, Coaldale, CO) and *S. elata* (collected in NV, 38°11'36"N 117°59"15"W) were surface-sterilized and cold stratified for 48 hours at 4º C. Seeds were germinated on sterile petri dishes and transferred to sealed Phytatrays™ (Sigma-Aldrich, St. Louis, MO) on ½ strength MS basal salts medium (Murashige & Skoog, 1962) with 1% sucrose and 0 µM or 20 µM sodium selenate. Plants were grown in a growth chamber at a light intensity of 150 µmol m^{-2} s^{-1} with a 16/8 L/D photoperiod at 23ºC. Three plants were grown per container, and three containers per species and treatment. After 30 days, one plant per container was harvested and its roots rinsed to remove external Se. The plants were separated into root and shoot and frozen in liquid nitrogen for RNA sequencing (n=3 bioreplicates per treatment). The remaining two plants from each container were harvested, the roots rinsed and separated from shoots and then used to obtain the fresh weights.

RNA-Sequencing

Frozen plants were shipped to the University of Missouri where total RNA was extracted using an RNA Mini Kit (Invitrogen, Carisbad, CA, USA). The mRNA was purified and used to construct Illumina cDNA libraries using the TruSeq RNA Kit, then sequenced on the Illumina HiSeq-2000 at the University of Missouri's DNA Core Facility. Pair-end 100 bp sequencing was performed for one biological replicate for each species, organ, Se treatment combination (8 samples). The sequence was quality filtered using Next GEN version 2.17 (SoftGenetics, State College, PA, USA); removing reads with a median quality score of less than 22, trimmed reads

at positons that had 3 consecutive bases with a quality score of less than 20, and removed any trimmed reads with a total length less than 40bp. The quality filtered data was assembled *de novo* using Trinity (Grabherr et al. 2011) using default parameters. Any contiguous sequence (contig) shorter than 300 bp was removed. Next, single-end 50 bp sequencing was performed on the remaining two biological replicates for each species, organ, Se treatment combination (16 samples). Quality filtered reads for all three biological replicates were aligned to the *de novo* assemblies using NextGENe version 2.17. Assembled reads were annotated using BLASTn against the *A. thaliana* cDNA database (TAIR, http://www.arabidopsis.org/) and assigned homologs with an e-value threshold of 0.00005. *A. thaliana* was used as a reference because it has a fully annotated genome, and is in the same family (Brassicaceae) as *Stanleya*. Finally, contigs annotated to the same ATID were associated with one gene and their RPKM values were summed. Only genes existing in both *S. pinnata* and *S. elata* libraries were used for further analysis. Following the conventional preliminary screening approach, we set the filter threshold to be 2% of sample quantiles across all groups, i.e. genes with negligible expression across all 24 samples were excluded if $r \in S_1 = \{g: max_{ijl} \sum_{k=1}^{3} Z_{g,ijkl}/3 < \varepsilon_1\}$ where Z stands for RPKM values and ε_1 is chosen to be the 2% grand quantiles of sample means (Gentleman et al., 2005). In addition, genes that essentially do not have any within-sample variations were excluded, i.e. gene r was removed if $r \in S_2 = \left\{g: max_{ijl} \sum_{k=1}^{3} \left(Z_{g,ijkl} - \sum_{k=1}^{3} Z_{g,ijkl}/3\right)^2 < 2\varepsilon_2\right\}$ where $2\varepsilon_2$ was selected to be the 2% grand quantiles of sample variations, as before.

Statistical analysis

Raw RPKMs were normalized using the trimmed mean of M-values (TMM) procedure (Oshlack et al., 2010). This was done because one of the treatment groups (*S. elata* roots, 20 μM Se) had on average ~3-fold lower RPKM levels than the other treatments, including for

commonly used housekeeping genes. The normalized RPKMs were further transformed by variance stabilization transformations. The experiment naturally follows a split-plot design and the processed libraries were therefore analyzed using the following linear mixed model (Morris 2010):

$$Y_{g,ijkl} = \mu_g + \alpha_{g,i} + \beta_{g,j} + (\alpha\beta)_{g,ij} + e_{g,ijk} + \gamma_{g,l} + (\alpha\gamma)_{g,il} + (\beta\gamma)_{g,jl} + (\alpha\beta\gamma)_{g,ijl} + \varepsilon_{g,ijkl}$$

where $Y_{g,ijkl}$ denotes the processed expression level of the g^{th} gene (g = 1, 2, … 19,129) of the l^{th} organ (l = 1, 2 stand for root and shoot, respectively) of the k^{th} biological replicate (k = 1, 2, 3) from the i^{th} species (i = 1, 2 stand for *S. elata* and *S. pinnata*, respectively) for the j^{th} treatment (j = 1, 2 stand for 0 and 20 μM Se, respectively). With the sub-index g suppressed for simplicity, we summarize the model parameters as following: α_i models the effect of species; β_j models the treatment effects; $(\alpha\beta)_{ij}$ models the interactions between species and treatment; γ_l models the organ effects; $(\alpha\gamma)_{il}$ models the interactions between species and organ; $(\beta\gamma)_{jl}$ models the interactions between treatment and organ; $(\alpha\beta\gamma)_{ijl}$ models the 3-way interaction between species, treatment, and organ; $e_{ijk} \sim i.i.d.N(0, \sigma_e^2)$ models correlations among samples within the same combination of species and treatment; and $\varepsilon_{ijkl} \sim i.i.d.N(0, \sigma^2)$ models measurement errors.

Data processing, model fitting and subsequent analyses were conducted using SAS ver. 9.4, R ver. 3.1.1, and bioconductor in R ver. 3.1.1 (Gentleman et al., 2005). Main effects of the (Se) treatment and species, as well as the simple effects of treatment for each species, were tested and estimated. In addition, the effect of treatment, segregated by organ type for each species; the effect of species for each organ type, segregated by treatments; and the interaction effect of species on the differences between treatments were tested for a more detailed analysis. Estimated model parameters, p-values for the corresponding tests and associated q-values were obtained. The Benjamini-Hochberg procedure was employed to control the false discovery rate (FDR) at

the 0.005 level (Benjamini & Hotchberg, 1995). Then for each of the above hypotheses of biological interest, the effects were estimated from model parameters for genes declared significant by the above general linear hypothesis testing procedure with FDR controlled at the 0.005 level. For example, the gene whose ATID is AT1G01030.1 has a q-value for the effect of Se treatment < 0.005 and is therefore considered a differentially expressed (DE) gene for the effect of Se treatment, whose 0 and 20 μM Se treatment effects were therefore estimated by the model parameters $\hat{\beta}_1$ and $\hat{\beta}_2$.

Mapman visualization

The estimated effects based on model parameters for significant DE ($q < 0.005$) genes were further visualized using Mapman ver. 3.5.1 (Thimm et al. 2004, Usadel et al. 2005). A total of 12 analysis files were generated (link: https://www.dropbox.com/sh/5fo1ikp4ca7my4x/AAD0S_lVuggP6I7WkXkx4WA0a?dl=0), and will be made available on DataDryad.org repository before publication. The mapping ATh_AGI_ISOFORM_MODEL_TAIR10_Aug2012 was used to visualize genes in pathways. To statistically compare a particular bin with other bins in a given pathway, numbers of significantly DE genes between *S. pinnata* and *S. elata* within each bin are treated as responses and the Wilcoxon rank-sum test, corrected for with the Benjamini-Hotchberg method, was conducted to identify bins significantly different from others (Benjamini & Hotchberg, 1995; Usadel et al., 2005). For those identified bins in a pathway ($p < 0.05$), we calculated the proportion of genes that were more expressed in *S. pinnata* than *S. elata*, as well as the proportion that were more expressed in *S. elata* than *S. pinnata*. This was investigated for genes that were DE between species for all combinations of organ and Se treatment. Using the Grubb's test, together with the median absolute deviation (MAD) score, we identified bins within which

the genes are more favored by *S. pinnata* than *S. elata*, deviated significantly from other bins ($p < 0.05$ for the Grubb test, or a MAD score larger than the 0.95 quantile).

ICP-AES analysis

A follow-up experiment was done to measure elemental concentrations and dry weight of plants grown under the same conditions as the samples used for RNA-seq. Each of the three containers per species and treatment housed 5 plants. After 30 days, plants were harvested and the shoots separated from the roots. These were dried for 72 hours at 50°C before being weighed and nitric-acid digested using Zarcinas et al. (1987) method. Digested material was analyzed for elemental concentrations using inductively-coupled plasma atomic emission spectroscopy (ICP-AES), using Fassel (1978) method. ANOVA followed by pairwise comparisons (Student's t-test) was completed in JMP (version 11) to test for significant differences between treatment groups. The roots were not analyzed due to pooling of samples with low root biomass (the final number of replicates was lower than 3).

RESULTS

Biomass and Se and S concentrations

We investigated whether Se would affect biomass in the two species. When Se hyperaccumulator *S. pinnata* and non-hyperaccumulator *S. elata* were grown on agar medium with or without 20 μM selenate, for transcriptome comparison, no significant ($p < 0.05$) differences in shoot fresh weight were observed between treatments (Fig. 2.1a). Similarly, in an identical experiment carried out for elemental analysis there were no differences in shoot DW between treatments (Fig. 2.1b). *S. pinnata* had a significantly higher shoot Se concentration than *S. elata*, both when supplied with selenate and without Se, and both species had higher Se levels when treated with Se than without (Fig. 2.1c). Because S competes with Se for uptake, the tissue

levels of S were also quantified. When treated with Se, *S. pinnata* had significantly higher shoot S concentrations than *S. elata*; in the absence of Se no significant difference was observed between the species (Fig. 2.1d). Within *S. elata*, Se treatment did not significantly affect S levels, while in *S. pinnata* S levels were higher in the presence of Se (Fig. 2.1d).

Transcriptome analysis overview

Illumina sequencing of the 24 cDNA libraries (two species, two organs, two Se treatments, and three biological replicates) generated 60,467,644 bp of sequences. A total of 205,543 contigs were assembled, with an average contig length of 594 bp. Contigs shorter than 300 bp were removed, leaving 101,675 contigs. Approximately 93% of these contigs were successfully annotated to *A. thaliana*, leaving 6,991 un-annotated contigs with abundant expression (>10 RPKM) that were excluded from further analysis. The ATID numbers to which the contigs BLASTed were used as IDs for the corresponding *Stanleya* genes, and the sum of RPKMs was used as a measure for gene expression. 19,572 genes found matches in both *Stanleya* species. After geometric means adjustment, an additional 443 genes were removed due to negligible expression and/or within-sample variations. The 19,129 remaining genes were used for all statistical analysis thereafter. In addition to expression comparisons within species, the expression levels of S. pinnata and S. elata genes associated with the same ATID were statistically compared to each other. These analyses included Se effect, species effect, organ effect, and their interactions, as described in detail in the Materials and Methods section. The 19,129 annotated genes with corresponding RPKMs for the 24 samples are listed in table S2.1.

An overview of gene expression responses to Se treatment is shown in Fig. 2.2. In roots, many more genes responded to Se treatment ($q < 0.005$) in *S. elata* compared to *S. pinnata* (Fig. 2.2a), while in shoots more genes were affected in *S. pinnata* than in *S. elata* (Fig. 2.2b). The

transcript levels of ~1,000 genes were similarly affected by Se in both plant species for roots, versus ~600 for shoots; both were relatively small fractions compared to genes differently affected by Se in the two species.

Gene expression differences between *S. pinnata* and *S. elata* were analyzed by comparing RPKM values of genes annotated to the same *A. thaliana* locus (Fig. S2.1). In both roots and shoots, the majority of genes were differently expressed between the two plant species, and a large proportion of these genes were differently expressed in both –Se and +Se treatments. Approximately half of the differently expressed genes were more expressed in *S. pinnata* than *S. elata*, and the other half more in *S. elata* than *S. pinnata*. Among genes that were differently expressed between species under only one treatment, the numbers of genes were similar for the +Se and –Se treatments; this was true for both organs (Fig. S2.1).

We were interested in which genes were most abundantly represented among the top 100 genes most affected by treatment, as they could reveal certain gene families that are involved in Se accumulation or tolerance. These genes can be found in Tables S2 – S4 for each of the 11 analyses generated from model parameters. Some gene families frequently present in multiple analysis include antioxidant-related genes (particularly peroxidases, which were more highly expressed in *S. pinnata* than *S. elata*), defense-related genes (particularly *Mlp*s, whose expression was dependent on both Se and species), sulfate assimilation genes (particularly ATP sulfurylases and APS reductases, which were more highly expressed in *S. pinnata*), transcription factors (particularly zinc finger protein genes, which differed for both Se presence and species), as well as glutathione-S-transferases (GSTs) and methyltransferases (particularly S-adenosyl methionine-dependent methyltransferases).

The genes that were DE between the two species were mapped into functional groups according to Mapman (see methods), to observe whether certain groups as a whole were more expressed in hyperaccumulator or nonaccumulator. Across all functional groups combined (Fig. 2.3, top bar), equal fractions of genes (50%) were more expressed in *S. pinnata* and *S. elata*. Among the functional groups, the percentage where *S. pinnata* > *S. elata* varied between 30% and 90%. Notable functional groups that were overall more expressed in the Se hyperaccumulator, regardless of organ and Se treatment, included gluconeogenesis/glyoxylate cycle genes, xenobiotic biodegradation, nitrogen assimilation and polyamine synthesis, metal handling and S assimilation. We did not identify any functional groups that were consistently (across treatments) more expressed in *S. elata*.

To gain insight into which functional groups of genes were most differentially expressed between the two plant species, the large-enzyme-family pathway was analyzed in Mapman for +Se and –Se, in both roots and shoots. Genes that were associated with peroxidases had significantly deviated expression ($p < 0.05$) compared with other gene groups displayed in the pathway for +Se and –Se in roots. The peroxidase group also had a significantly higher proportion of genes with greater expression in *S. pinnata* relative to other gene groups, as the p-value was < 0.05 (Grubb's test) or the MAD score was larger than 95th quantile for the majority of treatments. Additionally, in roots with Se treatment, glutathione S-transferase genes had significantly different expression ($p < 0.05$) compared with other gene groups as well as a higher proportion ($p < 0.05$, Grubb's test) of genes with greater expression in *S. pinnata* compared to other gene groups. No gene groups were found to deviate in expression from other gene groups in shoots for +Se or –Se treatments.

Transcript analysis of sulfate/selenate transporter genes

We analyzed the gene expressions of sulfate transporters (*Sultr)*, as they are thought to be responsible for greater S (and thus Se) uptake in hyperaccumulators. Figure 2.4a,b shows the transcript levels of *Sultr* genes DE between the plant species. In addition to these, high-affinity transporter *Sultr1;3*, thought to be involved in phloem loading, was more expressed in *S. pinnata* (~15 RPKM) than *S. elata* (not detected), and high-affinity transporter *Sultr1;1*, which is involved in root uptake (Rouached et al., 2008), was expressed at similar, very low levels in both species. Figure 2.4c shows the fold differences of *Sultr* expression levels between *S. pinnata* and *S. elata*, both in the presence and absence of Se, as part of cellular sulfate/selenate transport and root-to-shoot translocation. The high-affinity root transporter *Sultr1;2* (Takahashi et al., 2011) had extremely high levels of expression in *S. pinnata* roots, both for +Se and -Se treatments (Fig. 2.4b). *Sultr1;2* expression in *S. elata* roots showed a positive response to Se treatment (2-fold), while *S. pinnata* roots showed high constitutive expression. In shoots, *Sultr1;2* levels were overall much lower than in roots, and 2-fold lower in *S. pinnata* than *S. elata* (Fig. 2.4a, c).

Low-affinity transporter SULTR2;1, thought to mediate root-to-shoot translocation of sulfate/selenate into xylem parenchyma cells was somewhat more expressed in roots of *S. pinnata* than *S. elata*. In shoots, where SULTR2;1 may be involved in vascular unloading or loading (Kataoka et al., 2004), the expression was 5-fold higher in *S. pinnata* than *S. elata* in the absence of Se and only marginally higher in the presence of Se (Fig. 2.4). SULTR3;5, thought to co-facilitate transport with SULTR2;1 (Kataoka et al., 2004), was more expressed in roots of *S. pinnata* than *S. elata,* particularly in the presence of Se (~6 fold); in the shoot it was also somewhat more expressed in the hyperaccumulator (~2 fold, Fig. 2.4). For low-affinity transporter SULTR2;2, the expression level for either species in roots was at most ~100 RPKM, and the difference in expression between *S. pinnata* and *S. elata* was large: ~11- and 17-fold

higher for *S. pinnata* under –Se and +Se conditions, respectively. In shoots the ratio of *S. pinnata* to *S. elata* for *Sultr2;2* was ~2-fold, regardless of Se treatment. This transporter may control the amounts of sulfate/selenate in the phloem (Takahashi et al., 2011).

Sultr3;1, which is likely responsible for sulfate/selenate transport to the plastids (Cao et al., 2013), was expressed at somewhat lower levels in *S. pinnata* than *S. elata* roots, and somewhat higher levels in *S. pinnata* than *S. elata* shoots. In general, its expression was higher in shoots than roots, and its expression was somewhat lower in +Se than –Se (Fig. 2.4). *Sultr3;3* and *Sultr3;4* transcripts were present at 2 – 5 fold and 8 – 11 higher levels, respectively, in *S. pinnata* compared to *S. elata*, both in roots and shoots. The functions of these transporters are not well known; *Sultr3;3* was generally more expressed in shoots than roots, while *Sultr3;4* was more expressed in the roots than shoots of *S. pinnata* (Fig. 2.4).

Sultr4;1 and *Sultr4;2*, which are likely involved in vacuolar efflux (Takahashi et al., 2011), were both more expressed in roots than shoots, and *Sultr4;1* was more expressed than *Sultr4;2* (Fig. 2.4). The root *Sultr4;1* transcript levels were somewhat higher in *S. pinnata* than *S. elata* in –Se conditions, but lower in +Se conditions, because in the roots of *S. elata* but not *S. pinnata*, *Sultr4;1* expression was elevated under +Se conditions. In shoots, *Sultr4;1* levels were somewhat lower in *S. pinnata* than *S. elata*, regardless of Se treatment (Fig. 2.4). Lastly, the root and shoot transcript levels of *Sultr4;2* were over 10-fold higher in *S. pinnata* than *S. elata* without Se, while in the presence of Se they were only marginally higher (~2-fold). This was because there was a ~10-fold positive response to Se treatment for *Sultr4;2* in roots and shoots of *S. elata*, but not *S. pinnata* (Fig. 2.4).

Transcript analysis of genes involved in sulfate/selenate assimilation

As previous studies have shown that hyperaccumulators accumulate a higher fraction of organic Se than non-accumulators, as well as contain methylated Se forms not found in non-accumulators, we reasoned that they may have different expression levels of genes involved in S/Se assimilation. The flow diagram in figure 2.5 summarizes the RPKM levels of sulfate assimilation genes for comparison of species in different organs and Se treatments. In cases where different isozymes catalyze the same reaction, all corresponding genes are shown; often the expression levels within one species were quite different for these genes. Also, different isozyme genes often show expression differences in opposite directions between *S. pinnata* and *S. elata* (Fig. 2.5).

ATP sulfurylase (APS) and APS reductase (APR) have both been reported to be rate-limiting enzymes for S/Se assimilation (Bick & Leustek, 1998; Pilon-Smits et al., 1999). ATP sulfurylase 2 (*Aps2*), involved in the first step of S assimilation, had extremely high expression (>20,000 RPKM) in *S. pinnata* roots, >120-fold higher compared to *S. elata* roots, both for –Se and +Se treatments. In shoots, *Aps2* expression was 2-4 fold higher in *S. pinnata* than *S. elata*, dependent on Se presence. For –Se and +Se treatments, *Aps3* and *Aps4* transcript levels were 1.5 – 2 fold higher in *S. pinnata* than *S. elata* in roots. In shoots, *Aps3* expression was ~3-fold higher in *S. pinnata* than *S. elata*, but *Aps4* had similar, low expression in both species. In contrast to the other *Aps* genes, *Aps1* showed higher expression in *S. elata* compared to *S. pinnata* in roots (~5 fold) and shoots (~3-4 fold) for both –Se and +Se conditions.

Apr1, encoding APS reductase in the second step of S assimilation, was expressed in *S. elata* roots at ~1.5-2 fold higher levels compared to *S. pinnata* roots. In shoots, *Apr1* expression levels were similar in *S. pinnata* and *S. elata* regardless of Se treatment. Interestingly, *Apr3* was expressed at ~100 fold greater level in *S. pinnata* than *S. elata*, both in roots and shoots and for

both Se treatments. No *Apr2* homologue was detected in either species. All isoforms are chloroplastic in *A. thaliana* (TAIR).

In the cytosol, APS may also be phosphorylated to PAPS by APS kinase (APK), which is a starting point for the synthesis of a variety of sulfated metabolites including glucosinolates as well as PAP, a signal molecule that upregulates abiotic stress resistance genes (Bohrer et al., 2015). The expression of APK1 was 2-3 fold higher in *S. pinnata* than *S. elata* in both roots and shoots.

Sulfite reductase (*Sir*), involved in sulfite to sulfide reduction and perhaps also selenite to selenide reduction, was constitutively expressed at high levels across species, organs, and treatments (Fig. 2.5). Among genes encoding serine acetyltransferases (*Serat*), which provide O-acetylserine (OAS) to be combined with sulfide for Cys production (Kawashima et al., 2005), *Serat1;1* showed greater gene expression in *S. elata* compared to *S. pinnata* in both +Se and –Se treatments. However, *Serat3;1* showed much higher expression in *S. pinnata* than *S. elata*, with ~10 fold and 5 fold in roots and shoots, respectively. *Oas-tl A1 and Oas-tl A2*, which encode OAS thiol-lyases, were expressed at higher levels in *S. pinnata* than *S. elata* for both organs and treatments (Fig. 2.5). Cysteine synthase genes *Cs D1* and *Cs D2*, which mediate the same step as *Oas-tl*, showed comparable expression levels for +Se and –Se treatments but opposite expression between species. *S. elata* had 20-30 fold higher expression of *Cs D1* compared with *S. pinnata* in both organs, whereas *S. pinnata* had ~10 fold higher expression of *Cs D2* than *S. elata* in roots and ~4 fold higher in shoots. Cystathionine gamma synthase (*Cgs*), a key enzyme in the conversion of Cys to Met, showed similar high levels of gene expression across species, organs, and treatments; with the exception of *S. elata* and *S. pinnata* shoots grown with Se, where *S. elata* had ~5 fold greater *Cgs* expression than *S. pinnata* (Fig. 2.5). Cystathionine beta lyase

(*Cbl*) showed much higher gene expression (up to ~100 fold) in *S. pinnata* relative to *S. elata*, for both organs and Se treatments. Methionine synthase (*Ms2*), was expressed in *S. elata* roots and shoots at extremely high levels (23,000 RPKM), 5-10 fold greater than in *S. pinnata* roots and shoots. Although *Ms2* showed lower expression for both species with Se treatment, gene expression was relatively consistent between roots and shoots within each species (Fig 2.5).

Transcript analysis of genes involved in glutathione metabolism and other antioxidant systems

A key enzyme for biosynthesis of the important antioxidant glutathione (GSH) from Cys and Glu is gamma-glutamylcysteine ligase (also called synthetase), which is encoded by *Gsh1*. In both roots and shoots of *S. pinnata*, *Gsh1* had extremely high expression (~10,000 RPKM), regardless of Se treatment; this was ~4 fold higher than *Gsh1* transcript levels in *S. elata* (Fig. 2.6a, b). *Gsh2*, encoding GSH synthetase, the second enzyme for GSH synthesis, was only marginally more expressed in *S. pinnata*, and only in roots (Fig. 2.6a, b).

Among the GSH reductases (GR), *Gr1* was more expressed in *S. elata* while *Gr2* was more expressed in *S. pinnata*, regardless of organ or Se treatment (Fig. 2.6a, b). Among the glutathione S-transferase family, which conjugate GSH to various substrates (Marrs, 1996), *Gstf7* was 30-40 fold more expressed in the roots of *S. pinnata* than *S. elata* (Fig. 2.6a). Among the peroxidases, the GSH peroxidase genes *Gpx2*, *Gpx6* and *Gpx7* were more expressed in *S. pinnata* (up to 5 fold), while *Gpx5* was more expressed in *S. elata*; in general, *Gpx* expression was similar in root and shoot and not much affected by presence of Se (Fig. 2.6a, b). Ascorbate peroxidase (*Apx*) 1 expression was extremely high in *S. pinnata* (~5000 RPKM), up to ~5000 fold higher than in *S. elata* (Fig. 2.6a, b). Similarly, thioredoxin peroxidase (*Tpx*) was ~100-fold more expressed in *S. pinnata*, and thioredoxin reductase (*Trx*) 2 was ~10 fold more expressed in *S. pinnata* (Fig. 2.6a, b).

Transcript analysis of genes involved in JA, SA and ethylene signaling

The defense-related hormones JA, SA and ethylene were hypothesized in an earlier macroarray study to be involved in Se tolerance and accumulation in *S. pinnata* (Freeman et al., 2010), and were therefore also explored. Figure 2.7a and b show the expression of genes involved in JA synthesis. Genes that stood out because they were more expressed (at least 5 fold) in *S. pinnata* than *S. elata,* regardless of organ or Se presence include *Lox2* and *Lox6* (lipoxygenase, the first enzyme in JA synthesis), *Acx5* and *Aim1* (both acyl-CoA oxidases), *Opcl1* (At1g20480) and *Opcl3* (At1g20500). Genes more highly expressed (up to 6-fold) in *S. elata* than *S. pinnata* include *Acx1* (acyl-CoA oxidase) and *Opcl6*.

Figure 2.7c and d show the expression of genes involved in SA and ethylene biosynthesis as well as in JA, SA and ethylene signaling and defense responses. The overall trend was that these genes had constitutive higher expression in the Se hyperaccumulator, *S. pinnata*. Two genes with higher expression in *S. pinnata* than *S. elata* were *Pal1* and *Pal2*, encoding phenylalanine ammonia lyases, responsible for SA production via the shikimate pathway (Chen et al., 2009). *Pal* expression was lower for +Se than –Se treatment in roots of *S. elata* but not *S. pinnata*; in shoots Se had no marked effects on *Pal* expression. Isochorismate synthase (*Ics2*), also involved in SA biosynthesis, was more expressed in *S. pinnata* than *S. elata* for both organs and Se treatments. Genes encoding ethylene biosynthesis enzymes (SAM synthetase, ACC synthase, ACC oxidase) were expressed at similar levels in both species (not shown). However, the gene encoding EIN3, which responds to ethylene and functions as a transcription factor for downstream processes (Chao et al., 1997), was 10-20 fold more expressed in the Se hyperaccumulator.

Jar1, a response gene involved in JA activation and signaling (Laurie-Berry et al., 2006), was expressed at 10-20 fold higher levels in *S. pinnata* than *S. elata,* both in roots and shoots regardless of Se presence. Genes involved in SA signal transduction that were more expressed in *S. pinnata* than *S. elata* include the DNA-binding *Tga3*, *9* and *10,* which activate the expression of pathogenesis related (PR) proteins (Johnson et al., 2003). Indeed, *Pr4* was 4 – 20 times more expressed in the Se hyperaccumulator (Fig. 2.7c, d). There was only a marginal difference between the species in *Npr* expression; *Npr* encodes a receptor for SA. Transcription factor *Wrky70*, which is thought to activate SA-induced genes (Li et al., 2004), was more expressed in *S. pinnata*. The plant defensin factors *Pdf1.1* and (to a lesser extent) *Pdf1.2c* were more expressed in *S. pinnata* than *S. elata* (Fig. 2.7c, d). Since there appears to be a trend for plant defense mechanisms to be constitutively and highly expressed in the Se hyperaccumulator, we looked for a potential upstream initiating factor. In this context there were three notable genes that were more expressed in *S. pinnata* than *S. elata*, particularly in roots and in the presence of Se. The first one is *Mlo12* (mildew resistance locus), a plasma membrane protein involved in fungal resistance (Buschges et al., 1997), which was barely detectable in *S. elata* but present at up to 70-fold higher levels in *S. pinnata* (Fig. 2.7c). The other two (At5g36930 and At5g22690) are nucleotide-binding site–leucine-rich repeat encoding genes involved in pathogen sensing, although their exact functions are unknown.

DISCUSSION

The main question addressed in this study was: which genes play a direct role in the Se hyperaccumulator phenotype of *Stanleya pinnata*, and which other genes are involved in their regulation? Based on transcriptome comparison of *S. pinnata* with *S. elata*, the Se hyperaccumulator appears to use multiple mechanisms to accumulate and tolerate Se. These

include increased uptake and translocation of selenate through sulfate/selenate transporters, increased assimilation of selenate into organic forms, and increased antioxidant capacity. These processes may be regulated via the hormones JA, ethylene and SA in response to elevated levels of certain receptors and transcription factors. Defense pathways also appear to be upregulated in the hyperaccumulator, likely triggered by these same hormones.

We found that shoot biomass was not significantly different between *S. pinnata* and *S. elata* treated with 0 or 20 μM Se, indicating that the selenate concentration was not high enough to cause toxicity. The finding that Se levels were higher in shoots of *S. pinnata* than *S. elata* indicates that *S. pinnata* has a greater rate of uptake and/or root-to-shoot translocation. S levels in shoots were also higher in *S. pinnata* compared to *S. elata* when treated with Se. These results may be explained by elevated transcript levels of several sulfate/selenate transporters, as discussed below. *S. pinnata* also had higher Se levels than *S. elata* when not treated with external Se, probably because *S. pinnata* seeds contained higher levels of pre-existing Se.

Although toxicity was not observed in the shoots, Se significantly affected the transcriptome in both plant species. Se affected expression of more genes in the shoots of *S. pinnata* but more genes in the roots of *S. elata*, and only a small proportion of genes was similarly affected by Se in both species (Fig. 2.1). This indicates that the Se hyperaccumulator and non-accumulator respond differently to Se on an organ-specific level, and that the greater distribution of Se into the shoots of *S. pinnata* may trigger this response. A large fraction of genes were found to be differentially expressed between species, although they are closely related; *S. elata* is in the sister group to the *S. pinnata* species complex (Cappa et al., 2014). Differential gene expression between related species is not uncommon: a transcriptome study with maize and rice, both in the *Poaceae* family, showed large fractions of genes differentially

expressed between the species, even under the same growth conditions (Prasad et al., 2010; Wang et al., 2014). Interspecies transcriptome studies are inherently complicated because it is not known whether genes are orthologous. However, the overall differences in gene expression patterns that we observed agree well with earlier macroarray findings (Freeman et al., 2010).

When treated with Se, only *S. elata* showed increased expression of *Sultr1;2* and the *Sultr4* vacuolar exporter group, which indicates that the non-accumulator sensed sulfur starvation in the presence of Se. A similar response was reported for another non-accumulator, *A. thaliana* (Van Hoewyk et al., 2008). In comparison, *S. pinnata* roots had overall higher levels of *Sultr1;2* expression regardless of Se supply. It is possible that *S. pinnata* permanently senses S starvation. However, *Sultr1;1* which commonly responds to S starvation in other species (Rouached et al., 2008), was not constitutively upregulated. In any case, the elevated *Sultr1;2* expression levels may explain the hyperaccumulator's ability to uptake adequate S despite increased Se competition. Our finding of constitutively high expression of *Sultr1;2* in *S. pinnata* supports the general hypothesis that enhanced SULTR1;2 transport is the first and major step in the hyperaccumulation of Se. In *A. thaliana*, SULTR1;2 is also the main portal for selenate into the plant, and appears to have a higher Se/S specificity compared to the other root plasma membrane transporter, SULTR1;1, since null mutants were selenate-resistant and had a higher sulfate to selenate ratio in roots (El Kassis et al., 2007). The expression of *Sultr2;1*, *Sultr2;2* and *Sultr3;5*, which are thought to mediate the flux of sulfate through phloem and xylem parenchyma cells (Kataoka et al., 2004), was also higher in *S. pinnata* than *S. elata*, for the same organ and treatment. This higher expression indicates that *S. pinnata* has a greater rate of S/Se root-to-shoot translocation and source-to-sink remobilization than *S. elata*, which was indeed found in an earlier study (Cappa et al., 2014). Other *Sultr* genes more highly expressed in the

hyperaccumulator were *Sultr3;4* and *Sultr3;5*. *Lotus japonicus* SST1, which is a homolog of Arabidopsis SULTR3;5, is expressed in symbiosome membranes in root nodules and is required for nodule development (Krusell et al., 2005). Therefore, enhanced root expression of *S. pinnata Sultr3;5* (perhaps also *Sultr3;4*) may have implications for plant-microbe interactions; *S. pinnata* was shown recently to harbor a variety of highly Se-resistant bacterial endophytes (Sura-de Jong et al., 2015).

Based on transcript abundance of genes involved in S assimilation, *S. pinnata* appears to have an overall higher flux from inorganic to organic Se compared to *S. elata*. Higher levels of S assimilation would agree with an earlier finding that *S. pinnata* accumulated no detectable inorganic Se, while *S. elata* contained 20-25% inorganic Se (Cappa et al., 2015). The two plant species also differed in their apparent predominant isoforms APS, APR, SERAT and cysteine synthase, which may have different kinetic and substrate affinity properties, as well as cellular localization. In *A. thaliana*, APS2 is dual-localized to the cytosol and plastids, and constitutes the only cytosolic APS activity (Bohrer et al., 2015). The *S. pinnata* APS2 likely has similar dual localization. In earlier studies, APS was shown to be a rate-limiting enzyme for selenate assimilation to organic forms (Pilon-Smits et al., 1999). The extremely high expression of *Aps2* in the roots of *S. pinnata*, may suggest that selenate is assimilated in part in the roots, and that part of the Se may be transported in organic form in the xylem. Indeed, substantial quantities of organic Se, present as seleno-amino acids, have been detected in the roots of *S. pinnata* (Lindblom et al., 2013) as well as in guttation fluid (Freeman et al., 2006). It is not clear how these compounds are transported; we did not find high expression levels in either species for genes known in *A. thaliana* to encode amino acid transporters. *Apr3* expression levels were 100-fold higher in *S. pinnata*, but this may not have a physiological effect, since *Apr1* expression was

even two-fold higher than those of *Apr3* in *S. pinnata*, and two fold lower than the *Apr1* levels in *S. elata* (Fig. 2.5). Both *Stanleya* species had similarly high expression levels of *Sir*, which converts sulfite to sulfide. Selenite may also be reduced by GSH, either with or without the involvement of GR (Hsieh & Ganther, 1975; Sors et al., 2005). In the context of a GSH-mediated reduction, it is interesting that genes involved in GSH synthesis (*gsh1*) and reduction (*gr2*) were both much more highly expressed in *S. pinnata* than *S. elata* (Fig. 2.6). Serine acetyltransferases are known to be regulated by feedback inhibition from Cys, whose synthesis depends on combined SERAT and OASTL activity (Kawashima et al., 2005). *S. pinnata* roots had higher expression levels of *Serat3;1* than *S. elata* roots, which was reported to be insensitive to Cys levels (Kawashima et al., 2005), while *S. elata* had higher expression of *Serat1;1*, which was reported to be sensitive to Cys (Krueger et al., 2009). The DE of *Serat* between species suggest that *S. pinnata* bypasses feedback inhibition of (Se)Cys synthesis due to increasing levels of (Se)Cys, whereas *S. elata* SeCys synthesis could be inhibited with increasing Cys levels. It is worth noting that overexpression of a *Thlaspi goesingense* SERAT isoform in *A. thaliana* only produced modest increases in SeCys formation (Sors et al., 2005). Among the two CS isoforms with OAS-TL activity, CS D2 (mitochondrial and cytosolic) was much more highly expressed in *S. pinnata* and the CS D1 (cytosolic) was much more expressed in *S. elata*. The DE of CS between species could affect the rate of selenate uptake in *S. pinnata* versus *S. elata:* cytosolic CS was reported to negatively regulate root SULTR1;2 activity by binding its C-terminal STAS domain (Shibagaki & Grossman, 2010); it is possible that the *Stanleya* isoforms differ in this respect. Also interesting to note is that mitochondrial CS activity (for example, CS D2) was shown to be the most important CS for Cys synthesis in *A. thaliana* (Birke et al., 2012).

Transcript levels of genes mediating the three-step enzymatic conversion of (Se)Cys to (Se)Met also showed different flux between *S. pinnata* and *S. elata*, which may further affect the fate and accumulation of organic Se. Both species showed lower RPKM levels for *Cbl* than for *Cgs* and, especially, *Ms*. Furthermore, *Cgs* was more expressed in *S. elata*, *Cbl* was more expressed in *S. pinnata*, and *Ms2* levels were much higher in *S. elata*. The finding that *Cgs* expression was higher than *Cbl* expression in *S. pinnata* may explain why *S. pinnata* was reported to accumulate around 12% of its Se as selenocystathionine (Freeman et al., 2006). , The difference between *Cgs* and *Cbl* RPKM levels was even higher in *S. elata*, which suggests it may accumulate a larger fraction of its organic Se as selenocystathionine. Cappa et al. (2005) found 75% organic Se in *S. elata*. The related non-hyperaccumulator *Stanleya albescens* was shown to accumulate all of its organic Se (which was 75% of total Se) as selenocystathionine (Freeman et al., 2010). The finding that *S. elata* had higher *Ms2* expression than *S. pinnata* suggests that it more readily converts homoselenocysteine to SeMet. If so, it may have higher rates of non-specific incorporation of SeMet into protein, which could cause toxicity. *S. elata* was found in an earlier study to be much more Se sensitive than *S. pinnata* (El Mehdawi et al., 2012).

SeCys and SeMet may be further metabolized into volatile compounds by methyltransferases (James et al., 1995; Tagmount et al., 2002). One might expect one of these to be highly expressed in *S. pinnata*, since it accumulates 88% of its Se in the form of methyl-SeCys (Shrift & Virupaksha, 1965; Freeman et al., 2006). SeCys methyltransferase (SMT) was shown to be a major enzyme responsible for hyperaccumulation in Se hyperaccumulator *Astragalus bisulcatus* (Neuhierl and Bock, 1996; Sors et al., 2005, 2009). However, no SMT activity was found for the *A. thaliana* homologue, HMT (Sors et al., 2009). The expression levels of *Hmt2* and *Hmt3* were fairly low in both *Stanleya* species, and actually lower in *S. pinnata* (~20 RPKM) than

S. elata. However, a gene encoding an O-methyltransferase (At4g35160) was much more highly expressed in *S. pinnata* (~2500 RPKM) than *S. elata* (~15 RPKM). More research is needed to characterize the main methyltransferase(s) in *S. pinnata* responsible for the production of methyl-SeCys.

Although we hypothesized that SLIM1, a transcription factor regulating S assimilation (Kawashima et al., 2011), may be differentially expressed between the *Stanleya* species, we did not observe differences. Transcripts levels for microRNA395, also reported to regulate S assimilation (Kawashima et al., 2009), could not be compared because of the way the samples were processed.

Selenium is reactive and likely causes oxidative stress (Van Hoewyk, 2013). It has been found to induce the expression of genes coding for peroxidases and GSH-related enzymes (Rios et al., 2009; Freeman et al., 2010). Therefore, we hypothesized that free radical scavenging capacity may play a role in Se tolerance in *S. pinnata*. Indeed, Freeman et al. (2010) found that when supplied with Se, lower levels of reactive oxygen species accumulated in *S. pinnata* compared with the non-hyperaccumulator *S. albescens*, and higher transcript levels of antioxidant and redox-related genes were present in *S. pinnata* compared with *S. albescens*. Here, we report that several genes involved in GSH synthesis (*Gsh1*) and conjugation (*Gstf7*), and in free radical scavenging via peroxidase activity (*Gpx6*, *Apx1*, and *Tpx1*) were much more highly expressed in *S. pinnata* than *S. elata*. The peroxidase family category (Mapman) had the highest proportion of genes with greater expression in *S. pinnata* than *S. elata* for almost all treatments analyzed (Marrs, 1996). These results indicate that the Se hyperaccumulator has elevated GSH levels and antioxidant scavenging capacity, which may contribute to its Se tolerance. Higher GSH levels were indeed found in *S. pinnata* than in *S. albescens* by Freeman et

al. (2010). The constitutively elevated levels of GSH and peroxidase expression may "prime" *S. pinnata* for oxidative stress; this may be an advantage, given that it is chronically exposed to high levels of Se in its native soils (Cappa et al., 2014). The hyperaccumulators appear to be similarly "primed" for biotic stress, judged from their elevated expression levels of defense-related genes including PR proteins, PDF, and chitinases. Some of these responses may be triggered by shared upstream signaling pathways.

Three defense-related plant hormones that have been implicated to play a role in Se tolerance are JA, SA and ethylene. Transcriptome analysis by Tamaoki et al. (2008a) and Freeman et al. (2010) found that the expression levels of defense-related genes were constitutively higher in *S. pinnata* compared to *S. albescens*, and were also more induced by Se in Se-resistant than Se-sensitive *A. thaliana* accessions. Furthermore, treating Se-sensitive *A. thaliana* accessions with ethylene and JA restored Se tolerance (Tamaoki et al., 2008a), and application of 10 μM JA to *S. pinnata* increased leaf Se levels (Freeman et al., 2010). Moreover, tissue levels of JA and SA were higher in *S. pinnata* than *S. albescens* (Freeman et al., 2010). Our analysis of the expression of JA biosynthesis genes may explain the previously found elevated JA levels, since several *Lox* genes were more highly expressed in *S. pinnata* than *S. elata*, especially *Lox2* in *S. pinnata* roots. *Lox2* was reported by Tamaoki et al. (2008a) to be induced by Se in Se-resistant *A. thaliana* accessions. *Lox6* was also more highly expressed in both organs of *S. pinnata* compared to *S. elata*; interestingly, *Lox6* is currently the only lipoxygenase thought to positively regulate JA levels in roots as well as shoots (Grebner et al., 2013). A possible explanation for the higher expression levels of GSH biosynthesis genes in the Se tolerant species is that JA induces the expression of these genes. In *A. thaliana* (Xiang & Oliver, 1998) it was shown that JA, but not SA or ROS, was primarily responsible for increasing

the transcript levels of *Gsh1*, *Gsh2*, and *Gr1*. *Gsh1* responded with the greatest increase in transcript levels in dose-dependent JA tests, and we found that *Gsh1* had the highest expression in *S. pinnata* compared to *S. elata* among the GSH genes analyzed. JA, as well as ethylene, has also been reported to induce S assimilation (Tamaoki et al., 2008a), and thus may be responsible for the observed elevated levels of sulfate transporter and S assimilatory genes.

The greater expression of SA biosynthesis genes such as *Ics2* and *Pal*, as well as the SA-responsive genes such as *Wrky*, *Tga*, *Eps* and *Pr* in the Se hyperaccumulator indicates that these genes affect Se assimilation and, therefore, tolerance. The extremely high expression levels of *Pal* in *S. pinnata* may indicate that more SA is produced through the phenylpropanoid pathway. Tamaoki et al. (2008a) found increased SA levels in *A. thaliana* following Se treatment, although SA was thought to enhance Se sensitivity. Our findings of increased expression of *Pr4* in the Se hyperaccumulator is consistent with results from Freeman et al. (2010), where *Pr4* expression was greater in *S. pinnata* than *S. albescens*; and Tamaoki et al. (2008a), where *Pr4* was more induced in Se-tolerant *A. thaliana* accessions by Se treatment than in non-tolerant accessions. A potential upstream signaling gene for the SA-mediated responses may be *Mlo12*, which was ~65-fold more highly expressed in *S. pinnata* than *S. elata*, and had an RPKM level of >7000 in *S. pinnata*. MLO interacts with calmodulin (Kim et al., 2002 the expression of which was found by Tamaoki et al. (2008a) to be induced by Se in *A. thaliana*, along with many other genes encoding similar signaling proteins. Incidentally, calmodulin 3 was also 10-fold more highly expressed in *S. pinnata* than *S. elata* (~2500 vs ~250 RPKM).

Ethylene levels have been reported to induce PAL activity (Chalutz 1973), and here we found higher expression in the Se hyperaccumulator of ethylene-responsive gene *Ein3* and as well as the gene encoding MAPK6, a key protein in ethylene. Ethylene and JA may

cooperatively induce the expression of PDF (Penninckx et al., 1998; Leon-Reyes et al., 2010), which was found to be more expressed in *S. pinnata* compared to *S. albescens* (Freeman et al., 2010). In *A. thaliana* (Tamaoki et al., 2008b), PDF was more induced in tolerant accessions by Se treatment; furthermore, plants that overexpressed *Arabidopsis halleri* PDF1.1 showed a significant increase in tolerance to Se compared to wild-type. Here, we also report higher expression levels of *Pdf 1.1* and *Pdf 1.2C* in the Se hyperaccumulator, which could indicate that by the collective increase in ethylene and JA biosynthesis gene expression, SA-mediated expression and the associated increase in Se sensitivity may be inhibited, and plants may increase in tolerance to Se through the induction of PDF.

In conclusion, the analysis of the transcriptomes of *S. pinnata*, a Se hyperaccumulator, with *S. elata*, a closely related non-accumulator, yielded some new insights into Se hyperaccumulation and tolerance. At the level of large enzyme families as well as of individual analyses of GSH, ascorbate, and thioredoxin related genes, those genes involved in free-radical scavenging were some of the most abundant and differentially expressed between species, and may be involved in enzymatic or non-enzymatic (through their product, GSH) reduction of Se. In the *Sultr* family, the high expression levels of *Sultr1;2* in *S. pinnata* may be primarily responsible for Se uptake at the root level, and the elevated expression of several group 2, 3 and 4 *Sultr* genes in *S. pinnata* may contribute to increased root-to-shoot and source-to-sink transport of Se. The first and rate-limiting enzyme in S/Se assimilation, *Aps2*, was extremely highly expressed in *S. pinnata* but not *S. elata*, and may be localized in the cytosol in addition to the chloroplast (Bohrer et al., 2015). Other genes involved in S assimilation, particularly *Apr3*, were also expressed at higher levels in the hyperaccumulator, and may contribute to the accumulation of organic selenocompounds. The higher expression levels of several JA biosynthesis genes in *S.*

pinnata compared with *S. elata* implies greater amounts of certain JA precursors produced in the hyperaccumulator; JA has been previously shown to induce S assimilatory and GSH biosynthesis genes, and therefore may enhance Se tolerance. The potential Se sensing and downstream signaling mechanisms leading to the induction of these defense hormone genes provide a working model (Fig. 2.8), and will be an interesting area for further study. We propose several genes as possible candidates, MLO12 and two TIR-NB-LRR class genes (AT5G22690, AT5G36930), as they are known to trigger defense responses and were much more highly expressed in *S. pinnata* than *S. elata*. If a "key gene" could be identified that triggers the cascade of events that leads to the Se hyperaccumulation syndrome, such a gene would be very promising for the genetic engineering of plants with superior capacity for Se accumulation and tolerance, which would have applications in phytoremediation and biofortification.

FIGURES

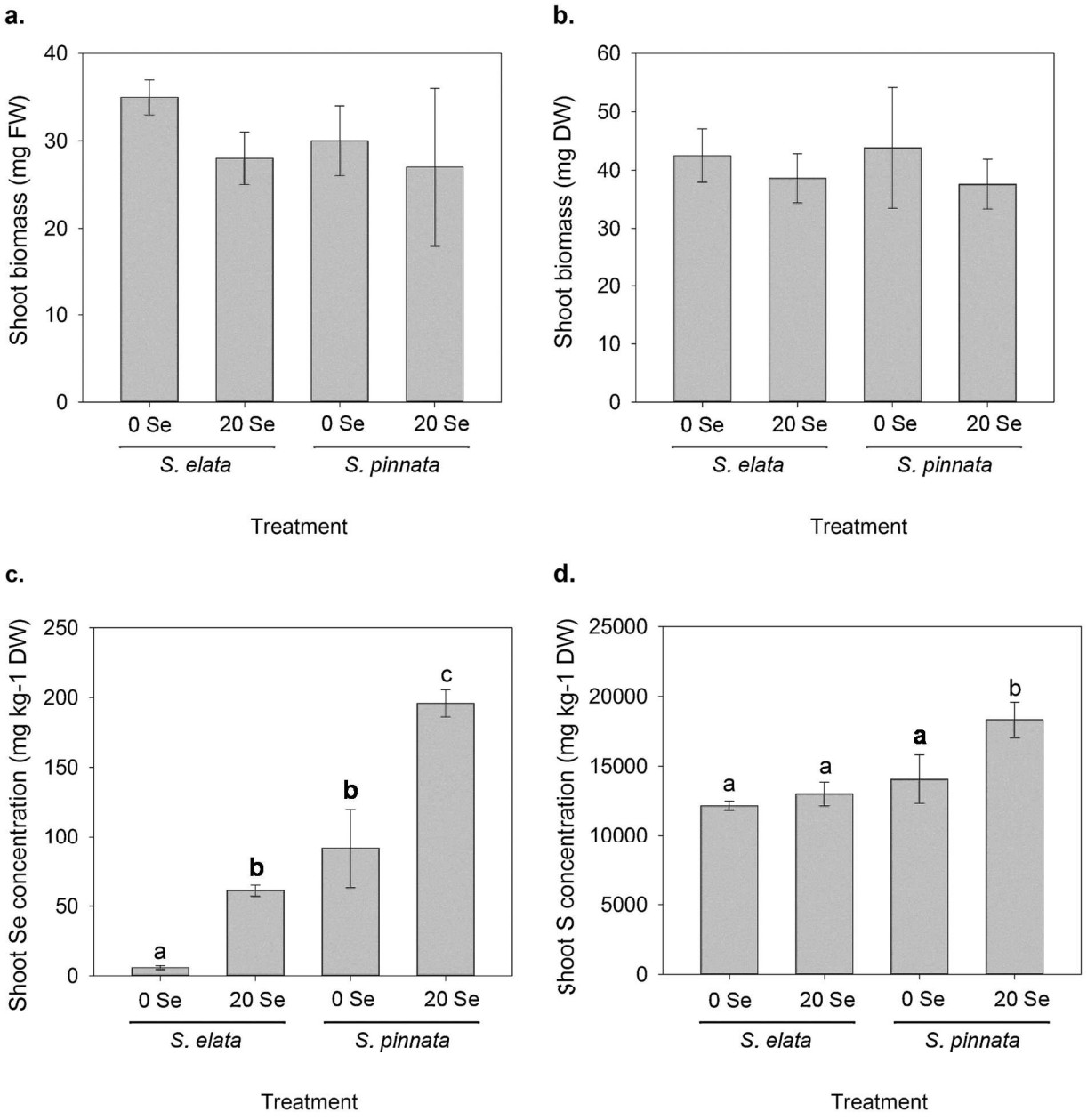

Figure 2.1 Biomass production and Se and S accumulation of Se hyperaccumulator S. pinnata and nonaccumulator S. elata grown on agar medium with 0 or 20 µM sodium selenate. (a) Shoot fresh weight of plants used for transcriptome analysis. (b) Dry weight of plants grown for elemental analysis. (c) Shoot Se concentration. (d) Shoot S concentration. Shown values

represent the mean of five replicates + SEM. Letters above bars indicate significant differences between treatments using ANOVA with post-hoc pairwise comparison (Student's t-test).

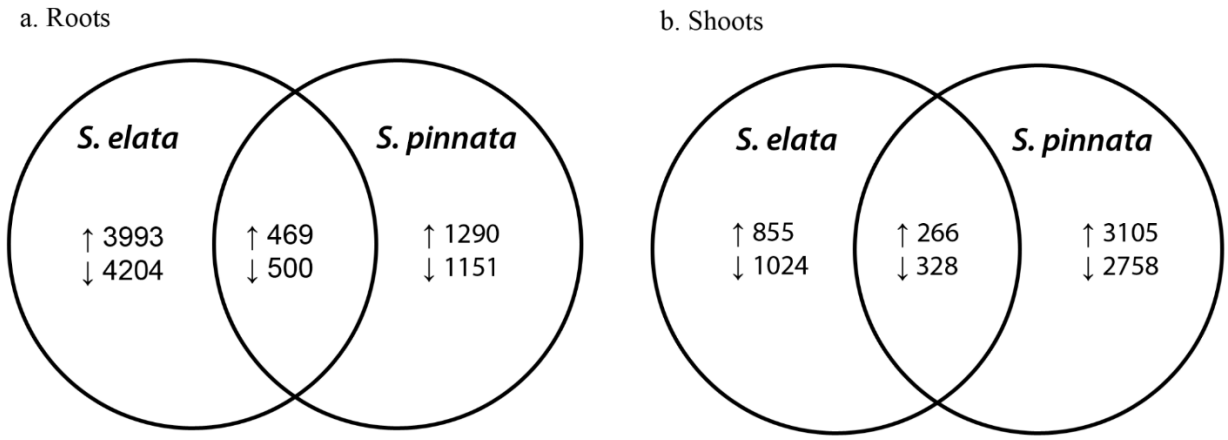

Figure 2.2 Venn diagrams showing the number of genes in *S. pinnata* or *S. elata* that are significantly increased (↑) or decreased (↓) in expression by 20 μM Se in roots **(a)** and shoots **(b)**. Overlapping areas represent genes with shared regulation patterns between species.

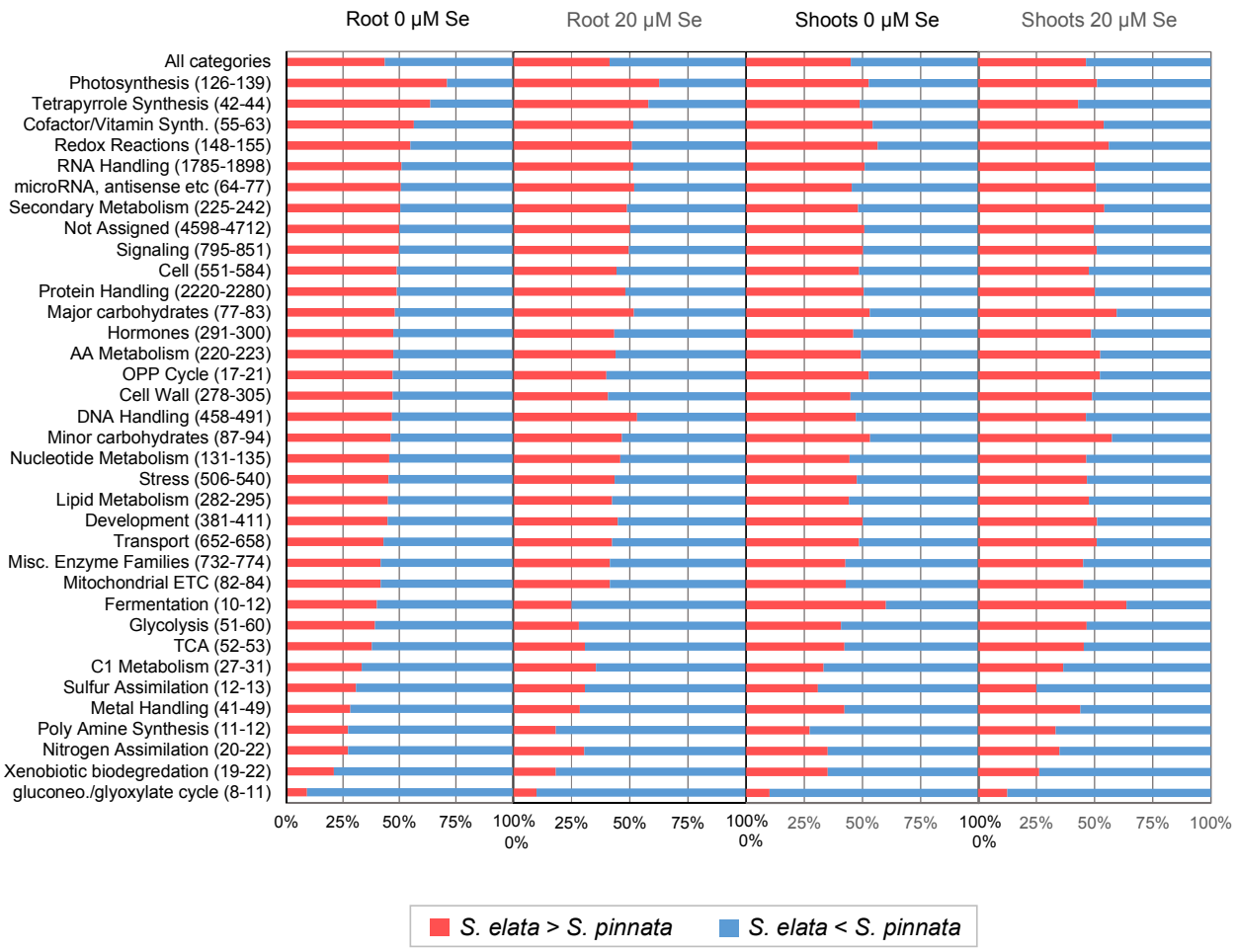

Figure 2.3 Differential expression patterns between *S. pinnata* and *S. elata* for major functional categories, as sorted by Mapman. The bracketed numbers to the right of the category names depict the range in the number of genes identified for that category for all 4 treatments: roots or shoots, 0 or 20 µM Se. For each treatment, red bars signify the percentage of genes with higher expression in *S. elata* than *S. pinnata* for a category, while blue bars signify the percentage of genes with higher expression in *S. pinnata* than *S. elata* ($q < 0.005$).

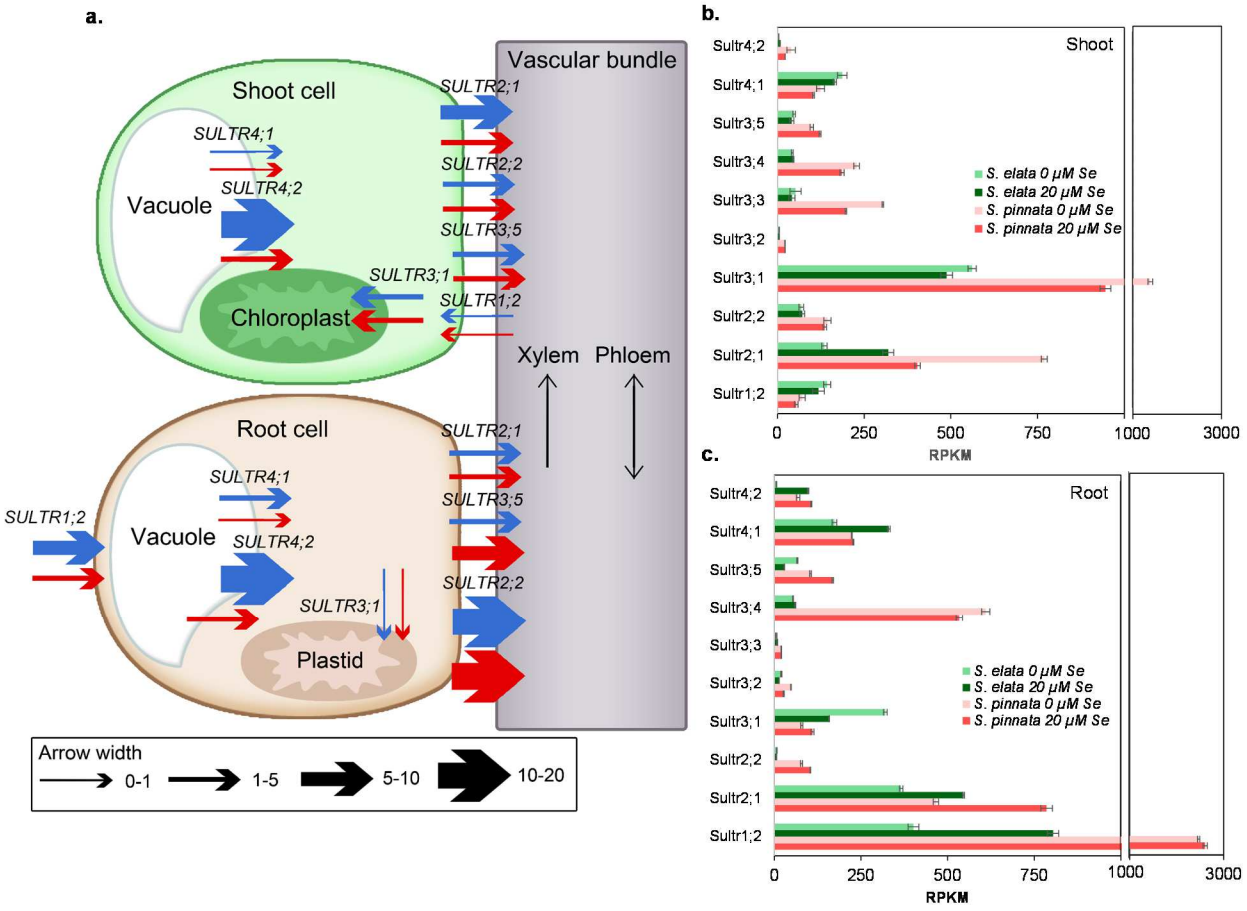

Figure 2.4 Expression levels of sulfate transporter (*Sultr*) genes in shoots and roots of *S. pinnata* and *S. elata* grown on 0 or 20 µM sodium selenate. **(a)** Schematic representation of the differences in expression levels between *S. pinnata* and *S. elata* for SULTRs with known transport functions in different cellular compartments and tissues. Width of arrows represents the fold difference between species (ratio of *S. pinnata* RPKM/*S. elata* RPKM) for a given treatment and organ. Blue arrows are for plants grown without Se and red arrows for plants grown with 20 µM Se. **(b)** Shoot and **(c)** root expression levels of *Sultr* genes (n=3, mean RPKM $\pm$ SD). Significant differences between treatments are presented in the text.

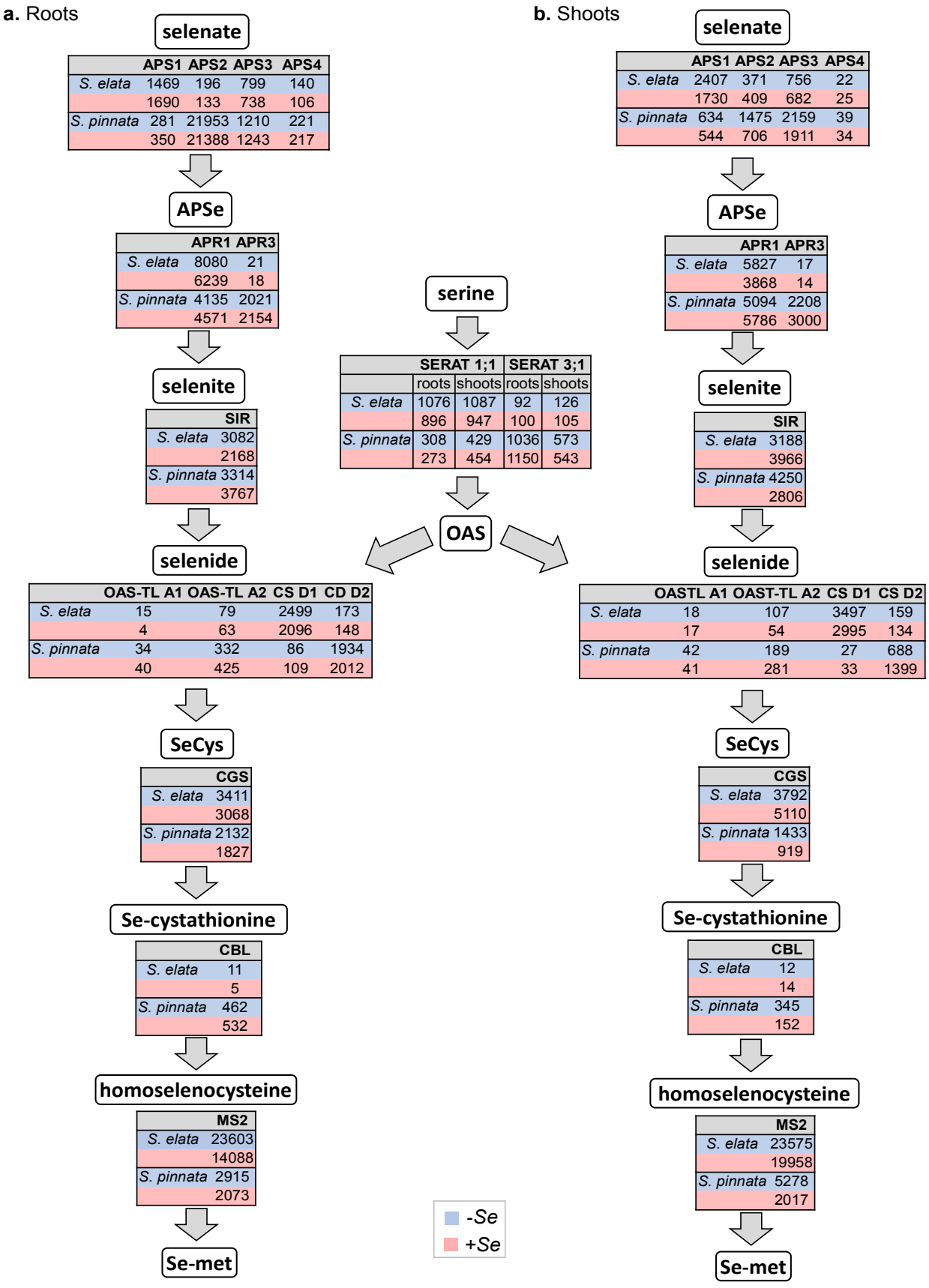
a. Roots
selenate
APS1 APS2 APS3 APS4
S. elata 1469 196 799 140
1690 133 738 106
S. pinnata 281 21953 1210 221
350 21388 1243 217
APSe
APR1 APR3
S. elata 8080 21
6239 18
S. pinnata 4135 2021
4571 2154
selenite
SIR
S. elata 3082
2168
S. pinnata 3314
3767
selenide
OAS-TL A1 OAS-TL A2 CS D1 CD D2
S. elata 15 79 2499 173
4 63 2096 148
S. pinnata 34 332 86 1934
40 425 109 2012
SeCys
CGS
S. elata 3411
3068
S. pinnata 2132
1827
Se-cystathionine
CBL
S. elata 11
5
S. pinnata 462
532
homoselenocysteine
MS2
S. elata 23603
14088
S. pinnata 2915
2073
Se-met
serine
SERAT 1;1 SERAT 3;1
roots shoots roots shoots
S. elata 1076 1087 92 126
896 947 100 105
S. pinnata 308 429 1036 573
273 454 1150 543
OAS
b. Shoots
selenate
APS1 APS2 APS3 APS4
S. elata 2407 371 756 22
1730 409 682 25
S. pinnata 634 1475 2159 39
544 706 1911 34
APSe
APR1 APR3
S. elata 5827 17
3868 14
S. pinnata 5094 2208
5786 3000
selenite
SIR
S. elata 3188
3966
S. pinnata 4250
2806
selenide
OASTL A1 OAST-TL A2 CS D1 CS D2
S. elata 18 107 3497 159
17 54 2995 134
S. pinnata 42 189 27 688
41 281 33 1399
SeCys
CGS
S. elata 3792
5110
S. pinnata 1433
919
Se-cystathionine
CBL
S. elata 12
14
S. pinnata 345
152
homoselenocysteine
MS2
S. elata 23575
19958
S. pinnata 5278
2017
Se-met
-Se
+Se

Figure 2.5 Expression levels of genes involved in Se/S assimilation in roots **(a)** and shoots **(b)** of *S. pinnata* and *S. elata* grown on 0 or 20 μM sodium selenate. Values displayed are the mean normalized RPKMs of 3 bioreplicates per treatment. Enzymes whose genes were significantly DE in *S. pinnata* and *S. elata* include APS (ATP sulfurylase), APR (APS reductase), SIR (sulfite reductase), SERAT (serine acetyl transferase), OAS-TL/CS (O-acetylserine thiol lyase / cysteine synthase), CGS (cystathionine gamma synthase), CBL (cystathionine beta lyase), MS (methionine synthase). Blue shaded cells represent plants treated with no Se, and red cells represent plants treated with 20 μM Se. The pathway metabolites (displayed in white cells) are APSe (adenosine-5-phosphoselenate), OAS (O-acetylserine), SeCys (seleno-cysteine), SeMet (selenomethionine).

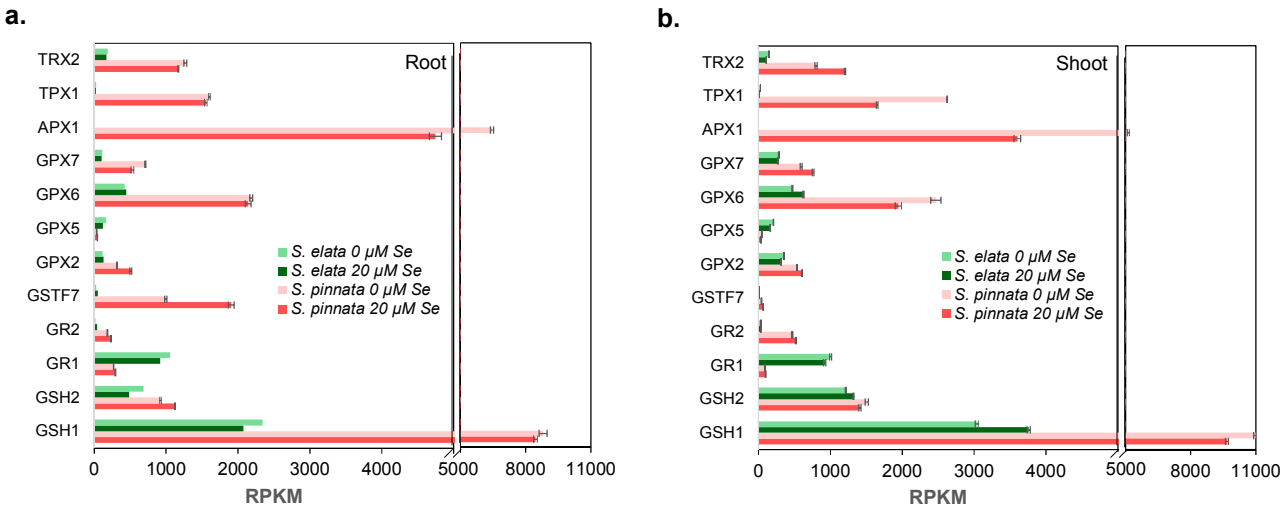

Figure 2.6 Expression levels of genes involved in antioxidant functions in roots **(a)** and shoots **(b)** of *S. pinnata* and *S. elata* grown on 0 or 20 µM sodium selenate. Shown values shown represent the mean RPKM (n=3 bioreplicates) ± SD. GSH1: gamma-glutamylcysteine synthetase; GSH2: glutathione synthetase; GR: glutathione reductase; GSTF: glutathione-S-transferase; GPX: glutathione peroxidase; APX: ascorbate peroxidase; TPX: thioredoxin peroxidase; TRX: thioredoxin reductase.

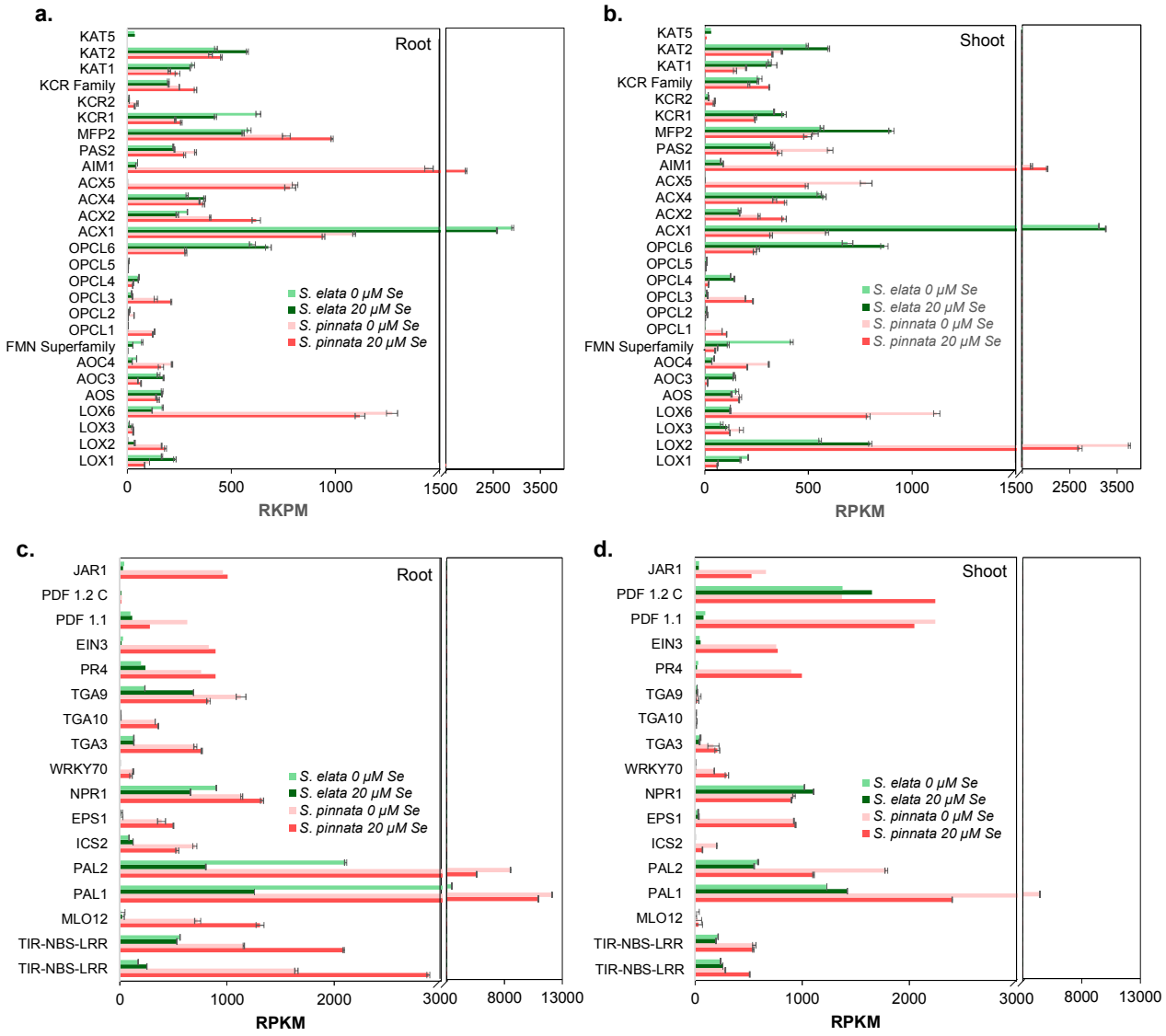

Figure 2.7 Expression levels of genes involved in synthesis and signaling of the defense-related plant hormones JA, ethylene and SA that were DE in roots **(a, c)** and shoots **(b, d)** of *S. pinnata* and *S. elata* grown on 0 or 20 µM sodium selenate. Shown values represent the mean RPKM (n=3 bioreplicates) ± SD. **(a, b)** Genes involved in JA biosynthesis. LOX: lipoxygenase; AOS: allene oxide synthase; AOC: allene oxide cyclase; ACX: acyl-CoA oxidase; AIM: acyl-CoA oxidase like protein; KCR: hydroxyacyl-CoA dehydrogenase; KAT: OPC4-3ketoacyl-CoA thiolase. **(c, d)** Genes involved in ethylene and SA biosynthesis, in JA/SA/ethylene signaling,

and defense. MLO: mildew resistance locus O; PAL: phenylalanine ammonia lyase; ICS: isochorismate synthase; EPS: enhanced *Pseudomonas* susceptibility; NPR: non-expressed pathogen resistance genes; WRKY: transcription factor; TGA: TGACG-binding protein; PR: pathogen resistant; EIN: ethylene insensitive; PDF: pathogen defensin factor; JAR: jasmonate responsive.

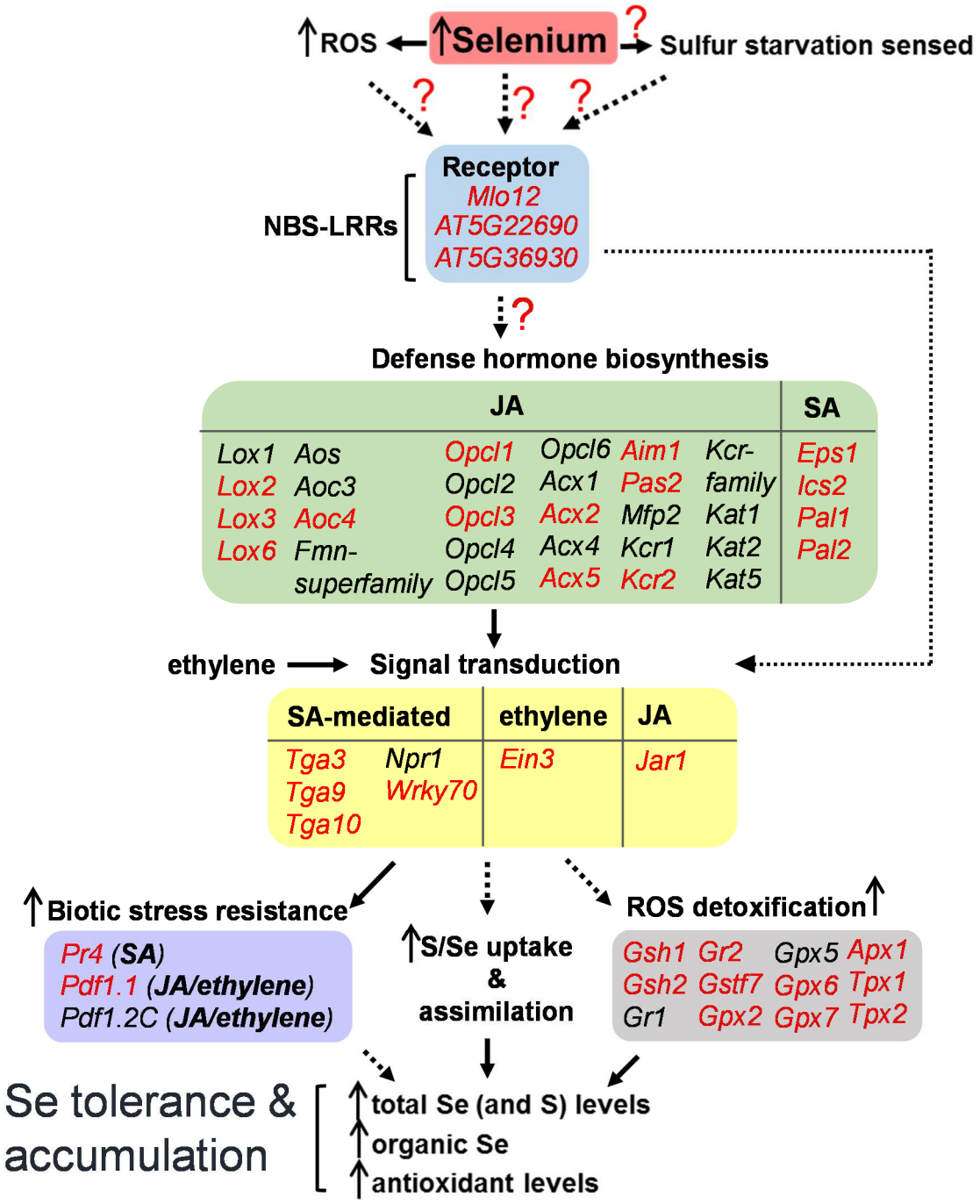

Figure 2.8 Schematic model of genes proposed to mediate Se sensing and response in Se hyperaccumulator *Stanleya pinnata*. Increased selenium supply may trigger the defense signaling pathways, leading to increased hormone synthesis and an increase in overall ROS scavenging ability and S/Se accumulation. Genes highlighted in red were found in this study to

be more highly expressed in *S. pinnata* than *S. elata* for all Se treatments. Solid arrows connecting gene groups represent well-known interactions from previous literature; dashed arrows represent tentative connections based on few studies; dashed arrows with question marks represent relationships proposed in this study requiring further analysis.

CHAPTER 2:

SUPPLEMENTARY MATERIAL

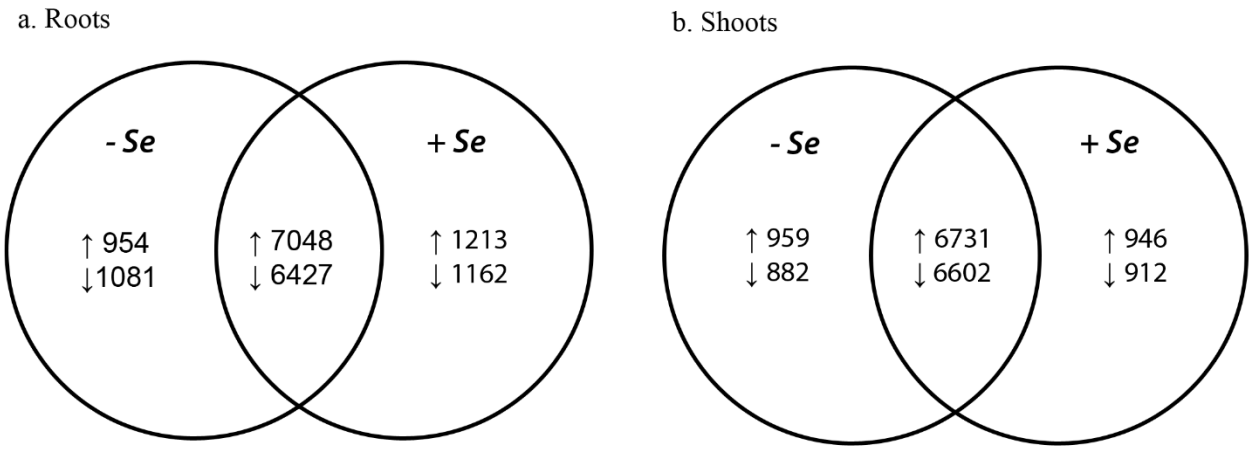

Fig. S2.1 Venn diagrams showing the number of genes in 0 µm Se (-Se) or 20 µm Se (+Se) conditions where expression in S. pinnata > S. elata (↑) and S. elata > S. pinnata (↓) in roots (a) and shoots (b). Overlapping areas show genes with shared regulation patterns regardless of treatment condition.

Table S2.1. Table of significantly differentially expressed (q<0.005) genes for all analyses based on model parameters. This file contains 19,000 rows and will be made available on DataDryad.org repository before publication.

link: ('gene_report.csv',

https://www.dropbox.com/s/ubso1zbb57dn89j/All%20Annotated%20Genes%20with%20RPKMs.xlsx?dl=0)

Table S2.2. Top 100 significant (q-value < 0.005) differentially expressed genes in response to Se treatment in **(a)** *S. elata*, **(b)** *S. pinnata*. Fold difference is calculated as the RPKM ratio of 0 µM/20 µM Se. Effect measures the extent by which the treatment affects (increases or decreases) gene expression, and is a more statistically reliable measure of gene response. The effect is on the transformed normalized scale (see methods section for model). (+) or (-) values indicate increased or decreased gene expression with Se treatment, respectively. The larger the absolute value of the effect is, the greater the treatment effect. Effect values were used to separate genes based on expression direction in descending order, with the most differentially expressed on top.

a. *S. elata*

ATID	fold change	effect	annotation
			Increased expression
AT3G41768.1	7.26	1.56	18SrRNA
AT2G07709.1	11.39	1.10	pseudogene, similar to NADH dehydrogenase
AT2G07717.1	15.84	1.01	pseudogene, similar to NADH-ubiquinone oxidoreductase chain 4
AT2G47230.2	14.60	0.95	DOMAIN OF UNKNOWN FUNCTION 724 6 (DUF6)
AT2G07711.1	18.05	0.85	pseudogene, similar to NADH dehydrogenase subunit 5
AT2G17430.1	43.38	0.77	MILDEW RESISTANCE LOCUS O 7 (MLO7)
AT2G07727.1	17.04	0.77	Di-haem cytochrome, transmembrane
AT2G07733.1	16.45	0.76	pseudogene, similar to NADH dehydrogenase subunit 2
AT1G16460.4	3.73	0.76	rhodanese homologue 2 (RDH2)
AT4G07668.1	2.70	0.71	gypsy-like retrotransposon family
AT2G19110.1	2.21	0.63	heavy metal atpase 4 (HMA4)
AT3G54010.2	3.57	0.62	PASTICCINO 1 (PAS1)
AT1G16440.1	28.64	0.61	root hair specific 3 (RSH3)
AT3G57120.1	7.39	0.61	Protein kinase superfamily protein
AT5G48320.1	25.04	0.55	Cysteine/Histidine-rich C1 domain family protein
AT1G10890.1	2.26	0.55	unknown protein
AT2G36420.1	1.90	0.53	unknown protein
AT5G40170.1	3.33	0.53	receptor like protein 54 (RLP54)
AT5G25310.1	5.24	0.52	Exostosin family protein
AT5G23110.1	1.78	0.51	Zinc finger, C3HC4 type (RING finger) family protein
AT2G06830.1	229.23	0.50	copia-like retrotransposon family

AT2G23000.1	1.73	0.49	serine carboxypeptidase-like 10 (scpl10)
AT5G49930.1	1.87	0.48	embryo defective 1441 (emb1441)
AT4G37330.1	2.19	0.47	cytochrome P450, family 81, subfamily D, polypeptide 4 (CYP81D4)
AT3G23790.1	2.74	0.47	acyl activating enzyme 16 (AAE16)
AT2G32415.2	2.48	0.45	Polynucleotidyl transferase, ribonuclease H fold protein with HRDC domain
AT1G72390.1	2.22	0.45	CONTAINS InterPro DOMAIN/s: Spt20 family
AT3G01770.1	1.84	0.45	bromodomain and extraterminal domain protein 10 (BET10)
AT2G07734.1	16.96	0.44	Alpha-L RNA-binding motif/Ribosomal protein S4 family protein
AT5G38383.1	4.53	0.44	gypsy-like retrotransposon family (Athila)
AT2G07783.1	13.38	0.44	pseudogene, similar to Ccl1
AT1G48090.1	1.64	0.44	calcium-dependent lipid-binding family protein
AT3G05820.1	375.23	0.44	invertase H (INVH)
AT1G10320.1	1.84	0.42	Zinc finger C-x8-C-x5-C-x3-H type family protein
AT2G07712.1	18.83	0.42	pseudogene, similar to maturase-related protein
			Decreased expression
AT3G20370.1	0.39	-1.05	TRAF-like family protein
AT5G25980.3	0.59	-0.84	glucoside glucohydrolase 2 (TGG2)
AT3G63200.1	0.39	-0.82	PATATIN-like protein 9 (PLP9)
AT3G03040.1	0.14	-0.80	F-box/RNI-like superfamily protein
AT3G16470.3	0.55	-0.78	JASMONATE RESPONSIVE 1 (JR1)
AT1G50010.1	0.52	-0.76	tubulin alpha-2 chain (TUA2)
AT1G48760.2	0.46	-0.76	delta-adaptin (delta-ADR)
AT2G22240.2	0.49	-0.72	myo-inositol-1-phosphate synthase 2 (MIPS2)
AT1G67870.1	0.57	-0.68	glycine-rich protein
AT1G48110.2	0.49	-0.66	evolutionarily conserved C-terminal region 7 (ECT7)
AT1G28400.1	0.55	-0.66	unknown protein
AT5G23020.1	0.62	-0.65	2-isopropylmalate synthase 2 (IMS2)
AT2G14247.1	0.22	-0.65	Expressed protein
AT2G33070.2	0.28	-0.62	nitrile specifier protein 2 (NSP2)
AT2G30860.2	0.52	-0.61	glutathione S-transferase PHI 9 (GSTF9)
AT3G16240.1	0.53	-0.61	delta tonoplast integral protein (DELTA-TIP)
AT2G01520.1	0.57	-0.60	MLP-like protein 328 (MLP328)
AT1G52000.1	0.59	-0.58	Mannose-binding lectin superfamily protein
AT4G23680.1	0.45	-0.58	Polyketide cyclase/dehydrase and lipid transport superfamily protein
AT4G11320.1	0.37	-0.57	Papain family cysteine protease
AT3G21180.1	0.33	-0.57	autoinhibited Ca(2+)-ATPase 9 (ACA9)
AT1G58270.1	0.49	-0.57	ZW9
AT5G07030.1	0.53	-0.56	Eukaryotic aspartyl protease family protein
AT5G56030.2	0.63	-0.55	heat shock protein 81-2 (HSP81-2)
AT2G38080.1	0.45	-0.53	IRREGULAR XYLEM 12 (IRX12)
AT1G52400.3	0.45	-0.52	beta glucosidase 18 (BGLU18)

AT4G32410.1	0.70	-0.52	cellulose synthase 1 (CESA1)
AT1G70850.3	0.64	-0.52	MLP-like protein 34 (MLP34)
AT3G17390.1	0.58	-0.52	METHIONINE OVER-ACCUMULATOR 3 (MTO3)
AT5G17920.2	0.65	-0.52	COBALAMIN-INDEPENDENT METHIONINE SYNTHASE (ATCIMS)
AT5G05170.1	0.79	-0.51	CONSTITUTIVE EXPRESSION OF VSP 1 (CEV1)
AT1G56070.1	0.73	-0.51	LOW EXPRESSION OF OSMOTICALLY RESPONSIVE GENES 1 (LOS1)
AT2G45470.1	0.54	-0.51	FASCICLIN-like arabinogalactan protein 8 (FLA8)
AT5G67360.1	0.70	-0.51	ARA12
AT3G09260.1	0.43	-0.50	PYK10
AT5G12250.1	0.67	-0.50	beta-6 tubulin (TUB6)
AT1G02500.2	0.61	-0.48	S-adenosylmethionine synthetase 1 (SAM1)
AT4G18780.1	0.48	-0.48	IRREGULAR XYLEM 1 (IRX1)
AT4G13930.1	0.61	-0.48	serine hydroxymethyltransferase 4 (SHM4)
AT4G13940.3	0.65	-0.48	HOMOLOGY-DEPENDENT GENE SILENCING 1 (HOG1)
AT5G26000.1	0.58	-0.48	thioglucoside glucohydrolase 1 (TGG1)
AT2G37180.1	0.64	-0.47	RESPONSIVE TO DESICCATION 28 (RD28)
AT3G03780.3	0.72	-0.47	methionine synthase 2 (MS2)
AT3G53260.1	0.50	-0.47	phenylalanine ammonia-lyase 2 (PAL2)
AT1G15690.2	0.78	-0.46	AVP1
AT2G38120.1	0.65	-0.46	AUXIN RESISTANT 1 (AUX1)
AT5G59870.1	0.62	-0.46	histone H2A 6 (HTA6)
AT1G51680.3	0.48	-0.46	4-coumarate:CoA ligase 1 (4CL1)
AT1G14900.1	0.52	-0.45	high mobility group A (HMGA)
AT5G10630.2	0.52	-0.45	Translation elongation factor EF1A/initiation factor IF2gamma family
AT1G54040.2	0.78	-0.45	epithiospecifier protein (ESP)
AT2G37040.1	0.58	-0.45	PHE ammonia lyase 1 (PAL1)
AT5G54160.1	0.64	-0.44	O-methyltransferase 1 (OMT1)
AT5G44340.1	0.68	-0.44	tubulin beta chain 4 (TUB4)
AT3G60750.2	0.90	-0.43	Transketolase
AT3G23800.1	0.56	-0.43	selenium-binding protein 3 (SBP3)
AT3G51070.1	0.10	-0.43	S-adenosyl-L-methionine-dependent methyltransferases superfamily protein
AT4G13770.1	0.77	-0.43	cytochrome P450, family 83, subfamily A, polypeptide 1 (CYP83A1)
AT4G00780.1	0.61	-0.43	TRAF-like family protein
AT1G15950.2	0.58	-0.43	cinnamoyl coa reductase 1 (CCR1)
AT5G04820.1	0.34	-0.42	ovate family protein 13 (OFP13)
AT1G19850.1	0.62	-0.42	MONOPTEROS (MP)
AT1G31280.1	0.55	-0.42	argonaute 2 (AGO2)
AT3G23255.2	0.32	-0.42	unknown protein
AT5G59320.1	0.40	-0.42	lipid transfer protein 3 (LTP3)

b. *S. pinnata*

ATID	fold change	effect	annotation
			Increased expression
AT4G32500.1	30.64	1.12	K+ transporter 5 (KT5)
AT1G17690.1	2.56	0.79	FUNCTIONS IN: molecular_function unknown
AT1G20440.1	2.03	0.77	cold-regulated 47 (COR47)
AT4G21060.2	2.62	0.77	Galactosyltransferase family protein
AT4G11320.1	44.85	0.76	Papain family cysteine protease
AT5G67310.1	3.17	0.72	cytochrome P450, family 81, subfamily G, polypeptide 1 (CYP81G1)
AT4G35160.1	1.87	0.70	O-methyltransferase family protein
AT5G53010.1	2.73	0.70	calcium-transporting ATPase, putative
AT5G66250.4	3.31	0.65	kinectin-related
AT5G12270.1	4.36	0.63	2-oxoglutarate (2OG) and Fe(II)-dependent oxygenase superfamily
AT5G53450.2	2.04	0.62	OBP3-responsive gene 1 (ORG1)
AT3G01420.1	3.86	0.60	DOX1
AT5G65220.1	2.08	0.55	Ribosomal L29 family protein
AT1G22360.2	2.25	0.54	UDP-glucosyl transferase 85A2 (UGT85A2)
AT1G13930.2	1.73	0.53	FUNCTIONS IN: molecular_function unknown
AT2G30670.1	1.51	0.51	NAD(P)-binding Rossmann-fold superfamily protein
AT5G38100.2	5.00	0.51	S-adenosyl-L-methionine-dependent methyltransferases superfamily protein
AT1G44542.1	1.70	0.51	Cyclase family protein
AT4G26630.2	1.71	0.50	DEK domain-containing chromatin associated protein
AT1G78860.1	1.56	0.50	D-mannose binding lectin protein with Apple-like carbohydrate-binding domain
AT5G40450.1	1.61	0.50	unknown protein
AT3G51920.1	2.34	0.50	calmodulin 9 (CAM9)
AT5G53460.3	1.27	0.49	NADH-dependent glutamate synthase 1 (GLT1)
AT2G42690.1	1.74	0.49	alpha/beta-Hydrolases superfamily protein
AT5G40340.1	1.98	0.48	Tudor/PWWP/MBT superfamily protein
AT5G41670.2	1.60	0.48	6-phosphogluconate dehydrogenase family protein
AT2G46572.1	33.97	0.47	Potential natural antisense gene
AT5G22690.1	1.76	0.47	Disease resistance protein (TIR-NBS-LRR class) family
AT1G79040.1	1.94	0.46	photosystem II subunit R (PSBR)
AT2G05380.2	1.61	0.46	glycine-rich protein 3 short isoform (GRP3S)
AT4G15530.6	1.63	0.46	pyruvate orthophosphate dikinase (PPDK)
AT4G33110.2	4.88	0.46	S-adenosyl-L-methionine-dependent methyltransferases superfamily protein
AT1G27950.1	2.59	0.44	glycosylphosphatidylinositol-anchored lipid protein transfer 1 (LTPG1)
AT2G21660.2	1.54	0.44	GLYCINE RICH PROTEIN 7 (ATGRP7)
AT2G16060.1	2.40	0.44	hemoglobin 1 (HB1)

AT2G05100.1	1.41	0.44	photosystem II light harvesting complex gene 2.1 (LHCB2.1)
AT1G74470.1	1.81	0.43	Pyridine nucleotide-disulphide oxidoreductase family protein
AT5G24660.1	1.90	0.43	RESPONSE TO LOW SULFUR 2 (LSU2)
AT1G77760.1	2.54	0.43	nitrate reductase 1 (NIA1)
AT1G64960.1	2.15	0.43	ARM repeat superfamily protein
AT5G64120.1	2.12	0.43	Peroxidase superfamily protein
AT2G15620.1	1.45	0.43	nitrite reductase 1 (NIR1)
AT5G64470.3	3.32	0.43	INVOLVED IN: biological_process unknown
AT5G66570.1	1.54	0.43	PS II oxygen-evolving complex 1 (PSBO1)
AT3G19930.1	1.60	0.43	sugar transporter 4 (STP4)
AT4G19810.1	1.46	0.42	Glycosyl hydrolase family protein with chitinase insertion domain
AT5G48180.1	1.90	0.42	nitrile specifier protein 5 (NSP5)
AT2G26560.1	4.07	0.42	phospholipase A 2A (PLA2A)
AT3G05900.1	2.01	0.42	neurofilament protein-related
AT1G22400.1	3.50	0.42	UGT85A1
AT2G43910.2	2.15	0.41	HARMLESS TO OZONE LAYER 1 (HOL1)
AT4G12550.1	2.26	0.41	Auxin-Induced in Root cultures 1 (AIR1)
AT3G54890.4	1.65	0.41	photosystem I light harvesting complex gene 1 (LHCA1)
AT4G32950.1	4.16	0.41	Protein phosphatase 2C family protein
AT1G13080.2	1.58	0.40	cytochrome P450, family 71, subfamily B, polypeptide 2 (CYP71B2)
			Decreased expression
AT1G07890.8	0.04	-2.61	ascorbate peroxidase 1 (APX1)
AT2G33770.1	0.30	-1.20	phosphate 2 (PHO2)
AT5G14200.3	0.11	-1.04	isopropylmalate dehydrogenase 1
AT3G16340.2	0.47	-0.83	pleiotropic drug resistance 1 (PDR1)
AT1G21140.1	0.41	-0.80	Vacuolar iron transporter (VIT) family protein
AT2G43150.1	0.50	-0.73	Proline-rich extensin-like family protein
AT5G48930.1	0.25	-0.68	hydroxycinnamoyl-CoA shikimate/quinate hydroxycinnamoyl transferase (HCT)
AT3G48770.1	0.00	-0.66	DNA binding
AT2G37040.1	0.35	-0.60	PHE ammonia lyase 1 (PAL1)
AT3G44300.1	0.39	-0.58	nitrilase 2 (NIT2)
AT4G25030.2	0.20	-0.58	unknown protein
AT5G64341.1	0.38	-0.58	conserved peptide upstream open reading frame 40 (CPuORF40)
AT2G30860.1	0.43	-0.58	glutathione S-transferase PHI 9 (GSTF9)
AT5G01595.1	0.01	-0.57	Potential natural antisense gene
AT2G47180.1	0.42	-0.57	galactinol synthase 1 (GolS1)
AT4G36648.1	0.35	-0.55	Unknown gene
AT5G66170.3	0.14	-0.54	sulfurtransferase 18 (STR18)
AT3G07390.1	0.12	-0.54	Auxin-Induced in Root cultures 12 (AIR12)
AT5G42530.1	0.53	-0.53	unknown protein
AT1G22410.1	0.75	-0.52	Class-II DAHP synthetase family protein

AT3G53260.1	0.23	-0.51	phenylalanine ammonia-lyase 2 (PAL2)
AT4G03050.1	0.64	-0.51	AOP3
AT5G05340.1	0.42	-0.50	Peroxidase superfamily protein
AT2G37180.1	0.17	-0.50	RESPONSIVE TO DESICCATION 28 (RD28)
AT5G17890.1	0.65	-0.50	DA1-related protein 4 (DAR4)
AT1G52400.3	0.59	-0.49	beta glucosidase 18 (BGLU18)
AT3G54600.1	0.38	-0.49	Class I glutamine amidotransferase-like superfamily protein
AT4G21510.1	0.54	-0.49	F-box family protein
AT1G72290.1	0.35	-0.48	Kunitz family trypsin and protease inhibitor protein
AT5G18370.1	0.67	-0.48	Disease resistance protein (TIR-NBS-LRR class) family
AT1G78360.1	0.34	-0.48	glutathione S-transferase TAU 21 (GSTU21)
AT5G37770.1	0.44	-0.48	TOUCH 2 (TCH2)
AT4G19690.2	0.65	-0.47	iron-regulated transporter 1 (IRT1)
AT5G06730.1	0.14	-0.47	Peroxidase superfamily protein
AT3G21240.1	0.45	-0.47	4-coumarate:CoA ligase 2 (4CL2)
AT3G19710.1	0.59	-0.46	branched-chain aminotransferase4 (BCAT4)
AT1G77520.1	0.80	-0.42	O-methyltransferase family protein
AT2G34210.1	0.59	-0.42	Transcription elongation factor Spt5
AT4G33720.1	0.55	-0.41	CAP (Cysteine-rich secretory proteins, Antigen 5, and Pathogenesis-related 1 protein) superfamily protein
AT3G03780.3	0.69	-0.41	methionine synthase 2 (MS2)
AT5G54090.1	0.33	-0.41	DNA mismatch repair protein MutS, type 2
AT1G73260.1	0.56	-0.41	kunitz trypsin inhibitor 1 (KTI1)
AT5G18360.1	0.41	-0.41	Disease resistance protein (TIR-NBS-LRR class) family
AT2G25450.1	0.81	-0.41	2-oxoglutarate (2OG) and Fe(II)-dependent oxygenase superfamily protein
AT4G36150.1	0.72	-0.40	Disease resistance protein (TIR-NBS-LRR class) family

Table S2.3 Top 100 significant (q-value < 0.005) differentially expressed genes in response to Se treatment in **(a)** *S. elata* roots, **(b)** *S. pinnata* roots, **(c)** *S. elata* shoots, **(d)** *S. pinnata* shoots. Fold difference is calculated as the RPKM ratio of 0 μM/20 μM Se. Effect measures the extent by which the treatment affects (increases or decreases) gene expression, and is a more statistically reliable measure of gene response. The effect is on the transformed normalized scale (see methods section for model). (+) or (-) values indicate increased or decreased gene expression with Se treatment, respectively. The larger the absolute value of the effect is, the greater the treatment effect. Effect values were used to separate genes based on expression direction in descending order, with the most differentially expressed on top.

a. *S. elata* roots

ATID	fold change	effect	Annotation
			Increased expression
AT3G41768.1	9.89	3.28	18SrRNA
AT2G07709.1	13.08	2.24	pseudogene, similar to NADH dehydrogenase,
AT2G07717.1	18.32	2.04	pseudogene, similar to NADH-ubiquinone
AT2G07711.1	20.23	1.69	pseudogene, similar to NADH dehydrogenase subunit 5
AT2G07727.1	18.96	1.53	Di-haem cytochrome, transmembrane; Cytochrome b/b6, C-terminal
AT2G07733.1	18.44	1.51	pseudogene, similar to NADH dehydrogenase subunit 2
AT2G47230.2	21.67	1.15	DOMAIN OF UNKNOWN FUNCTION 724 6 (DUF6)
AT1G10890.1	3.15	1.13	unknown protein
AT2G19110.1	2.48	1.00	heavy metal atpase 4 (HMA4)
AT5G40170.1	3.92	0.98	receptor like protein 54 (RLP54)
AT2G36420.1	2.23	0.94	unknown protein
AT5G49930.1	2.42	0.90	embryo defective 1441 (emb1441)
AT3G54010.2	4.42	0.90	PASTICCINO 1 (PAS1)
AT1G65860.1	2.06	0.89	flavin-monooxygenase glucosinolate S-oxygenase 1 (FMO GS-OX1)
AT3G14460.1	3.83	0.89	LRR and NB-ARC domains-containing disease resistance protein
AT2G07734.1	18.89	0.88	Alpha-L RNA-binding motif/Ribosomal protein S4 family protein
AT2G07783.1	15.61	0.86	pseudogene, similar to Ccl1
AT2G17430.1	33.59	0.85	MILDEW RESISTANCE LOCUS O 7 (MLO7)
AT2G07712.1	22.90	0.82	pseudogene, similar to maturase-related protein

AT5G25310.1	6.98	0.82	Exostosin family protein
AT1G10320.1	2.54	0.82	Zinc finger C-x8-C-x5-C-x3-H type family protein
AT4G07668.1	2.80	0.81	gypsy-like retrotransposon family
AT1G16440.1	33.05	0.78	root hair specific 3 (RSH3)
AT3G19670.1	1.94	0.77	pre-mRNA-processing protein 40B (PRP40b)
AT3G57120.1	10.60	0.76	Protein kinase superfamily protein
AT5G23110.1	2.01	0.76	Zinc finger, C3HC4 type (RING finger) family protein
AT3G19190.1	2.19	0.75	AUTOPHAGY 2 (ATG2)
AT3G01770.1	2.34	0.75	bromodomain and extraterminal domain protein 10 (BET10)
AT5G38383.1	8.52	0.75	gypsy-like retrotransposon family (Athila)
AT1G19485.2	3.21	0.74	Transducin/WD40 repeat-like superfamily protein
AT1G79950.1	2.70	0.73	RAD3-like DNA-binding helicase protein
AT1G06490.1	2.78	0.73	glucan synthase-like 7 (GSL07)
AT2G07715.1	26.63	0.73	Nucleic acid-binding, OB-fold-like protein
AT3G13790.2	2.22	0.72	ATBFRUCT1
AT1G16460.4	3.88	0.72	rhodanese homologue 2 (RDH2)
AT1G54490.1	2.99	0.72	exoribonuclease 4 (XRN4)
AT2G07687.1	15.51	0.72	Cytochrome c oxidase, subunit III
AT4G02660.1	2.18	0.72	Beige/BEACH domain ;WD domain, G-beta repeat protein
AT1G48090.1	1.99	0.72	calcium-dependent lipid-binding family protein
AT3G02070.1	2.26	0.71	Cysteine proteinases superfamily protein
AT3G20475.1	2.69	0.70	MUTS-homologue 5 (MSH5)
			Decreased expression
AT2G22240.2	0.16	-1.28	myo-inositol-1-phosphate synthase 2 (MIPS2)
AT4G23680.1	0.33	-1.28	Polyketide cyclase/dehydrase and lipid transport superfamily protein
AT1G50010.1	0.35	-1.25	tubulin alpha-2 chain (TUA2)
AT5G05170.1	0.36	-1.23	CONSTITUTIVE EXPRESSION OF VSP 1 (CEV1)
AT5G25980.3	0.33	-1.18	glucoside glucohydrolase 2 (TGG2)
AT1G52000.1	0.39	-1.17	Mannose-binding lectin superfamily protein
AT3G20370.1	0.35	-1.15	TRAF-like family protein
AT4G11320.1	0.36	-1.10	Papain family cysteine protease
AT2G33070.2	0.27	-1.09	nitrile specifier protein 2 (NSP2)
AT5G23020.1	0.42	-1.08	2-isopropylmalate synthase 2 (IMS2)
AT3G63200.1	0.36	-1.07	PATATIN-like protein 9 (PLP9)
AT1G56070.1	0.44	-1.06	LOW EXPRESSION OF OSMOTICALLY RESPONSIVE GENES 1 (LOS1)
AT3G09260.1	0.42	-1.06	PYK10
AT5G56030.2	0.35	-1.05	heat shock protein 81-2 (HSP81-2)
AT2G30860.2	0.31	-1.05	glutathione S-transferase PHI 9 (GSTF9)
AT2G37040.1	0.37	-1.03	PHE ammonia lyase 1 (PAL1)
AT4G32410.1	0.46	-1.01	cellulose synthase 1 (CESA1)

AT2G38080.1	0.19	-0.99	IRREGULAR XYLEM 12 (IRX12)
AT1G48760.2	0.38	-0.98	delta-adaptin (delta-ADR)
AT5G12250.1	0.41	-0.98	beta-6 tubulin (TUB6)
AT4G05050.1	0.43	-0.97	ubiquitin 11 (UBQ11)
AT1G02500.2	0.41	-0.96	S-adenosylmethionine synthetase 1 (SAM1)
AT1G15690.2	**0.35**	-0.91	AVP1
AT1G28400.1	0.47	-0.90	unknown protein
AT3G53260.1	0.38	-0.89	phenylalanine ammonia-lyase 2 (PAL2)
AT4G13940.3	0.47	-0.87	HOMOLOGY-DEPENDENT GENE SILENCING 1 (HOG1)
AT2G01520.1	0.54	-0.86	MLP-like protein 328 (MLP328)
AT3G60750.2	0.43	-0.86	Transketolase
AT3G03040.1	0.11	-0.85	F-box/RNI-like superfamily protein
AT1G52400.3	0.32	-0.84	beta glucosidase 18 (BGLU18)
AT1G54040.2	0.46	-0.84	epithiospecifier protein (ESP)
AT5G44340.1	0.41	-0.82	tubulin beta chain 4 (TUB4)
AT3G16470.3	0.55	-0.81	JASMONATE RESPONSIVE 1 (JR1)
AT1G51680.3	0.38	-0.81	4-coumarate:CoA ligase 1 (4CL1)
AT1G78120.1	0.46	-0.81	Tetratricopeptide repeat (TPR)-like superfamily protein
AT4G38770.1	0.46	-0.80	proline-rich protein 4 (PRP4)
AT5G67360.1	0.53	-0.80	ARA12; FUNCTIONS IN: serine-type endopeptidase activity
AT3G47470.1	0.52	-0.80	light-harvesting chlorophyll-protein complex I subunit A4 (LHCA4)
AT4G13930.1	0.41	-0.80	serine hydroxymethyltransferase 4 (SHM4)
AT1G07890.6	0.39	-0.79	ascorbate peroxidase 1 (APX1)
AT4G18780.1	0.29	-0.79	IRREGULAR XYLEM 1 (IRX1)
AT1G48110.2	0.48	-0.78	evolutionarily conserved C-terminal region 7 (ECT7)
AT1G44575.2	0.49	-0.78	NONPHOTOCHEMICAL QUENCHING 4 (NPQ4)
AT5G38480.2	0.46	-0.77	general regulatory factor 3 (GRF3_
AT5G17920.2	0.53	-0.77	COBALAMIN-INDEPENDENT METHIONINE SYNTHASE (ATCIMS)
AT5G44790.1	0.47	-0.77	RESPONSIVE-TO-ANTAGONIST 1 (RAN1)
AT3G15950.1	0.24	-0.75	NAI2
AT5G07030.1	0.49	-0.75	Eukaryotic aspartyl protease family protein
AT2G38120.1	0.51	-0.75	AUXIN RESISTANT 1 (AUX1)
AT2G41840.1	0.53	-0.74	Ribosomal protein S5 family protein
AT4G21960.1	0.57	-0.74	PRXR1
AT3G16240.1	0.32	-0.74	delta tonoplast integral protein (DELTA-TIP)
AT3G16410.1	0.20	-0.74	nitrile specifier protein 4 (NSP4)
AT4G33090.1	0.45	-0.74	aminopeptidase M1 (APM1)
AT4G03050.1	0.42	-0.73	AOP3
AT1G73330.1	0.19	-0.71	drought-repressed 4 (DR4)
AT5G17420.1	0.23	-0.71	IRREGULAR XYLEM 3 (IRX3)
AT3G03780.3	0.60	-0.71	methionine synthase 2 (MS2)

AT2G36880.2	0.44	-0.71	methionine adenosyltransferase 3 (MAT3)

b. *S. elata* shoots

ATID	fold change	effect	Annotation
			Increased expression
AT1G16460.4	3.63	0.79	rhodanese homologue 2 (RDH2)
AT2G47230.2	9.19	0.75	DOMAIN OF UNKNOWN FUNCTION 724 6 (DUF6)
AT2G17430.1	93.25	0.69	MILDEW RESISTANCE LOCUS O 7 (MLO7)
AT2G23000.1	1.94	0.65	serine carboxypeptidase-like 10 (scpl10)
AT4G07668.1	2.54	0.60	gypsy-like retrotransposon family
AT4G37330.1	2.97	0.59	cytochrome P450, family 81, subfamily D, polypeptide 4 (CYP81D4)
AT5G01595.1	3.69	0.59	Potential natural antisense gene
AT2G38230.1	35.45	0.53	pyridoxine biosynthesis 1.1 (PDX1.1)
AT4G24120.1	1.81	0.51	YELLOW STRIPE like 1 (YSL1)
AT4G25100.5	1.63	0.47	Fe superoxide dismutase 1 (FSD1)
AT5G56870.1	1.48	0.47	beta-galactosidase 4 (BGAL4)
AT3G23790.1	2.57	0.46	acyl activating enzyme 16 (AAE16)
AT3G57120.1	4.85	0.46	Protein kinase superfamily protein
AT1G69990.1	2.19	0.45	Leucine-rich repeat protein kinase family protein
AT5G43530.1	50.85	0.44	Helicase protein with RING/U-box domain
AT1G16440.1	20.55	0.44	root hair specific 3 (RSH3)
AT5G48320.1	12.54	0.43	Cysteine/Histidine-rich C1 domain family protein
AT1G27110.3	2.03	0.43	Tetratricopeptide repeat (TPR)-like superfamily protein
AT5G13630.2	1.36	0.42	GENOMES UNCOUPLED 5 (GUN5)
AT1G29720.1	2.05	0.42	Leucine-rich repeat transmembrane protein kinase
AT5G04460.2	1.93	0.42	RING/U-box superfamily protein
AT4G14370.1	59.09	0.41	Disease resistance protein (TIR-NBS-LRR class) family
AT1G07110.1	1.55	0.41	fructose-2,6-bisphosphatase (F2KP)
AT3G56090.1	3.12	0.41	ferritin 3 (FER3)
AT5G61820.1	1.63	0.41	FUNCTIONS IN: molecular_function unknown
AT2G31660.1	1.56	0.39	SUPER SENSITIVE TO ABA AND DROUGHT2 (SAD2)
AT5G43060.1	1.43	0.39	Granulin repeat cysteine protease family protein
AT5G10180.1	2.36	0.39	slufate transporter 2
AT1G79460.1	3.07	0.39	GA REQUIRING 2 (GA2)
AT1G53510.1	2.85	0.39	mitogen-activated protein kinase 18 (MPK18)
AT5G02100.1	3E+11	0.39	UNFERTILIZED EMBRYO SAC 18 (UNE18)
AT3G19170.2	1.40	0.39	presequence protease 1 (PREP1)
AT1G36160.2	1.47	0.39	acetyl-CoA carboxylase 1 (ACC1)
AT1G58290.1	2.04	0.38	HEMA1
AT3G26770.1	2.73	0.38	NAD(P)-binding Rossmann-fold superfamily protein

AT1G02640.1	1.52	0.38	beta-xylosidase 2 (BXL2)
AT4G03050.1	1.42	0.37	AOP3
AT3G11930.4	1.53	0.37	Adenine nucleotide alpha hydrolases-like superfamily protein
AT5G45650.1	1.46	0.37	subtilase family protein
			Decreased expression
AT2G14247.1	0.15	-1.55	Expressed protein
AT3G20370.1	0.43	-0.95	TRAF-like family protein
AT5G26000.1	0.52	-0.79	thioglucoside glucohydrolase 1 (TGG1)
AT3G03040.1	0.16	-0.76	F-box/RNI-like superfamily protein
AT3G16470.3	0.51	-0.75	JASMONATE RESPONSIVE 1 (JR1)
AT1G67870.1	0.57	-0.70	glycine-rich protein
AT5G67370.1	0.46	-0.65	Protein of unknown function (DUF1230)
AT5G59320.1	0.40	-0.63	lipid transfer protein 3 (LTP3)
AT3G23800.1	0.56	-0.62	selenium-binding protein 3 (SBP3)
AT5G53450.2	0.36	-0.61	OBP3-responsive gene 1 (ORG1)
AT1G17990.2	0.27	-0.61	FMN-linked oxidoreductases superfamily protein
AT4G14365.1	0.32	-0.61	XB3 ortholog 4 in Arabidopsis thaliana (XBAT34)
AT2G37180.1	0.61	-0.61	RESPONSIVE TO DESICCATION 28 (RD28)
AT1G31580.1	0.11	-0.60	ECS1
AT5G63520.1	0.50	-0.60	CONTAINS InterPro DOMAIN/s: F-box domain, Skp2-like
AT5G05250.1	0.40	-0.59	unknown protein
AT3G63200.1	0.47	-0.57	PATATIN-like protein 9 (PLP9)
AT3G27060.1	0.46	-0.54	TSO MEANING 'UGLY' IN CHINESE 2 (TSO2)
AT3G21180.1	0.28	-0.54	autoinhibited Ca(2+)-ATPase 9 (ACA9)
AT1G48110.2	0.52	-0.53	evolutionarily conserved C-terminal region 7 (ECT7)
AT1G48760.2	0.58	-0.53	delta-adaptin (delta-ADR)
AT1G22690.3	0.44	-0.53	Gibberellin-regulated family protein
AT4G00780.1	0.61	-0.52	TRAF-like family protein
AT5G25980.3	0.68	-0.51	glucoside glucohydrolase 2 (TGG2)
AT4G04610.1	0.66	-0.50	APS reductase 1 (APR1)
AT1G62420.1	0.22	-0.50	Protein of unknown function (DUF506)
AT1G58270.1	0.34	-0.49	ZW9
AT5G24660.1	0.27	-0.48	RESPONSE TO LOW SULFUR 2 (LSU2)
AT3G17390.1	0.62	-0.48	METHIONINE OVER-ACCUMULATOR 3 (MTO3)
AT1G68890.1	0.69	-0.48	magnesium ion binding
AT3G16240.1	0.61	-0.48	delta tonoplast integral protein (DELTA-TIP)
AT5G19120.1	0.60	-0.47	Eukaryotic aspartyl protease family protein
AT3G56360.1	0.50	-0.47	unknown protein
AT5G44190.1	0.52	-0.47	GOLDEN2-like 2 (GLK2)
AT3G18290.1	0.67	-0.46	BRUTUS (BTS)
AT2G46660.1	0.29	-0.46	cytochrome P450, family 78, subfamily A, polypeptide 6 (CYP78A6)

AT1G12080.2	0.51	-0.46	Vacuolar calcium-binding protein-related
AT3G51070.1	0.09	-0.44	S-adenosyl-L-methionine-dependent methyltransferases superfamily protein
AT4G16000.1	0.34	-0.44	unknown protein
AT5G04150.1	0.37	-0.43	BHLH101
AT1G61120.1	0.17	-0.43	terpene synthase 04 (TPS04)
AT1G73602.1	0.64	-0.43	conserved peptide upstream open reading frame 32 (CPuORF32)
AT5G64770.1	0.62	-0.43	root meristem growth factor 9 (RGF9)
AT3G23255.2	0.31	-0.43	unknown protein
AT4G09150.2	0.63	-0.42	T-complex protein 11
AT1G70850.3	0.66	-0.42	MLP-like protein 34 (MLP34)
AT1G28400.1	0.69	-0.41	unknown protein
AT3G22060.1	0.43	-0.41	Receptor-like protein kinase-related family protein
AT2G31880.1	0.57	-0.41	SUPPRESSOR OF BIR1 1 (SOBIR1)
AT1G20693.3	0.63	-0.41	high mobility group B2 (HMGB2)
AT1G09530.2	0.60	-0.40	phytochrome interacting factor 3 (PIF3)
AT4G21990.2	0.53	-0.40	APS reductase 3 (APR3)
AT5G13740.1	0.69	-0.39	zinc induced facilitator 1 (ZIF1)
AT4G35110.4	0.59	-0.39	Arabidopsis phospholipase-like protein (PEARLI 4) family
AT3G17510.1	0.59	-0.39	CBL-interacting protein kinase 1 (CIPK1)
AT5G52300.2	0.53	-0.38	LOW-TEMPERATURE-INDUCED 65 (LTI65)
AT2G36830.1	0.68	-0.38	gamma tonoplast intrinsic protein (GAMMA-TIP)
AT3G16230.3	0.57	-0.38	Predicted eukaryotic LigT
AT1G64510.1	0.70	-0.37	Translation elongation factor EF1B/ribosomal protein S6 family protein
AT3G63160.1	0.68	-0.37	FUNCTIONS IN: molecular_function unknown
AT2G37170.1	0.62	-0.37	plasma membrane intrinsic protein 2 (PIP2b)

c. *S. pinnata* roots

ATID	fold change	effect	Annotation
			Increased expression
AT4G11310.1	37.12	1.52	Papain family cysteine protease
AT4G32500.1	132.20	1.31	K+ transporter 5 (KT5)
AT4G21060.2	3.08	0.97	Galactosyltransferase family protein
AT5G38100.2	5.18	0.97	S-adenosyl-L-methionine-dependent methyltransferases superfamily protein
AT5G53010.1	3.60	0.95	calcium-transporting ATPase, putative
AT4G11320.1	43.27	0.90	Papain family cysteine protease
AT4G12550.1	2.27	0.89	Auxin-Induced in Root cultures 1 (AIR1)
AT1G17690.1	2.79	0.88	FUNCTIONS IN: molecular_function unknown
AT5G48570.1	3.11	0.87	FKBP-type peptidyl-prolyl cis-trans isomerase family protein

AT2G16060.1	2.45	0.86	hemoglobin 1 (HB1)
AT1G74590.1	2.67	0.85	glutathione S-transferase TAU 10 (GSTU10)
AT4G35160.1	2.90	0.85	O-methyltransferase family protein
AT5G12270.1	4.22	0.84	2-oxoglutarate (2OG) and Fe(II)-dependent oxygenase superfamily protein
AT3G12500.1	2.12	0.81	basic chitinase (HCHIb)
AT2G36120.1	2.07	0.80	DEFECTIVELY ORGANIZED TRIBUTARIES 1 (DOT1)
AT2G30670.1	3.05	0.74	NAD(P)-binding Rossmann-fold superfamily protein
AT1G17745.2	2.07	0.74	D-3-phosphoglycerate dehydrogenase
AT1G78340.1	2.37	0.68	glutathione S-transferase TAU 22 (GSTU22)
AT4G33110.2	4.97	0.67	S-adenosyl-L-methionine-dependent methyltransferases superfamily protein
AT3G47730.1	1.72	0.63	ATP-binding cassette A2 (ABCA2)
AT2G26560.1	4.53	0.62	phospholipase A 2A (PLA2A)
AT5G43360.1	5.77	0.61	phosphate transporter 1
AT4G32950.1	4.06	0.61	Protein phosphatase 2C family protein
AT1G02920.1	1.91	0.61	glutathione S-transferase 7 (GSTF7)
AT1G21310.1	1.56	0.60	extensin 3 (EXT3)
AT5G08260.1	3.13	0.60	serine carboxypeptidase-like 35 (scpl35)
AT5G22690.1	1.75	0.59	Disease resistance protein (TIR-NBS-LRR class) family
AT1G52050.1	2.64	0.59	Mannose-binding lectin superfamily protein
AT1G56430.1	2.30	0.57	nicotianamine synthase 4 (NAS4)
AT2G43840.1	3.05	0.57	UDP-glycosyltransferase 74 F1 (UGT74F1)
AT5G36930.2	1.81	0.57	Disease resistance protein (TIR-NBS-LRR class) family
AT4G19810.1	1.67	0.57	Glycosyl hydrolase family protein with chitinase insertion domain
AT1G70830.4	2.59	0.57	MLP-like protein 28 (MLP28)
AT3G47780.1	1.80	0.56	ABC2 homolog 6 (ATH6)
AT3G61390.2	2.38	0.56	RING/U-box superfamily protein
AT2G18960.1	1.49	0.56	H(+)-ATPase 1 (HA1)
AT1G44542.1	1.87	0.55	Cyclase family protein
AT5G38100.1	4.69	0.55	S-adenosyl-L-methionine-dependent methyltransferases superfamily protein
AT2G44220.1	2.61	0.53	Protein of Unknown Function (DUF239)
AT4G13770.1	1.57	0.52	cytochrome P450, family 83, subfamily A, polypeptide 1 (CYP83A1)
AT2G43100.1	1.89	0.51	isopropylmalate isomerase 2 (IPMI2)
AT5G23010.1	1.59	0.51	methylthioalkylmalate synthase 1 (MAM1)
AT5G17330.1	1.94	0.50	glutamate decarboxylase (GAD)
AT3G51920.1	2.14	0.50	calmodulin 9 (CAM9)
AT4G23010.3	2.11	0.50	UDP-galactose transporter 2 (UTR2)
AT3G53280.1	7.80	0.50	cytochrome p450 71b5 (CYP71B5)
AT2G39200.1	1.80	0.49	MILDEW RESISTANCE LOCUS O 12 (MLO12)
AT2G46572.1	39.72	0.49	Potential natural antisense gene
AT4G10340.1	1.50	0.49	light harvesting complex of photosystem II 5 (LHCB5)

AT3G19930.1	1.62	0.48	sugar transporter 4 (STP4)
AT1G19715.3	1.53	0.48	Mannose-binding lectin superfamily protein
AT5G40820.1	1.79	0.48	Ataxia telangiectasia-mutated and RAD3-related (ATR)
AT5G67310.1	2.13	0.47	cytochrome P450, family 81, subfamily G, polypeptide 1 (CYP81G1)
AT5G66690.1	1.72	0.47	UGT72E2
AT2G42690.1	2.28	0.47	alpha/beta-Hydrolases superfamily protein
AT5G08640.2	4.09	0.47	flavonol synthase 1 (FLS1)
AT5G64470.3	3.64	0.47	INVOLVED IN: biological_process unknown
AT1G12110.1	1.57	0.46	nitrate transporter 1.1 (NRT1.1)
AT1G48760.2	1.51	0.46	delta-adaptin (delta-ADR)
AT1G21110.1	2.11	0.46	O-methyltransferase family protein
			Decreased expression
AT4G36150.1	0.03	-3.22	Disease resistance protein (TIR-NBS-LRR class) family
AT4G33720.1	0.25	-1.28	CAP (Cysteine-rich secretory proteins, Antigen 5, and Pathogenesis-related 1 protein) superfamily protein
AT1G73260.1	0.43	-1.15	kunitz trypsin inhibitor 1 (KTI1)
AT5G18360.1	0.12	-1.07	Disease resistance protein (TIR-NBS-LRR class) family
AT3G47340.2	0.18	-1.05	glutamine-dependent asparagine synthase 1 (ASN1)
AT1G77520.1	0.34	-1.04	O-methyltransferase family protein
AT4G19690.2	0.43	-0.96	iron-regulated transporter 1 (IRT1)
AT5G54090.1	0.39	-0.94	DNA mismatch repair protein MutS, type 2
AT2G25450.1	0.45	-0.81	2-oxoglutarate (2OG) and Fe(II)-dependent oxygenase superfamily protein
AT1G21140.1	0.32	-0.80	Vacuolar iron transporter (VIT) family protein
AT4G21510.1	0.08	-0.78	F-box family protein
AT1G63220.1	0.11	-0.76	Calcium-dependent lipid-binding (CaLB domain) family protein
AT5G06730.1	0.38	-0.74	Peroxidase superfamily protein
AT4G01870.1	0.41	-0.74	tolB protein-related
AT3G21240.1	0.19	-0.71	4-coumarate:CoA ligase 2 (4CL2)
AT1G78360.1	0.44	-0.70	glutathione S-transferase TAU 21 (GSTU21)
AT2G34210.1	0.00	-0.70	Transcription elongation factor Spt5
AT5G05340.1	0.26	-0.67	Peroxidase superfamily protein
AT5G66170.3	0.32	-0.61	sulfurtransferase 18 (STR18)
AT2G37180.1	0.58	-0.61	RESPONSIVE TO DESICCATION 28 (RD28)
AT1G01580.1	0.42	-0.59	ferric reduction oxidase 2 (FRO2)
AT1G52810.1	0.21	-0.58	2-oxoglutarate (2OG) and Fe(II)-dependent oxygenase superfamily protein
AT5G19440.1	0.58	-0.58	NAD(P)-binding Rossmann-fold superfamily protein
AT3G53260.1	0.65	-0.54	phenylalanine ammonia-lyase 2 (PAL2)
AT4G17030.1	0.28	-0.54	expansin-like B1 (EXLB1)
AT5G01595.1	0.36	-0.51	Potential natural antisense gene
AT1G50060.1	0.28	-0.51	CAP (Cysteine-rich secretory proteins, Antigen 5, and Pathogenesis-related 1 protein) superfamily protein

AT1G15040.2	0.33	-0.50	Class I glutamine amidotransferase-like superfamily protein
AT1G22410.1	0.61	-0.50	Class-II DAHP synthetase family protein
AT5G20620.1	0.60	-0.50	ubiquitin 4 (UBQ4)
AT1G75830.1	0.45	-0.49	low-molecular-weight cysteine-rich 67 (LCR67)
AT5G18370.1	0.40	-0.49	Disease resistance protein (TIR-NBS-LRR class) family
AT1G09780.1	0.62	-0.48	Phosphoglycerate mutase, 2,3-bisphosphoglycerate-independent
AT3G25510.1	0.38	-0.48	disease resistance protein (TIR-NBS-LRR class), putative
AT5G04950.1	0.48	-0.47	nicotianamine synthase 1 (NAS1)
AT3G21690.1	0.60	-0.47	MATE efflux family protein
AT2G41705.2	0.55	-0.46	camphor resistance CrcB family protein
AT3G61430.2	0.60	-0.46	plasma membrane intrinsic protein 1A (PIP1A)
AT4G12290.1	0.49	-0.46	Copper amine oxidase family protein
AT5G48930.1	0.55	-0.46	hydroxycinnamoyl-CoA shikimate/quinate hydroxycinnamoyl transferase (HCT)

d. *S. pinnata* shoots

ATID	fold change	effect	Annotation
			Increased expression
AT1G59900.1	2.58	1.18	cold-regulated 47 (COR47)
AT1G68890.1	3.97	1.13	UDP-glucosyl transferase 85A2 (UGT85A2)
AT5G54390.1	26.99	1.08	DOX1
AT4G15530.6	2.56	1.05	unknown protein
AT1G18590.1	4.50	1.02	glutamine-dependent asparagine synthase 1 (ASN1)
AT4G01800.2	2.26	1.01	glycine-rich protein 3 short isoform (GRP3S)
AT5G65220.1	4.87	0.97	cytochrome P450, family 81, subfamily G, polypeptide 1 (CYP81G1)
AT5G64040.1	6.26	0.96	kinectin-related
AT2G38120.1	15.14	0.92	K+ transporter 5 (KT5)
AT1G78860.1	2.14	0.92	Hyaluronan / mRNA binding family
AT5G61290.1	2.16	0.90	Ribosomal L29 family protein
AT1G78630.1	2.69	0.90	glycosylphosphatidylinositol-anchored lipid protein transfer 1 (LTPG1)
AT5G17890.1	1.96	0.88	NADH-dependent glutamate synthase 1 (GLT1)
AT1G08830.2	2.01	0.85	FUNCTIONS IN: molecular_function unknown
AT4G11310.1	2.06	0.84	GLYCINE RICH PROTEIN 7 (ATGRP7)
AT4G13430.1	2.82	0.84	Tudor/PWWP/MBT superfamily protein
AT5G09220.1	2.14	0.83	OBP3-responsive gene 1 (ORG1)
AT1G70890.1	3.52	0.82	UGT85A1
AT2G21660.2	2.08	0.80	DEK domain-containing chromatin associated protein
AT2G28950.1	1.95	0.78	CP5
AT2G38540.1	2.06	0.78	RNA-binding (RRM/RBD/RNP motifs) family protein
AT3G52930.1	1.98	0.77	photosystem II subunit R (PSBR)

AT4G32500.1	2.03	0.77	beta-xylosidase 1 (BXL1)
AT1G75750.2	1.91	0.76	pyruvate orthophosphate dikinase (PPDK)
AT1G22400.1	15.48	0.75	UDP-Glycosyltransferase superfamily protein
AT1G15810.1	1.79	0.75	S15/NS1, RNA-binding protein
AT4G26630.2	2.24	0.74	nitrile specifier protein 5 (NSP5)
AT1G27950.1	2.42	0.71	Tropomyosin-related
AT4G37800.1	1.87	0.70	LOW-TEMPERATURE-INDUCED 65 (LTI65)
AT1G35720.1	2.33	0.70	FUNCTIONS IN: molecular_function unknown
AT4G03050.1	1.71	0.69	aldehyde oxidase 1 (AAO1)
AT5G55660.1	1.85	0.68	PSAN
AT3G12780.1	1.84	0.68	GAST1 protein homolog 1 (GASA1)
AT3G02020.1	1.84	0.67	Pyridine nucleotide-disulphide oxidoreductase family protein
AT5G37770.1	1.80	0.66	myosin 2 (ATM2)
AT3G16470.3	3.42	0.66	nitrate reductase 1 (NIA1)
AT4G13615.1	2.08	0.64	unknown protein
AT1G03630.2	2.31	0.64	cytochrome P450, family 71, subfamily B, polypeptide 2 (CYP71B2)
AT2G31790.1	3.23	0.63	FUNCTIONS IN: molecular_function unknown
AT1G64720.1	1.67	0.62	eukaryotic translation initiation factor 3A (EIF3A)
AT5G46110.4	2.24	0.62	HARMLESS TO OZONE LAYER 1 (HOL1)
AT3G51950.2	2.78	0.62	D-mannose binding lectin protein with Apple-like carbohydrate-binding domain
AT5G48180.1	2.19	0.62	DEK domain-containing chromatin associated protein
AT1G58270.1	48.85	0.62	Papain family cysteine protease
AT2G43100.1	3.60	0.62	unknown protein
AT5G13630.2	1.89	0.61	ortholog of sugar beet HS1 PRO-1 2 (HSPRO2)
AT5G61790.1	2.30	0.61	pseudogene, similar to pathogen- and wound-inducible antifungal protein CBP20 precursor, similar to pathogen- and wound-inducible antifungal protein
		Decreased expression	
AT2G47180.1	0.06	-2.00	Disease resistance protein (TIR-NBS-LRR class) family
AT1G52190.1	0.28	-1.64	Papain family cysteine protease
AT4G13940.4	0.21	-1.59	2-oxoglutarate (2OG) and Fe(II)-dependent oxygenase superfamily protein
AT1G61520.1	0.28	-1.36	extensin 3 (EXT3)
AT2G34210.1	0.31	-1.23	methylthioalkylmalate synthase 1 (MAM1)
AT1G13080.2	0.18	-1.22	branched-chain aminotransferase4 (BCAT4)
AT1G72290.1	0.41	-1.22	cytochrome P450, family 83, subfamily A, polypeptide 1 (CYP83A1)
AT5G56000.1	0.38	-1.10	methionine synthase 2 (MS2)
AT5G26000.1	0.33	-1.08	isopropylmalate isomerase 2 (IPMI2)
AT1G21440.1	0.46	-1.05	Class I glutamine amidotransferase-like superfamily protein
AT3G55700.1	0.08	-1.01	Disease resistance protein (TIR-NBS-LRR class) family
AT3G47340.2	0.25	-1.00	isopropylmalate dehydrogenase 1
AT2G45960.3	0.09	-0.99	Kunitz family trypsin and protease inhibitor protein

AT2G21660.2	0.45	-0.98	beta glucosidase 18 (BGLU18)
AT2G26890.1	0.38	-0.96	O-methyltransferase family protein
AT1G17745.2	0.18	-0.95	cytochrome p450 79f1 (CYP79F1)
AT4G32260.1	0.45	-0.92	phosphate 2 (PHO2)
AT3G03780.3	0.50	-0.92	xyloglucan endotransglucosylase/hydrolase 7 (XTH7)
AT4G17520.1	0.36	-0.89	unknown protein
AT5G53300.4	0.23	-0.84	galactinol synthase 1 (GolS1)
AT4G26690.1	0.41	-0.82	UDP-Glycosyltransferase superfamily protein
AT1G52000.1	0.08	-0.82	AOP3
AT5G64040.1	0.31	-0.82	Auxin-Induced in Root cultures 12 (AIR12)
AT2G05380.2	0.36	-0.80	Mannose-binding lectin superfamily protein
AT2G05520.6	0.45	-0.79	Major facilitator superfamily protein
AT3G54600.1	0.07	-0.78	DA1-related protein 4 (DAR4)
AT1G74090.1	0.17	-0.76	ZW9
AT4G05050.1	0.36	-0.76	APS kinase (APK)
AT3G07390.1	0.16	-0.75	polygalacturonase inhibiting protein 2 (PGIP2)
AT3G58610.3	0.23	-0.73	NOD26-like intrinsic protein 6
AT1G65980.2	0.33	-0.71	Phosphoenolpyruvate carboxylase family protein
AT4G11320.1	0.01	-0.70	TOUCH 2 (TCH2)
AT4G37800.1	0.54	-0.70	PHE ammonia lyase 1 (PAL1)
AT2G32870.1	0.36	-0.69	flavin-monooxygenase glucosinolate S-oxygenase 1 (FMO GS-OX1)
AT5G01220.1	0.49	-0.69	AUXIN RESISTANT 1 (AUX1)
AT3G19710.1	0.43	-0.68	amino acid permease 2 (AAP2)
AT1G51400.1	0.46	-0.68	sulfotransferase 17 (SOT17)
AT1G77760.1	0.24	-0.67	cellulose synthase-like A01 (CSLA01)
AT4G21990.1	0.57	-0.67	glutathione S-transferase PHI 9 (GSTF9)
AT5G20960.2	0.45	-0.66	DNA mismatch repair protein MutS, type 2
AT5G53460.3	0.48	-0.66	Flavin-binding monooxygenase family protein
AT5G52300.2	0.49	-0.66	COBRA (COb)
AT5G54280.2	0.47	-0.66	myb domain protein 28 (MYB28)
AT3G44300.1	0.46	-0.65	glutathione S-transferase TAU 20 (GSTU20)
AT1G19920.1	0.52	-0.64	Plant invertase/pectin methylesterase inhibitor superfamily
AT1G52400.3	0.48	-0.63	APS2
AT5G42530.1	0.57	-0.63	HAL2-like (HL)
AT1G80760.1	0.63	-0.63	PRXR1
AT4G35160.1	0.00	-0.62	Transcription elongation factor Spt5
AT1G65860.1	0.61	-0.62	isopropyl malate isomerase large subunit 1 (IIL1)
AT2G01140.1	0.64	-0.62	glyceraldehyde-3-phosphate dehydrogenase B subunit (GAPb)
AT5G65220.1	0.24	-0.62	pleiotropic drug resistance 1 (PDR1)
AT1G16410.1	0.50	-0.61	Transmembrane amino acid transporter family protein

Table S2.4. Top 100 significant (q-value < 0.005) differentially expressed genes between species in **(a)** roots with 0 µM Se, **(b)** roots with 20 µM Se, **(c)** shoots with 0 µM Se, and **(d)** shoots with 20 µM Se. Fold difference is calculated as the RPKM ratio of *S. pinnata*/*S. elata*. Effect measures the extent by which the treatment affects (increases or decreases) gene expression, and is a more statistically reliable measure of gene response. The effect is on the transformed normalized scale (see methods section for model). (+) or (-) values indicate more or less gene expression in *S. pinnata* relative to *S. elata*, respectively. The larger the absolute value of the effect is, the greater the treatment effect. Effect values were used to separate genes based on expression direction in descending order, with the most differentially expressed on top.

a. Root -Se

ATID	fold change	effect	Annotation
			More expressed
AT3G52930.1	212.56	4.95	Aldolase superfamily protein
AT1G19920.1	111.72	4.68	APS2
AT3G16460.2	221.44	4.44	Mannose-binding lectin superfamily protein
AT2G45960.3	61.89	4.23	plasma membrane intrinsic protein 1B (PIP1b)
AT1G73260.1	31.34	3.97	kunitz trypsin inhibitor 1 (KTI1)
AT1G07890.8	6E+13	3.95	ascorbate peroxidase 1 (APX1)
AT4G36150.1	225.37	3.84	Disease resistance protein (TIR-NBS-LRR class) family
AT2G21045.1	119.45	3.62	Rhodanese/Cell cycle control phosphatase superfamily protein
AT2G01140.1	41.77	3.58	Aldolase superfamily protein
AT4G13940.4	557.14	3.58	HOMOLOGY-DEPENDENT GENE SILENCING 1 (HOG1)
AT5G62700.1	2772.81	3.56	tubulin beta chain 3 (TUB3)
AT5G40780.2	507.39	3.37	lysine histidine transporter 1
AT4G13615.1	460.08	3.31	Uncharacterised protein family SERF
AT5G09810.1	77.26	3.28	actin 7 (ACT7)
AT3G23640.2	74.07	3.28	heteroglycan glucosidase 1 (HGL1)
AT4G16260.1	158.57	3.26	Glycosyl hydrolase superfamily protein
AT4G26690.1	157.74	3.25	SHAVEN 3 (SHV3)
AT2G05380.2	6558.44	3.14	glycine-rich protein 3 short isoform (GRP3S)
AT3G13330.1	120.56	3.12	proteasome activating protein 200 (PA200)
AT2G44790.1	150.33	2.96	uclacyanin 2 (UCC2)

AT4G33720.1	1020.03	2.79	CAP (Cysteine-rich secretory proteins, Antigen 5, and Pathogenesis-related 1 protein) superfamily protein
AT4G19690.2	28.54	2.75	iron-regulated transporter 1 (IRT1)
AT2G25490.1	36.05	2.66	EIN3-binding F box protein 1 (EBF1)
AT3G51950.2	188.20	2.63	Zinc finger (CCCH-type) family protein / RNA recognition motif (RRM)-containing protein
AT2G43610.1	26.38	2.60	Chitinase family protein
AT2G28780.1	34.75	2.57	unknown protein
AT3G28510.1	228.65	2.56	P-loop containing nucleoside triphosphate hydrolases superfamily protein
AT2G25450.1	72.44	2.52	2-oxoglutarate (2OG) and Fe(II)-dependent oxygenase superfamily protein
AT3G52590.1	18.94	2.52	ubiquitin extension protein 1 (UBQ1)
AT4G38920.1	73.31	2.50	vacuolar-type H(+)-ATPase C3 (VHA-C3)
AT5G54090.1	49.56	2.48	DNA mismatch repair protein MutS, type 2
AT1G52400.3	8.56	2.46	beta glucosidase 18 (BGLU18)
AT1G32450.1	9.51	2.42	nitrate transporter 1.5 (NRT1.5)
AT4G10340.1	27.17	2.42	light harvesting complex of photosystem II 5 (LHCB5)
AT3G26200.1	58.23	2.40	cytochrome P450, family 71, subfamily B, polypeptide 22 (CYP71B22)
AT2G46750.1	16.58	2.38	D-arabinono-1,4-lactone oxidase family protein
AT1G08830.2	12.78	2.37	copper/zinc superoxide dismutase 1 (CSD1)
AT5G54770.1	3214.15	2.37	THI1
AT5G13490.2	6.77	2.37	ADP/ATP carrier 2 (AAC2)
AT5G37600.1	15.73	2.35	glutamine synthase clone R1 (GSR 1)
AT2G21660.2	36.39	2.33	GLYCINE RICH PROTEIN 7 (ATGRP7)
AT5G53300.4	7.08	2.32	ubiquitin-conjugating enzyme 10 (UBC10)
AT5G56630.1	22.22	2.31	phosphofructokinase 7 (PFK7)
AT4G21990.1	95.84	2.30	APS reductase 3 (APR3)
AT2G18960.1	5.52	2.29	H(+)-ATPase 1 (HA1)
AT1G19715.3	41.31	2.28	Mannose-binding lectin superfamily protein
AT4G15310.1	5639.31	2.26	cytochrome P450, family 702, subfamily A, polypeptide 3 (CYP702A3)
AT1G32790.2	52.58	2.25	CTC-interacting domain 11 (CID11)
AT1G15690.2	6.51	2.25	AVP1
AT3G62830.2	64.32	2.22	UDP-GLUCURONIC ACID DECARBOXYLASE 2 (UXS2)
AT4G29040.1	59.89	2.22	regulatory particle AAA-ATPase 2A (RPT2a)
AT4G01290.2	36.51	2.19	unknown protein
AT3G02090.2	66.24	2.16	MPPBETA
AT5G64100.1	31.59	2.16	Peroxidase superfamily protein
AT4G33420.1	28.72	2.16	Peroxidase superfamily protein
AT5G19440.1	16.44	2.15	NAD(P)-binding Rossmann-fold superfamily protein
		Less expressed	
AT5G23020.1	0.00	-4.07	2-isopropylmalate synthase 2 (IMS2)
AT3G47470.1	0.00	-4.06	light-harvesting chlorophyll-protein complex I subunit A4 (LHCA4)

AT3G16470.3	0.04	-3.86	JASMONATE RESPONSIVE 1 (JR1)
AT5G13630.2	0.00	-3.71	GENOMES UNCOUPLED 5 (GUN5)
AT1G70850.3	0.06	-3.45	MLP-like protein 34 (MLP34)
AT1G68890.1	0.01	-3.19	magnesium ion binding
AT4G11320.1	0.00	-3.18	Papain family cysteine protease
AT2G26890.1	0.01	-2.98	GRAVITROPISM DEFECTIVE 2 (GRV2)
AT1G45201.1	0.02	-2.91	triacylglycerol lipase-like 1 (TLL1)
AT3G02020.1	0.03	-2.84	aspartate kinase 3 (AK3)
AT5G52040.4	0.02	-2.82	RNA-binding (RRM/RBD/RNP motifs) family protein
AT4G22100.1	0.08	-2.80	beta glucosidase 2 (BGLU3)
AT1G78080.1	0.00	-2.74	related to AP2 4 (RAP2.4)
AT3G03780.3	0.12	-2.69	methionine synthase 2 (MS2)
AT3G26460.1	0.00	-2.68	Polyketide cyclase/dehydrase and lipid transport superfamily protein
AT2G40130.2	0.02	-2.61	Double Clp-N motif-containing P-loop nucleoside triphosphate hydrolases superfamily protein
AT1G52000.1	0.09	-2.60	Mannose-binding lectin superfamily protein
AT3G63200.1	0.03	-2.59	PATATIN-like protein 9 (PLP9)
AT2G38040.2	0.05	-2.57	acetyl Co-enzyme a carboxylase carboxyltransferase alpha subunit (CAC3)
AT4G05050.1	0.05	-2.56	ubiquitin 11 (UBQ11)
AT4G27640.1	0.01	-2.55	ARM repeat superfamily protein
AT1G67090.2	0.02	-2.54	ribulose bisphosphate carboxylase small chain 1A (RBCS1A)
AT1G65860.1	0.04	-2.51	flavin-monooxygenase glucosinolate S-oxygenase 1 (FMO GS-OX1)
AT3G16640.1	0.06	-2.50	translationally controlled tumor protein (TCTP)
AT3G02360.1	0.04	-2.46	6-phosphogluconate dehydrogenase family protein
AT1G09000.1	0.02	-2.43	NPK1-related protein kinase 1 (NP1)
AT1G62770.1	0.03	-2.42	Plant invertase/pectin methylesterase inhibitor superfamily protein
AT5G61790.1	0.04	-2.39	calnexin 1 (CNX1)
AT4G39420.2	0.04	-2.35	unknown protein
AT1G68750.1	0.06	-2.30	phosphoenolpyruvate carboxylase 4 (PPC4)
AT3G19710.1	0.09	-2.30	branched-chain aminotransferase4 (BCAT4)
AT3G54890.4	0.05	-2.30	photosystem I light harvesting complex gene 1 (LHCA1)
AT1G48110.2	0.05	-2.29	evolutionarily conserved C-terminal region 7 (ECT7)
AT1G15820.1	0.03	-2.28	light harvesting complex photosystem II subunit 6 (LHCB6)
AT2G41840.1	0.10	-2.27	Ribosomal protein S5 family protein
AT2G48130.1	0.03	-2.25	Bifunctional inhibitor/lipid-transfer protein/seed storage 2S albumin superfamily protein
AT4G08150.1	0.06	-2.24	KNOTTED-like from Arabidopsis thaliana (KNAT1)
AT5G44790.1	0.05	-2.23	RESPONSIVE-TO-ANTAGONIST 1 (RAN1)
AT5G23010.1	0.16	-2.23	methylthioalkylmalate synthase 1 (MAM1)
AT1G48920.1	0.09	-2.23	nucleolin like 1 (NUC-L1)
AT3G04940.1	0.03	-2.22	cysteine synthase D1 (CYSD1)
AT1G36160.2	0.02	-2.20	acetyl-CoA carboxylase 1 (ACC1)

AT5G59950.5	0.00	-2.18	RNA-binding (RRM/RBD/RNP motifs) family protein
AT5G23110.1	0.01	-2.16	Zinc finger, C3HC4 type (RING finger) family protein

a. Root +Se

ATID	fold change	effect	annotation
			More expressed
AT1G19920.1	160.55	4.80	APS2
AT3G52930.1	125.43	4.56	Aldolase superfamily protein
AT3G16460.2	702.61	4.36	Mannose-binding lectin superfamily protein
AT2G45960.3	73.74	4.08	plasma membrane intrinsic protein 1B (PIP1B)
AT2G21045.1	76.44	3.80	Rhodanese/Cell cycle control phosphatase superfamily protein
AT2G01140.1	82.18	3.70	Aldolase superfamily protein
AT5G62700.1	5E+13	3.61	tubulin beta chain 3 (TUB3)
AT5G40780.2	665.57	3.59	lysine histidine transporter 1
AT2G18960.1	14.56	3.54	H(+)-ATPase 1 (HA1)
AT1G07890.8	5680.91	3.54	ascorbate peroxidase 1 (APX1)
AT3G23640.2	92.39	3.42	heteroglycan glucosidase 1 (HGL1)
AT4G13940.4	442.87	3.39	HOMOLOGY-DEPENDENT GENE SILENCING 1 (HOG1)
AT3G13330.1	191.27	3.30	proteasome activating protein 200 (PA200)
AT4G26690.1	87.77	3.30	SHAVEN 3 (SHV3)
AT4G13615.1	336.52	3.29	Uncharacterised protein family SERF
AT5G09810.1	54.24	3.26	actin 7 (ACT7)
AT4G16260.1	100.14	3.25	Glycosyl hydrolase superfamily protein
AT1G52400.3	25.56	3.25	beta glucosidase 18 (BGLU18)
AT1G73260.1	23.02	3.20	kunitz trypsin inhibitor 1 (KTI1)
AT5G54160.1	12.12	3.13	O-methyltransferase 1 (OMT1)
AT2G43610.1	84.04	3.11	Chitinase family protein
AT2G05380.2	1906.50	3.03	glycine-rich protein 3 short isoform (GRP3S)
AT1G15690.2	15.73	2.94	AVP1
AT1G35720.1	11.14	2.86	annexin 1 (ANNAT1)
AT4G10340.1	33.41	2.83	light harvesting complex of photosystem II 5 (LHCB5)
AT2G44790.1	174.19	2.79	uclacyanin 2 (UCC2)
AT3G09260.1	8.43	2.78	PYK10
AT1G21310.1	9.99	2.78	extensin 3 (EXT3)
AT2G25490.1	50.85	2.74	EIN3-binding F box protein 1 (EBF1)
AT5G54770.1	2E+13	2.73	THI1
AT5G13490.2	10.29	2.71	ADP/ATP carrier 2 (AAC2)
AT3G51950.2	294.60	2.64	Zinc finger (CCCH-type) family protein / RNA recognition motif (RRM)-containing protein
AT1G19715.3	36.94	2.61	Mannose-binding lectin superfamily protein

AT5G37600.1	17.88	2.59	glutamine synthase clone R1 (GSR 1)
AT2G37040.1	8.65	2.49	PHE ammonia lyase 1 (PAL1)
AT3G12500.1	27.49	2.49	basic chitinase (HCHIB)
AT3G26200.1	35.26	2.41	cytochrome P450, family 71, subfamily B, polypeptide 22 (CYP71B22)
AT4G21990.1	120.75	2.40	APS reductase 3 (APR3)
AT4G38920.1	44.43	2.39	vacuolar-type H(+)-ATPase C3 (VHA-C3)
AT2G46750.1	11.64	2.38	D-arabinono-1,4-lactone oxidase family protein
AT1G32790.2	111.59	2.35	CTC-interacting domain 11 (CID11)
AT1G75220.1	182.66	2.31	Major facilitator superfamily protein
AT3G62830.2	62.93	2.30	UDP-GLUCURONIC ACID DECARBOXYLASE 2 (UXS2)
AT5G41670.2	26.51	2.29	6-phosphogluconate dehydrogenase family protein
AT3G47730.1	12.53	2.29	ATP-binding cassette A2 (ABCA2)
AT1G59900.1	51.81	2.28	pyruvate dehydrogenase complex E1 alpha subunit (E1 ALPHA)
AT2G21660.2	26.29	2.27	GLYCINE RICH PROTEIN 7 (ATGRP7)
AT1G66580.1	9.12	2.25	senescence associated gene 24 (SAG24)
AT1G50010.1	6.08	2.23	tubulin alpha-2 chain (TUA2)
AT5G40510.1	28.39	2.23	Sucrase/ferredoxin-like family protein
AT4G15530.6	61.16	2.23	pyruvate orthophosphate dikinase (PPDK)
AT2G28780.1	23.28	2.23	unknown protein
AT1G32450.1	8.24	2.22	nitrate transporter 1.5 (NRT1.5)
AT2G15620.1	12.72	2.21	nitrite reductase 1 (NIR1)
AT3G28510.1	76.53	2.20	P-loop containing nucleoside triphosphate hydrolases superfamily protein
AT5G53300.4	6.18	2.20	ubiquitin-conjugating enzyme 10 (UBC10)
AT5G64100.1	20.75	2.17	Peroxidase superfamily protein
AT4G29010.1	47.35	2.13	ABNORMAL INFLORESCENCE MERISTEM (AIM1)
AT3G58610.3	8.89	2.13	ketol-acid reductoisomerase
AT1G20440.1	10.51	2.12	cold-regulated 47 (COR47)
			Less expressed
AT3G41768.1	0.08	-3.67	18SrRNA
AT1G65860.1	0.02	-3.42	flavin-monooxygenase glucosinolate S-oxygenase 1 (FMO GS-OX1)
AT5G13630.2	0.00	-3.35	GENOMES UNCOUPLED 5 (GUN5)
AT1G68890.1	0.01	-3.21	magnesium ion binding
AT3G47470.1	0.00	-3.21	light-harvesting chlorophyll-protein complex I subunit A4 (LHCA4)
AT2G26890.1	0.01	-3.14	GRAVITROPISM DEFECTIVE 2 (GRV2)
AT1G09000.1	0.01	-3.13	NPK1-related protein kinase 1 (NP1)
AT1G78080.1	0.00	-3.11	related to AP2 4 (RAP2.4)
AT1G45201.1	0.02	-3.04	triacylglycerol lipase-like 1 (TLL1)
AT5G23110.1	0.01	-2.92	Zinc finger, C3HC4 type (RING finger) family protein
AT4G22100.1	0.09	-2.91	beta glucosidase 2 (BGLU3)
AT5G23020.1	0.01	-2.90	2-isopropylmalate synthase 2 (IMS2)
AT3G16640.1	0.05	-2.84	translationally controlled tumor protein (TCTP)

AT5G52040.4	0.01	-2.82	RNA-binding (RRM/RBD/RNP motifs) family protein
AT4G39420.2	0.03	-2.82	unknown protein
AT3G16470.3	0.09	-2.80	JASMONATE RESPONSIVE 1 (JR1)
AT3G02020.1	0.05	-2.78	aspartate kinase 3 (AK3)
AT2G36420.1	0.04	-2.78	unknown protein
AT1G70850.3	0.11	-2.76	MLP-like protein 34 (MLP34)
AT5G49660.1	0.07	-2.59	Leucine-rich repeat transmembrane protein kinase family protein
AT2G46950.1	0.04	-2.54	cytochrome P450, family 709, subfamily B, polypeptide 2 (CYP709B2)
AT2G07709.1	0.04	-2.53	pseudogene, similar to NADH dehydrogenase
AT4G02660.1	0.00	-2.45	Beige/BEACH domain
AT3G63520.1	0.09	-2.44	carotenoid cleavage dioxygenase 1 (CCD1)
AT5G02770.1	0.01	-2.36	unknown protein
AT3G03780.3	0.15	-2.35	methionine synthase 2 (MS2)
AT5G04380.1	0.03	-2.35	S-adenosyl-L-methionine-dependent methyltransferases superfamily protein
AT4G01120.1	0.01	-2.34	G-box binding factor 2 (GBF2)
AT3G28730.1	0.03	-2.28	high mobility group (HMG)
AT3G22968.1	0.10	-2.25	conserved peptide upstream open reading frame 59 (CPuORF59)
AT1G67090.2	0.04	-2.23	ribulose bisphosphate carboxylase small chain 1A (RBCS1A)
AT1G15820.1	0.04	-2.23	light harvesting complex photosystem II subunit 6 (LHCB6)
AT2G48130.1	0.03	-2.21	Bifunctional inhibitor/lipid-transfer protein/seed storage 2S albumin superfamily protein
AT1G68750.1	0.07	-2.21	phosphoenolpyruvate carboxylase 4 (PPC4)
AT5G49930.1	0.05	-2.20	embryo defective 1441 (emb1441)
AT2G40130.2	0.04	-2.18	Double Clp-N motif-containing P-loop nucleoside triphosphate hydrolases superfamily protein
AT1G36160.2	0.03	-2.18	acetyl-CoA carboxylase 1 (ACC1)
AT4G08150.1	0.08	-2.16	KNOTTED-like from Arabidopsis thaliana (KNAT1)
AT3G55460.1	0.06	-2.16	SC35-like splicing factor 30 (SCL30)
AT3G56990.1	0.01	-2.16	embryo sac development arrest 7 (EDA7)

c. Shoot –Se

ATID	fold change	effect	annotation
			More expressed
AT5G54770.1	2.44E+14	5.73	THI1
AT4G10340.1	84.26	5.68	light harvesting complex of photosystem II 5 (LHCB5)
AT2G05100.1	10199.15	5.44	photosystem II light harvesting complex gene 2.1 (LHCB2.1)
AT4G11310.1	78.24	4.22	Papain family cysteine protease
AT2G45960.3	73.51	4.13	plasma membrane intrinsic protein 1B (PIP1b)
AT1G60950.1	25.12	3.75	FED A
AT1G07890.8	5E+13	3.67	ascorbate peroxidase 1 (APX1)

AT5G62700.1	2288.39	3.63	tubulin beta chain 3 (TUB3)
AT2G34410.2	149.25	3.50	O-acetyltransferase family protein
AT5G09810.1	122.16	3.48	actin 7 (ACT7)
AT1G73260.1	918.65	3.45	kunitz trypsin inhibitor 1 (KTI1)
AT1G03630.2	107.21	3.43	protochlorophyllide oxidoreductase C (POR C)
AT2G25450.1	660.28	3.28	2-oxoglutarate (2OG) and Fe(II)-dependent oxygenase superfamily protein
AT4G03280.2	18.76	3.25	photosynthetic electron transfer C (PETC)
AT1G15810.1	74.17	3.19	S15/NS1, RNA-binding protein
AT3G52930.1	99.82	3.10	Aldolase superfamily protein
AT4G13615.1	314.24	3.05	Uncharacterised protein family SERF
AT3G54600.1	11.04	3.04	Class I glutamine amidotransferase-like superfamily protein
AT1G72600.2	13.09	3.00	hydroxyproline-rich glycoprotein family protein
AT4G37800.1	14.28	2.99	xyloglucan endotransglucosylase/hydrolase 7 (XTH7)
AT1G78630.1	24.98	2.98	embryo defective 1473 (emb1473)
AT2G38540.1	15.02	2.96	lipid transfer protein 1 (LP1)
AT1G74090.1	23.70	2.95	desulfo-glucosinolate sulfotransferase 18 (SOT18)
AT3G51950.2	450.85	2.93	Zinc finger (CCCH-type) family protein / RNA recognition motif (RRM)-containing protein
AT4G13940.4	532.49	2.92	HOMOLOGY-DEPENDENT GENE SILENCING 1 (HOG1)
AT3G12780.1	31.37	2.89	phosphoglycerate kinase 1 (PGK1)
AT4G21960.1	9.70	2.86	PRXR1
AT2G01140.1	43.74	2.86	Aldolase superfamily protein
AT2G05380.2	108.12	2.84	glycine-rich protein 3 short isoform (GRP3S)
AT4G38920.1	78.55	2.72	vacuolar-type H(+)-ATPase C3 (VHA-C3)
AT4G26690.1	43.00	2.72	SHAVEN 3 (SHV3)
AT2G46820.2	80.46	2.72	photosystem I P subunit (PSI-P)
AT1G08830.2	18.67	2.70	copper/zinc superoxide dismutase 1 (CSD1)
AT1G51400.1	88.96	2.69	Photosystem II 5 kD protein
AT1G21310.1	30.12	2.68	extensin 3 (EXT3)
AT1G42970.1	8.03	2.67	glyceraldehyde-3-phosphate dehydrogenase B subunit (GAPb)
AT3G44300.1	2E+13	2.64	nitrilase 2 (NIT2)
AT5G46110.4	7.90	2.64	ACCLIMATION OF PHOTOSYNTHESIS TO ENVIRONMENT 2 (APE2)
AT1G35720.1	9.13	2.63	annexin 1 (ANNAT1)
AT2G25490.1	33.73	2.61	EIN3-binding F box protein 1 (EBF1)
AT1G52400.3	12.78	2.60	beta glucosidase 18 (BGLU18)
AT1G70830.4	32.31	2.60	MLP-like protein 28 (MLP28)
AT4G28750.1	9.41	2.59	PSA E1 KNOCKOUT (PSAE-1)
AT5G56000.1	9.28	2.57	HEAT SHOCK PROTEIN 81.4 (Hsp81.4)
AT1G65980.2	102.19	2.55	thioredoxin-dependent peroxidase 1 (TPX1)
AT1G20440.1	31.28	2.52	cold-regulated 47 (COR47)
AT3G52590.1	23.43	2.52	ubiquitin extension protein 1 (UBQ1)

AT1G70890.1	25.40	2.48	MLP-like protein 43 (MLP43)
AT4G35160.1	115.74	2.43	O-methyltransferase family protein
AT2G21660.2	63.30	2.42	GLYCINE RICH PROTEIN 7 (ATGRP7)
AT4G21990.1	128.86	2.42	APS reductase 3 (APR3)
AT2G30670.1	158.83	2.41	NAD(P)-binding Rossmann-fold superfamily protein
AT2G05520.6	9.29	2.39	glycine-rich protein 3 (GRP-3)
AT3G13330.1	43.92	2.38	proteasome activating protein 200 (PA200)
AT2G28950.1	17.56	2.35	expansin A6 (EXPA6)
AT2G26900.1	11.69	2.34	Sodium Bile acid symporter family
AT4G36150.1	54.21	2.34	Disease resistance protein (TIR-NBS-LRR class) family
AT1G17745.2	29.55	2.33	D-3-phosphoglycerate dehydrogenase
AT2G13360.1	332.27	2.31	alanine:glyoxylate aminotransferase (AGT)
AT3G58610.3	7.55	2.31	ketol-acid reductoisomerase
AT1G59900.1	20.70	2.30	pyruvate dehydrogenase complex E1 alpha subunit (E1 ALPHA)
AT5G54390.1	17.46	2.30	HAL2-like (HL)
AT2G40100.1	117.81	2.30	light harvesting complex photosystem II (LHCB4.3)
AT5G53300.4	7.11	2.28	ubiquitin-conjugating enzyme 10 (UBC10)
		Less expressed	
AT3G47470.1	0.00	-6.69	light-harvesting chlorophyll-protein complex I subunit A4 (LHCA4)
AT5G13630.2	0.00	-5.25	GENOMES UNCOUPLED 5 (GUN5)
AT4G35090.2	0.00	-4.21	catalase 2 (CAT2)
AT2G46950.1	0.01	-4.02	cytochrome P450, family 709, subfamily B, polypeptide 2 (CYP709B2)
AT4G32260.1	0.00	-3.86	ATPase, F0 complex, subunit B/B', bacterial/chloroplast
AT5G23020.1	0.01	-3.75	2-isopropylmalate synthase 2 (IMS2)
AT1G67090.2	0.07	-3.57	ribulose bisphosphate carboxylase small chain 1A (RBCS1A)
AT1G68890.1	0.01	-3.57	magnesium ion binding
AT5G54270.1	0.00	-3.53	light-harvesting chlorophyll B-binding protein 3 (LHCB3)
AT1G15820.1	0.04	-3.53	light harvesting complex photosystem II subunit 6 (LHCB6)
AT1G61520.3	0.00	-3.44	photosystem I light harvesting complex gene 3 (LHCA3)
AT5G26000.1	0.01	-3.40	thioglucoside glucohydrolase 1 (TGG1)
AT4G11960.2	0.00	-3.01	PGR5-like B (PGRL1b)
AT3G23800.1	0.00	-2.90	selenium-binding protein 3 (SBP3)
AT5G52040.4	0.01	-2.90	RNA-binding (RRM/RBD/RNP motifs) family protein
AT3G04940.1	0.01	-2.87	cysteine synthase D1 (CYSD1)
AT1G61520.1	0.08	-2.83	photosystem I light harvesting complex gene 3 (LHCA3)
AT2G26890.1	0.01	-2.80	GRAVITROPISM DEFECTIVE 2 (GRV2)
AT1G52340.1	0.02	-2.75	ABA DEFICIENT 2 (ABA2)
AT2G32870.1	0.04	-2.74	TRAF-like family protein
AT3G59780.1	0.05	-2.63	Rhodanese/Cell cycle control phosphatase superfamily protein
AT4G22100.1	0.10	-2.63	beta glucosidase 2 (BGLU3)
AT3G54890.4	0.14	-2.61	photosystem I light harvesting complex gene 1 (LHCA1)

AT3G02020.1	0.04	-2.59	aspartate kinase 3 (AK3)
AT1G79040.1	0.13	-2.56	photosystem II subunit R (PSBR)
AT5G02020.2	0.02	-2.52	unknown protein
AT4G05050.1	0.07	-2.50	ubiquitin 11 (UBQ11)
AT5G58070.1	0.05	-2.50	temperature-induced lipocalin (TIL)
AT5G01220.1	0.08	-2.46	sulfoquinovosyldiacylglycerol 2 (SQD2)
AT5G40450.1	0.13	-2.45	unknown protein
AT3G16470.3	0.05	-2.42	JASMONATE RESPONSIVE 1 (JR1)
AT1G09000.1	0.02	-2.39	NPK1-related protein kinase 1 (NP1)
AT2G38040.2	0.08	-2.37	acetyl Co-enzyme a carboxylase carboxyltransferase alpha subunit (CAC3)
AT1G55480.1	0.02	-2.35	protein containing PDZ domain, a K-box domain, and a TPR region (ZKT)
AT5G61790.1	0.04	-2.35	calnexin 1 (CNX1)
AT4G01800.2	0.00	-2.30	Albino or Glassy Yellow 1 (AGY1)

d. Shoot +Se

ATID	fold change	effect	annotation
			More expressed
AT2G05100.1	51346.62	5.96	photosystem II light harvesting complex gene 2.1 (LHCB2.1)
AT5G54770.1	3E+14	5.90	THI1
AT4G10340.1	98.55	5.88	light harvesting complex of photosystem II 5 (LHCB5)
AT2G45960.3	74.83	4.02	plasma membrane intrinsic protein 1B (PIP1b)
AT1G15810.1	118.46	3.90	S15/NS1, RNA-binding protein
AT2G05380.2	260.92	3.86	glycine-rich protein 3 short isoform (GRP3S)
AT1G03630.2	169.98	3.80	protochlorophyllide oxidoreductase C (POR C)
AT5G62700.1	5161.80	3.79	tubulin beta chain 3 (TUB3)
AT2G38540.1	35.04	3.76	lipid transfer protein 1 (LP1)
AT1G20440.1	75.89	3.68	cold-regulated 47 (COR47)
AT2G34410.2	160.14	3.68	O-acetyltransferase family protein
AT1G60950.1	21.81	3.60	FED A
AT4G13615.1	522.75	3.59	Uncharacterised protein family SERF
AT5G09810.1	137.20	3.55	actin 7 (ACT7)
AT1G78630.1	34.33	3.39	embryo defective 1473 (emb1473)
AT4G03280.2	20.33	3.33	photosynthetic electron transfer C (PETC)
AT2G21660.2	148.40	3.29	GLYCINE RICH PROTEIN 7 (ATGRP7)
AT1G07890.8	4E+14	3.24	ascorbate peroxidase 1 (APX1)
AT2G05520.6	20.64	3.21	glycine-rich protein 3 (GRP-3)
AT1G74090.1	24.36	3.10	desulfo-glucosinolate sulfotransferase 18 (SOT18)
AT4G35160.1	242.86	3.02	O-methyltransferase family protein
AT3G12780.1	34.00	2.98	phosphoglycerate kinase 1 (PGK1)

AT1G51400.1	71.56	2.97	Photosystem II 5 kD protein
AT4G28750.1	11.29	2.89	PSA E1 KNOCKOUT (PSAE-1)
AT5G56000.1	12.25	2.87	HEAT SHOCK PROTEIN 81.4 (Hsp81.4)
AT3G52590.1	35.57	2.87	ubiquitin extension protein 1 (UBQ1)
AT3G52930.1	89.02	2.86	Aldolase superfamily protein
AT1G75750.2	79.58	2.80	GAST1 protein homolog 1 (GASA1)
AT1G72600.2	12.19	2.80	hydroxyproline-rich glycoprotein family protein
AT4G11310.1	38.14	2.80	Papain family cysteine protease
AT4G13940.4	502.80	2.79	HOMOLOGY-DEPENDENT GENE SILENCING 1 (HOG1)
AT4G21990.1	207.58	2.78	APS reductase 3 (APR3)
AT1G73260.1	93.49	2.72	kunitz trypsin inhibitor 1 (KTI1)
AT2G30670.1	221.07	2.70	NAD(P)-binding Rossmann-fold superfamily protein
AT3G51950.2	238.95	2.64	Zinc finger (CCCH-type) family protein / RNA recognition motif (RRM)-containing protein
AT2G01140.1	34.30	2.63	Aldolase superfamily protein
AT1G75350.1	388.13	2.56	embryo defective 2184 (emb2184)
AT1G35720.1	8.15	2.56	annexin 1 (ANNAT1)
AT5G53300.4	8.85	2.51	ubiquitin-conjugating enzyme 10 (UBC10)
AT1G70890.1	38.34	2.49	MLP-like protein 43 (MLP43)
AT1G08830.2	19.14	2.48	copper/zinc superoxide dismutase 1 (CSD1)
AT4G34350.1	9.32	2.46	4-hydroxy-3-methylbut-2-enyl diphosphate reductase (HDR)
AT1G15340.2	278.76	2.46	methyl-CPG-binding domain 10 (MBD10)
AT2G13360.1	268.41	2.42	alanine:glyoxylate aminotransferase (AGT)
AT1G20693.3	9.24	2.42	high mobility group B2 (HMGB2)
AT1G59900.1	21.70	2.40	pyruvate dehydrogenase complex E1 alpha subunit (E1 ALPHA)
AT1G70830.4	28.20	2.39	MLP-like protein 28 (MLP28)
AT1G17745.2	28.21	2.35	D-3-phosphoglycerate dehydrogenase
AT5G46110.4	6.22	2.31	ACCLIMATION OF PHOTOSYNTHESIS TO ENVIRONMENT 2 (APE2)
AT2G26900.1	12.49	2.30	Sodium Bile acid symporter family
AT3G58610.3	7.19	2.30	ketol-acid reductoisomerase
AT5G53450.2	15.59	2.29	OBP3-responsive gene 1 (ORG1)
AT4G38920.1	66.02	2.29	vacuolar-type H(+)-ATPase C3 (VHA-C3)
AT4G37800.1	9.14	2.27	xyloglucan endotransglucosylase/hydrolase 7 (XTH7)
AT5G52300.2	13.41	2.23	LOW-TEMPERATURE-INDUCED 65 (LTI65)
			Less expressed
AT3G47470.1	0.00	-7.05	light-harvesting chlorophyll-protein complex I subunit A4 (LHCA4)
AT5G13630.2	0.00	-5.84	GENOMES UNCOUPLED 5 (GUN5)
AT4G35090.2	0.00	-4.34	catalase 2 (CAT2)
AT2G46950.1	0.01	-4.20	cytochrome P450, family 709, subfamily B, polypeptide 2 (CYP709B2)
AT4G32260.1	0.00	-3.76	ATPase, F0 complex, subunit B/B', bacterial/chloroplast
AT5G54270.1	0.00	-3.76	light-harvesting chlorophyll B-binding protein 3 (LHCB3)
AT1G67090.2	0.06	-3.75	ribulose bisphosphate carboxylase small chain 1A (RBCS1A)

AT5G23020.1	0.00	-3.74	2-isopropylmalate synthase 2 (IMS2)
AT1G61520.3	0.00	-3.56	photosystem I light harvesting complex gene 3 (LHCA3)
AT1G15820.1	0.06	-3.34	light harvesting complex photosystem II subunit 6 (LHCB6)
AT1G68890.1	0.02	-3.13	magnesium ion binding
AT1G61520.1	0.06	-3.06	photosystem I light harvesting complex gene 3 (LHCA3)
AT4G11960.2	0.00	-3.04	PGR5-like B (PGRL1b)
AT2G26890.1	0.01	-2.99	GRAVITROPISM DEFECTIVE 2 (GRV2)
AT1G62380.1	0.08	-2.89	ACC oxidase 2 (ACO2)
AT3G02020.1	0.01	-2.89	aspartate kinase 3 (AK3)
AT3G03780.3	0.10	-2.85	methionine synthase 2 (MS2)
AT4G05050.1	0.04	-2.83	ubiquitin 11 (UBQ11)
AT1G52340.1	0.02	-2.82	ABA DEFICIENT 2 (ABA2)
AT3G59780.1	0.03	-2.72	Rhodanese/Cell cycle control phosphatase superfamily protein
AT5G52040.4	0.02	-2.66	RNA-binding (RRM/RBD/RNP motifs) family protein
AT3G04940.1	0.01	-2.65	cysteine synthase D1 (CYSD1)
AT5G26000.1	0.02	-2.61	thioglucoside glucohydrolase 1 (TGG1)
AT1G54780.1	0.00	-2.56	TLP18.3
AT4G03050.1	0.01	-2.55	AOP3
AT1G01790.1	0.02	-2.53	K+ efflux antiporter 1 (KEA1)
AT2G32870.1	0.06	-2.49	TRAF-like family protein
AT4G19840.1	0.08	-2.47	phloem protein 2-A1 (PP2-A1)
AT3G19710.1	0.06	-2.39	branched-chain aminotransferase4 (BCAT4)
AT1G55480.1	0.02	-2.36	protein containing PDZ domain, a K-box domain, and a TPR region (ZKT)
AT1G09000.1	0.02	-2.35	NPK1-related protein kinase 1 (NP1)
AT1G16410.1	0.04	-2.34	cytochrome p450 79f1 (CYP79F1)
AT5G02020.2	0.03	-2.32	unknown protein
AT4G22100.1	0.13	-2.32	beta glucosidase 2 (BGLU3)
AT5G58070.1	0.07	-2.32	temperature-induced lipocalin (TIL)
AT3G23800.1	0.00	-2.31	selenium-binding protein 3 (SBP3)
AT5G23010.1	0.13	-2.30	methylthioalkylmalate synthase 1 (MAM1)
AT3G25920.1	0.05	-2.30	ribosomal protein L15 (RPL15)
AT5G49660.1	0.05	-2.28	Leucine-rich repeat transmembrane protein kinase family protein
AT4G01800.2	0.00	-2.26	Albino or Glassy Yellow 1 (AGY1)
AT5G01220.1	0.11	-2.26	sulfoquinovosyldiacylglycerol 2 (SQD2)
AT3G63520.1	0.13	-2.26	carotenoid cleavage dioxygenase 1 (CCD1)
AT4G39420.2	0.04	-2.26	unknown protein
AT2G38040.2	0.11	-2.25	acetyl Co-enzyme a carboxylase carboxyltransferase alpha subunit (CAC3)
AT5G61790.1	0.05	-2.25	calnexin 1 (CNX1)

REFERENCES

Altschul, S. F., T. L. Madden, A. A. Schäffer, J. Zhang, Z. Zhang, W. Miller and D. J. Lipman. 1997. Gapped BLAST and PSI-BLAST: a new generation of protein database search programs. *Nucleic Acids Research* 25: 3389-3402.

Banuelos GS, Ajwa HA, Mackey B, Wu L, Cook C, Akohoue S, Zambruzuski S. 1997. Evaluation of different plant species used for phytoremediation of high soil selenium. *Journal of Environmental Quality* 26: 639-646.

Banuelos GS, Da Roche J, Robinson J. 2010. Developing selenium-enriched animal feed and biofuel from canola planted for managing Se-laden drainage waters in the westside of central California. *International Journal of Phytoremediation* 12: 243-254.

Benjamini Y, Hochberg Y. 1995. Controlling the false discovery rate: a practical and powerful approach to multiple testing. *Journal of the Royal Statistical Society* (Series B) 57: 289-300.

Bick JA, Leustek T. 1998. Plant sulfur metabolism - the reduction of sulfate to sulfite. *Current Opinion in Plant Biology* 1: 240-244.

Birke H, Haas FH, De Kok LJ, Balk J, Wirtz M, Hell R. 2012. Cysteine biosynthesis, in concert with a novel mechanism, contributes to sulfide detoxification in mitochondria of *Arabidopsis thaliana*. *Biochemical Journal* 445: 275-283.

Bohrer AS, Yoshimoto N, Sekiguchi A, Rykulski N, Saito K, Takahashi H. 2014. Alternative translational initiation of ATP sulfurylase underlying dual localization of sulfate assimilation pathways in plastids and cytosol in *Arabidopsis thaliana*. *Frontiers in Plant Science* 5.

Brown TA, Shrift A. 1981. Exclusion of selenium from proteins of selenium-tolerant Astragalus species. *Plant Physiology* 67: 1051-1053.

Buschges R, Hollricher K, Panstruga R, Simons G, Wolter M, Frijters A, vanDaelen R, vanderLee T, Diergaarde P, Groenendijk J, Topsch S, Vos P, Salamini F, Schulze-Lefert P. 1997. The barley mlo gene: A novel control element of plant pathogen resistance. *Cell* 88: 695-705.

Cakir O, Ari S. 2013. Cloning and molecular characterization of selenocysteine methyltransferase (AchSMT) cDNA from *Astragalus chrysochlorus*. *Plant Omics* 6: 100-106.

Cao MJ, Wang Z, Wirtz M, Hell R, Oliver DJ, Xiang CB. 2013. SULTR3;1 is a chloroplast

localized sulfate transporter in *Arabidopsis thaliana*. *Plant Journal* 73: 607-616.

Cappa JJ, Cappa PJ, El Mehdawi AF, McAleer JM, Simmons MP, Pilon-Smits EAH. 2014. Characterization of selenium and sulfur accumulation across the genus Stanleya (Brassicaceae): a field survey and common-garden experiment. *American Journal of Botany* 101: 830-839.

Cappa JJ, Yetter C, Fakra S, Cappa PJ, DeTar R, Landes C, Pilon-Smits EAH, Simmons MP. 2015. Evolution of selenium hyperaccumulation in Stanleya (Brassicaceae) as inferred from phylogeny, physiology and X-ray microprobe analysis. *New Phytologist* 205: 583-595.

Chalutz E. 1973. Ethylene-induced phenylalanine ammonia-lyase activity in carrot roots. *Plant physiology* 51: 1033-1036.

Chao QM, Rothenberg M, Solano R, Roman G, Terzaghi W, Ecker JR. 1997. Activation of the ethylene gas response pathway in Arabidopsis by the nuclear protein ETHYLENE-INSENSITIVE3 and related proteins. *Cell* 89: 1133-1144.

Chen Z, Zheng Z, Huang J, Lai Z, Fan B. 2009. Biosynthesis of salicylic acid in plants. *Plant Signaling & Behavior* 4: 493-496.

El Kassis E, Cathala N, Rouached H, Fourcroy P, Berthomieu P, Terry N, Davidian JC. 2007. Characterization of a selenate-resistant Arabidopsis mutant. Root growth as a potential target for selenate toxicity. *Plant Physiology* 143: 1231-1241.

El Mehdawi AF, Cappa JJ, Fakra SC, Self J, Pilon-Smits EAH. 2012. Interactions of Selenium and Non-accumulators during Co-cultivation on Seleniferous or Non-Seleniferous Soil – The Importance of Having Good Neighbors. *New Phytologist* 194: 264-277.

Eshdat Y, Holland D, Faltin Z, BenHayyim G. 1997. Plant glutathione peroxidases. *Physiologia Plantarum* 1997: 234-240.

Fassel VA. 1978. Quantitative elemental analyses by plasma emission spectroscopy. *Science* 202: 183–191.

Foster LH, Sumar S. 1997. Selenium in health and disease: *Critical Reviews in Food Science and Nutrition* 37: 211-228.

Freeman JL, Zhang LH, Marcus MA, Fakra S, McGrath SP, Pilon-Smits EAH. 2006. Spatial imaging, speciation, and quantification of selenium in the hyperaccumulator plants *Astragalus bisulcatus* and *Stanleya pinnata*. *Plant Physiology* 142: 124-134.

Freeman JL, Lindblom SD*, Quinn CF, Fakra S, Marcus MA, Pilon-Smits EAH. 2007. Selenium accumulation protects plants from herbivory by Orthoptera due to toxicity and deterrence. *New Phytologist* 175: 490-500.

Freeman JL, Quinn CF, Lindblom SD, Klamper EM, Pilon-Smits EAH. 2009. Selenium protects the hyperaccumulator *Stanleya pinnata* against black-tailed prairie dog herbivory in native seleniferous habitats. *American Journal of Botany* 96: 1075-1085.

Freeman JL, Tamaoki M, Stushnoff C, Quinn CF, Cappa JJ, Devonshire J, Fakra SC, Marcus MA, McGrath SP, Hoewyk DV, Pilon-Smits EAH. 2010. Molecular mechanisms of selenium tolerance and hyperaccumulation in *Stanleya pinnata*. *Plant Physiology* 153: 1630-1652.

Galeas ML, Zhang LH, Freeman JL, Wegner M, Pilon-Smits EAH. 2007. Seasonal fluctuations of selenium and sulfur accumulation in selenium hyperaccumulators and related nonaccumulators. *New Phytologist* 173: 517-525.

Geering HR, Cary EE, Jones L HP, Allaway WH. 1968. Solubility and redox criteria for the possible forms of selenium in soils. *Soil Science Society of America Proceedings* 32: 35-40.

Gentleman R, Carey VJ, Huber W, Irizarry RA, and Dudoit S. 2005. Bioinformatics and computational biology solutions using R and Bioconductor. Spring-Verlag New York.

Grabherr MG, Haas BJ, Yassour M, Levin JZ, Thompson DA, Amit I, Adiconis X, Fan L, Raychowdhury R, Zeng Q, Chen Z, Mauceli E, Hacohen N, Gnirke A, Rhind N, di Palma F, Birren BW, Nusbaum C, Lindblad-Toh K, Friedman N, Regev A. 2011. Full-length transcriptome assembly from RNA-seq data without a reference genome. *Nature Biotechnology* 297: 644-52.

Grebner W, Stingl NE, Oenel A, Mueller MJ, Berger S. 2013. Lipoxygenase6-Dependent Oxylipin Synthesis in Roots Is Required for Abiotic and Biotic Stress Resistance of Arabidopsis. *American Society of Plant Biologists* 161: 2159-2170.

Hanson BR, Lindblom SD, Loeffler ML, Pilon-Smits EAH. 2004. Selenium protects plants from phloem-feeding aphids due to both deterrence and toxicity. *New Phytologist* 162: 655-662.

Hsieh HS, Ganther HE. 1975. Acid-volatile selenium formation catalyzed by glutathione reductase. *Biochemistry* 14: 1631-1636.

James F, Nolte KD, Hanson AD. 1995. Purification and properties of S-Adenosyl-L methionine: L-Methionine S-Methyltransferase from *Wollastonia biflora* leaves. *The Journal of Biological Chemistry* 270: 22344-22350.

Johnson C, Boden E, Arias J. 2003. Salicylic acid and NPR1 induce the recruitment of trans-activating TGA factors to a defense gene promoter in Arabidopsis. *Plant Cell* 8: 1846-1858.

Kataoka T, Hayashi N, Yamaya T, Takahashi H. 2004. Root-to-shoot transport of sulfate in Arabidopsis. Evidence for the role of SULTR3;5 as a component of low-affinity sulfate transport system in the root vasculature. *Plant Physiology* 136: 4198-4204.

Kawashima CG, Berkowitz O, Hell R, Noji M, Saito K. 2005. Characterization and expression analysis of a serine acetyltransferase gene family involved in a key step of the sulfur assimilation pathway in Arabidopsis. *Plant Physiology* 137: 220-230.

Kawashima CG, Yoshimoto N, Maruyama-Nakashita A, Tsuchiya YN, Saito K, Takahashi H, Dalmay T. 2009. Sulphur starvation induces the expression of microRNA-395 and one of its target genes but in different cell types. *Plant Journal* 57: 313-321.

Kawashima CG, Matthewman CA, Huang SQ, Lee BR, Yoshimoto N, Koprivova A, Rubio Somoza I, Todesco M, Rathjen T, Saito K, Takahashi H, Dalmay T, Kopriva S. 2011. Interplay of SLIM1 and miR395 in the regulation of sulfate assimilation in Arabidopsis. *Plant Journal* 66: 863-876.

Kim MC, Panstruga R, Elliott C, Müller J, Devoto A, Yoon HW, Park HC, Cho MJ, Schulze Lefert P. 2002. Calmodulin interacts with MLO protein to regulate defense against mildew in barley. *Nature* 416: 447-51.

Krueger S, Niehl A, Martin MC, Steinhauser D, Donath A, Hildebrandt T, Romero LC, Hoefgen R, Gotor C, Hesse H. 2009. Analysis of cytosolic and plastidic serine acetyltransferase mutants and subcellular metabolite distributions suggests interplay of the cellular compartments for cysteine biosynthesis in Arabidopsis. *Plant Cell and Environment* 32: 349-367.

Laurie-Berry N, Joardar V, Street IH, Kunkel BN. 2006. The *Arabidopsis thaliana* JASMONATE INSENSITIVE 1 gene is required for suppression of salicylic acid-dependent defenses during infection by *Pseudomonas syringae*. *Molecular Plant-Microbe Interactions* 19:789-800.

Leon-Reyes A, Du Y, Koornneef A, Proietti S, Körbes AP, Memelink J, Pieterse CMJ, Ritsema T. 2010. Ethylene signaling renders the jasmonate response of Arabidopsis insensitive to future suppression by salicylic acid. *Molecular Plant-Microbe Interactions* 23: 187-197.

Leves FP, Tierney ML, Howitt SM. 2008. Polar residues in a conserved motif spanning helices 1 and 2 are functionally important in the *SulP* transporter family. *The International Journal of Biochemistry and Cell Biology* 40: 2596-2605.

Li J, Brader G, Palva ET. 2004. The WRKY70 Transcription Factor: A Node of Convergence for Jasmonate-Mediated and Salicylate-Mediated Signals in Plant Defense. *Plant Cell* 16: 319-331.

Lower M, Anders S, Huber W. 2014. Differential analysis of count data -- the DESeq 2 package manual.

Marrs KA. 1996. The functions and regulation of glutathione-s-transferases in plants. *Annual Review of Plant Physiology and Plant Molecular Biology* 47: 127-158.

Meija J, Montes-Bayón M, Le Duc DL, Terry N, Caruso JA. 2002. Simultaneous monitoring of volatile selenium and sulfur species from se accumulating plants (wild type and genetically modified) by GC/MS and GC/ICP-MS using solid-phase microextraction for sample introduction. *Analytical Chemistry* 74: 5837-5844.

Morris MD. 2010. Design of Experiments: An Introduction Based on Linear Models. Chapman and Hall/CRC.

Murashige T, Skoog F (1962) A revised medium for rapid growth and bioassays with tobacco tissue culture. *Physiologia Plantarum* 15: 437-497.

Neuhierl B, Bock A. 1996. On the mechanism of selenium tolerance in selenium-accumulating plants - Purification and characterization of a specific selenocysteine methyltransferase from cultured cells of *Astragalus bisculatus*. *European Journal of Biochemistry* 239: 235-238.

Ng BH, Anderson JW. 1978. Synthesis of selenocysteine by cysteine synthase from selenium accumulator and non-accumulator plants. *Phytochemistry* 17: 2069–2074.

Ohno M, Uraji M, Shimoishi Y, Mori IC, Nakamura Y, Murata Y. 2012. Mechanisms of the selenium tolerance of the *Arabidopsis thaliana* knockout mutant of sulfate transporter SULTR1;2. *Bioscience, Biotechnology, and Biochemistry* 76: 993-998.

Oshlack A, Robinson MD, Young MD. 2010. From RNA-seq reads to differential expression results. *Genome Biology* 11: 200.

Penninckx IAMA, Thomma BPHJ, Buchala A, Métraux JP, Broekaert WF. 1998. Concomitant Activation of Jasmonate and Ethylene Response Pathways Is Required for Induction of a Plant Defensin Gene in Arabidopsis. *Plant Cell* 10: 2103-2113.

Pilon-Smits EAH, Quinn CF, Tapken W, Malagoli M, Schiavon M. 2009. Physiological functions of beneficial elements. *Current Opinion in Plant Biology* 12: 267-274.

Prasad V, Strömberg CAE, Leaché AD, Samant B, Patnaik R, Tang L, Mohabey DM, Ge S, Sahni A. 2010. Late Cretaceous origin of the rice tribe provides evidence for early diversification in Poaceae. *Nature Communications* 2: 480.

Rios JJ, Blasco B, Cervilla LM, Rosales MA, Sanchez-Rodriguez E, Romero L, Ruiz JM. 2009. Production and detoxification of H202 in lettuce plants exposed to selenium. *Annals of Applied Biology* 154: 107-116.

Rouached H, Wirtz M, Alary R, Hell R, Arpat AB, Davidian JC, Fourcroy P, Berthomieu P.

2008. Differential regulation of the expression of two high-affinity sulfate transporters, SULTR1.1 and SULTR1.2, in Arabidopsis. *Plant Physiology* 147: 897-911.

Shibagaki N, Grossman AR. 2010. Binding of cysteine synthase to the STAS domain of sulfate transporter and its regulatory consequences. *Journal of Biological Chemistry* 285: 25094-25102.

Shrift A, Virupaksha TK. 1965. Seleno-amino acids in selenium-accumulating plants. *Biochimica Biophysica Acta* 100: 65-75.

Sors TG, Ellis DR, Na GN, Lahner B, Lee S, Leustek T, Pickering IJ, Salt DE. 2005. Analysis of sulfur and selenium assimilation in Astragalus plants with varying capacities to accumulate selenium. *Plant Journal* 42: 785-797.

Sors TG, Martin CP, Salt DE. 2009. Characterization of selenocysteine methyltransferases from Astragalus species with contrasting selenium accumulation capacity. *Plant Journal* 59: 110-122.

Sura-de Jong M, Reynolds RJ, Richterova K, Musilova L, Hrochova I, Frantik T, Sakmaryova I, Strejcek M, Cochran A, Staicu L, Cappa JJ, van der Lelie D, and Pilon-Smits EAH (2015) Selenium hyperaccumulators harbor a diverse endophytic bacterial community characterized by extreme selenium tolerance and plant growth promoting properties. *Frontiers in Plant Science*, in press.

Tagmount A, Berken A, Terry N. 2002. An essential role of S-adenosyl-L-methionine : L methionine S-methyltransferase in selenium volatilization by plants. Methylation of selenomethionine to selenium-methyl-L-selenium-methionine, the precursor of volatile selenium. *Plant Physiology* 130: 847-856.

Takahashi H, Kopriva S, Giordano M, Saito K, Hell R. 2011. Sulfur assimilation in photosynthetic organisms: molecular functions and regulations of transporters and assimilatory enzymes. *Annual Review of Plant Biology* 62: 157-84.

Tamaoki M, Freeman JL, Pilon-Smits EAH. 2008a. Cooperative ethylene and jasmonic acid signaling regulates selenite resistance in Arabidopsis. *Plant Physiology* 146: 1219-1230.

Tamaoki M, Freeman JL, Marques L, Pilon-Smits EAH. 2008b. New insights into the roles of ethylene and jasmonic acid in the acquisition of selenium resistance in plants. *Plant Signaling and Behavior* 3: 865-867.

Thimm O, Blasing O, Gibon Y, Nagel A, Meyer S, Kruger P, Selbig J, Muller LA, Rhee SY, Stitt M. 2004. MAPMAN: a user-driven tool to display genomics data sets onto diagrams of metabolic pathways and other biological processes. *Plant Journal* 37: 914–939.

Usadel B, Nagel A, Thimm O, Redestig H, Blaesing OE, Palacios-Rojas N, Selbig J,

Hannermann J, Piques MC, Steinhauser D, Scheible WR, Gibon Y, Morcuende R, Weicht D, Meyer S, Sitt M. 2005. Extension of the visualization tool MapMan to allow statistical analysis of arrays, display of coresponding genes, and comparison with known responses. *Plant Physiology* 2005: 1195-1204.

Van Hoewyk D. 2013. A tale of two toxicities: malformed selenoproteins and oxidative stress both contribute to selenium stress in plants. *Annals of Botany* 112: 965-972.

Van Huysen T, Abdel-Ghany S, Hale KL, LeDuc D, Terry N, Pilon-Smits EAH. 2003. Overexpression of cystathionine-gamma-synthase enhances selenium volatilization in *Brassica juncea*. *Planta* 218: 71-78.

Wilber C. Toxicology of Selenium: 1980. A review. *Clinical Toxicology* 17: 171-230.

Zarcinas BA, Cartwright B, Spouncer LR (1987) Nitric acid digestion and multi element analysis of plant material by inductively coupled plasma spectrometry. *Communications in Soil Science and Plant Analysis* 18: 131-146.

Zayed A, Lytle CM, Terry N. 1998. Accumulation and volatilization of different chemical species of selenium by plants. *Planta* 206: 284-92.

APPENDIX:

ADDITIONAL OBSERVATIONS

INTRODUCTION

While the exact mechanism of plant selenate uptake is unknown, it likely is mediated by sulfate transporters, such as the high-affinity *Sultr1;2* in *Arabidopsis thaliana*. A study has shown that *A. thaliana* wildtype plants had a higher Se to S ratio when provided with sulfate and selenate compared to *A. thaliana* mutants unable to express *Sultr1;2;* the mutants also had enhanced selenate tolerance (El Kassis et al., 2007). Another study found that increased sulfate supply severely inhibited Se accumulation from selenate in tissues of *Brassica juncea*, a secondary Se accumulator. In contrast, increasing the sulfate supply to two ecotypes of the hyperaccumulator *Stanleya pinnata* did not significantly inhibit Se accumulation (Harris et al., 2014). This indicates that this hyperaccumulator has a transporter with enhanced specificity for selenate relative to sulfate, perhaps even a selenate-specific transporter. This finding is interesting, since no selenate-specific transporter has been reported for any organism. If indeed a selenate-specific transporter exists, this could be applicable for phytoremediation and biofortification, since Se accumulation is often inhibited by high S levels. *B. juncea*, currently one of the most popular plants for these phytotechnologies, obviously suffers from this limitation (Banuelos et al., 2005; Prins et al., 2011).

These sulfate-selenate interaction experiments using *S. pinnata* and *B. juncea* have given valuable new insight into the mechanism of Se accumulation. However, no studies so far have determined S-dependent Se uptake in non-hyperaccumulator *Stanleya* species. The experiment

described in the following pages analyzed the elemental concentrations of Se and S *S. elata*, a non-accumulator species, when supplied with various concentrations of Se and S, and compares the results to those obtained earlier for *S. pinnata*. S. elata was chosen because among the Stanleya species it accumulates the least Se. *S. elata* and *S. pinnata* were also compared using RNAseq, as described in Chapter 2 of this thesis. The physiological data shown here complement the transcript analyses of the *Sultr* gene family in the previous chapter, where many *Sultr* genes, notably *Sultr1;2*, had higher expression levels in *S. pinnata* than *S. elata*.

METHODS

ICP-AES analysis

Seeds of *S. elata* (NV, 36°16'36"N 115°30'12"W) were germinated on MS-agar in sterile petri dishes and transferred to pots with pre-washed Turface MVP (Profile Products LLC, Buffalo Grove, IL, USA), a clay-based substrate. After three weeks, the seedling were transferred to an aerated hydroponic setup. Three bio-replicates were housed per hydroponic container, with one container for each of the three treatments. Plants were grown on ½ strength Hoagland's Solution (Murashige & Skoog, 1962) under halogen lamps with a 16/8hr light period at room temperature. Plants were then pretreated with either 0.5 or 5 mM S five days prior to harvest, and treated with 0 or 20 μM Se three days prior to harvest (all treatment groups: 0 μM Se with 0.5 mM S; 20 μM Se with 0.5 mM S; and 20 μM Se with 5 mM S). After 3 days, plants were harvested and the roots rinsed and separated from the shoots. Plant tissues were dried for 72 hours at 50 °C before being weighed and nitric-acid digested following method in Zarcinas et al. (1987). The roots were excluded from further analysis due to pooling of low biomass samples from bioreplicates. The shoots were used to obtain elemental concentrations using inductively-coupled plasma atomic emission spectroscopy (ICP-AES), following method in Fassel (1978).

The elemental concentrations for *S. pinnata*, grown under similar conditions, were obtained from a previous study by Schiavon et al. (2015). Statistical significance between treatments were calculated using ANOVA with Tukey-Kramer multiple comparisons test in JMP (version 11).

RESULTS & DISCUSSION

Almost no Se was detected in the shoots of *S. elata* grown in 0.5 mM S and no Se supplied (Appendix Fig 1.1a); therefore, *S. elata* did not contain pre-existing Se in seed. While *S. elata* accumulated over 600 mg kg^{-1} Se in shoots when supplied with the same S levels but 20 μM Se, Se concentrations significantly diminished when S supply increased to 5 mM. The severe reduction in Se accumulation (>41 fold) by 10-fold increasing the S supply from 0.5 to 5 mM suggests that in the non-accumulator, Se accumulation is largely dependent on the activity of S transporters, and that these may have a higher specificity for sulfate relative to selenate. *S. elata* also accumulated more S in shoots when supplied with 0.5 mM S and 0 μM Se, relative to plants supplied with 0.5 mM S and 20 μM Se; the level of S in shoots also decreased when plants were supplied 20 μM Se with an excess of 5 mM S (Appendix Fig 1.1b). The observation that S amounts supplied affect Se accumulation, and *vice versa*, supports the idea that Se competes with S for transport by the same protein(s). The finding that S concentration went up in *S. elata* treated with Se may suggest that 20 μM Se induces S starvation in non-accumulators, resulting in the increased uptake and/or translocation of S and Se; the addition of excess (5 mM) S may have restored S homeostasis in the non-accumulator, resulting in similar levels of S as found for the 0.5S 0Se treatment (Appendix Fig 1.1b).

When supplied with 0.5 mM S and 20 μM Se, *S. elata* had proportionally more Se relative to S in the shoots than plants supplied with 5 mM S and 20 μM Se (Appendix Fig 1.1c). In a recent study by Schiavon et al. (2015), hyperaccumulator *S. pinnata* showed a similar trend:

a decrease in Se concentration relative to S when supplied with ten-fold higher sulfate levels (5 mM S and 20 μM Se, as compared to 0.5 mM S and 20 μM Se). However, *S. pinnata* had greater ratios of Se relative to S for all treatments when compared to *S. elata* (Appendix Fig 1.1d). Indeed, when Se supply was held constant but S supply increased by 10-fold, *S. pinnata* showed only a 2.6-fold decrease in Se levels relative to S, whereas *S. elata* showed a 22-fold decrease in Se levels relative to S. When the amount of Se relative to S supplied was taken into account, *S. elata* had a Se enrichment factor (Se:S ratio in the plant divided by the Se:S ratio supplied) that was less than 1 for all treatments, indicating it preferentially takes up sulfate over selenate. It had a lower Se enrichment factor when supplied with excess (5 mM) S and 20 μM Se, compared to normal (0.5 mM) S and 20 μM Se (Appendix Fig 1.1e). In *S. pinnata*, the Se enrichment factor was >1 for all treatments, indicating it preferentially takes up selenate over sulfate. Its Se enrichment ratio actually increased when excess (5 mM) S was supplied (Appendix Fig 1.1f). In conclusion, these findings indicate that while *S. elata* has transporters that do not have a higher affinity for Se and may even prefer sulfate over selenate as a substrate, based on enrichment factor, in the hyperaccumulator *S. pinnata* a Se-specific transporter may exist, or a sulfate/selenate transporter with increased specificity for selenate over sulfate.

FIGURES

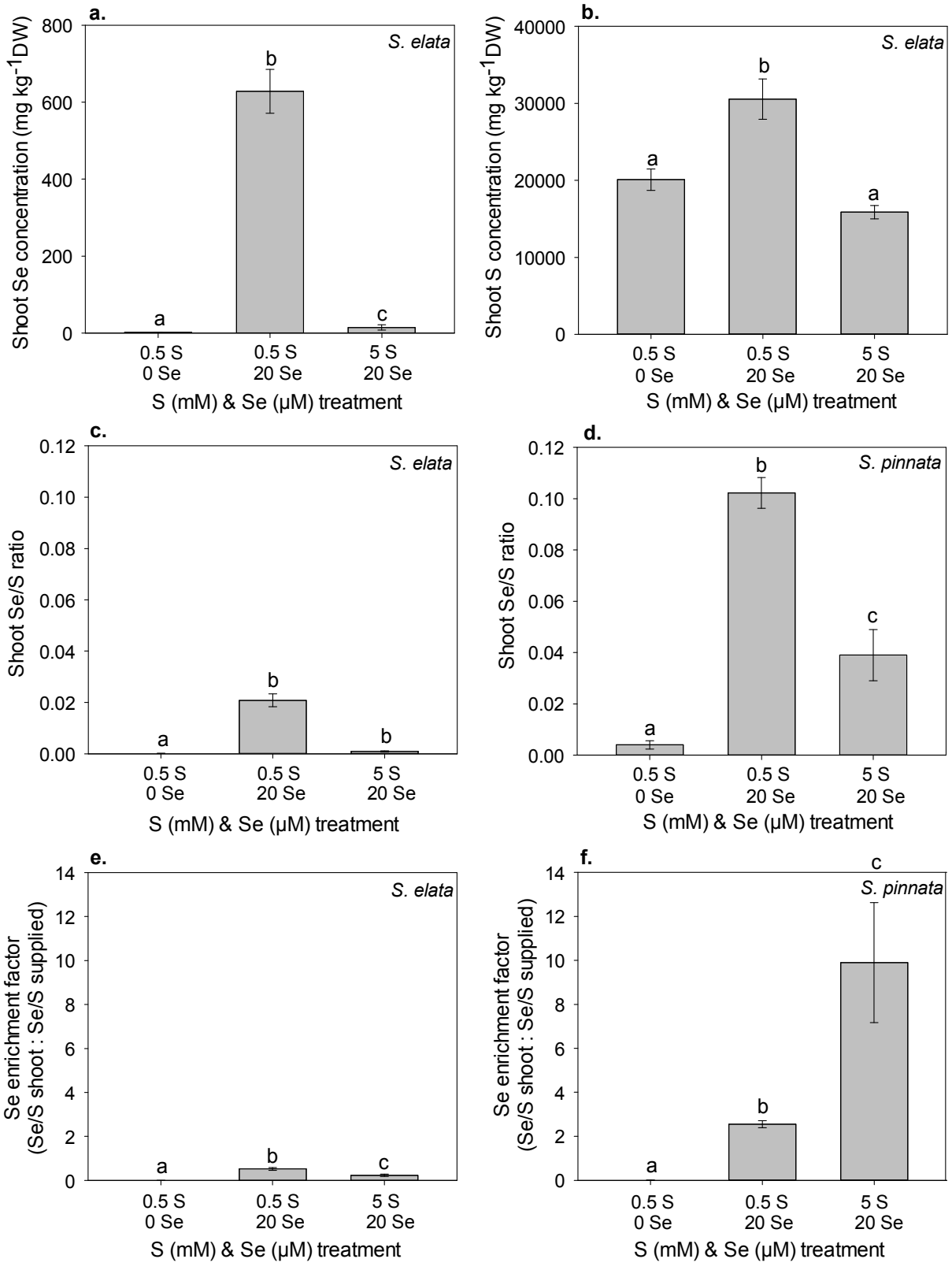
a.
S. elata
Shoot Se concentration (mg kg-1DW)
800
600
400
200
0
a
b
c
0.5 S 0 Se
0.5 S 20 Se
5 S 20 Se
S (mM) & Se (µM) treatment
b.
S. elata
Shoot S concentration (mg kg-1DW)
40000
30000
20000
10000
0
a
b
a
0.5 S 0 Se
0.5 S 20 Se
5 S 20 Se
S (mM) & Se (µM) treatment
c.
S. elata
Shoot Se/S ratio
0.12
0.10
0.08
0.06
0.04
0.02
0.00
a
b
b
0.5 S 0 Se
0.5 S 20 Se
5 S 20 Se
S (mM) & Se (µM) treatment
d.
S. pinnata
Shoot Se/S ratio
0.12
0.10
0.08
0.06
0.04
0.02
0.00
a
b
c
0.5 S 0 Se
0.5 S 20 Se
5 S 20 Se
S (mM) & Se (µM) treatment
e.
S. elata
Se enrichment factor (Se/S shoot : Se/S supplied)
14
12
10
8
6
4
2
0
a
b
c
0.5 S 0 Se
0.5 S 20 Se
5 S 20 Se
S (mM) & Se (µM) treatment
f.
S. pinnata
Se enrichment factor (Se/S shoot : Se/S supplied)
14
12
10
8
6
4
2
0
a
b
c
0.5 S 0 Se
0.5 S 20 Se
5 S 20 Se
S (mM) & Se (µM) treatment

Appendix Fig. 1.1 Selenium and sulfur concentrations and enrichment ratios in plants grown in liquid medium with 0 or 20 μM sodium selenate, and 0.5 or 5 mM sulfate. (a) Shoot Se concentration in *S. elata*. (b) Shoot S concentration.in *S. elata*. (c) Shoot ratio of Se relative to S in *S. elata*. (d) Shoot ratio of Se relative to S in *S. pinnata*. (e) The enrichment ratio of Se relative to S, accounting for the amounts of Se to S supplied, in *S. elata*. (f) The enrichment ratio of Se relative to S, accounting for the amounts of Se to S supplied, in *S. elata*. Shown values represent the mean of three replicates + SEM. Letters above bars indicate significant differences between treatments using ANOVA with post-hoc Tukey-Kramer multiple comparisons test.

REFERENCES

Banuelos G, Terry N, Leduc DL, Pilon-Smits EAH, Mackey B. 2005. Field trial of transgenic Indian mustard plants shows enhanced phytoremediation of selenium-contaminated sediment. *Environmental Science & Technology* 39: 1771-1777.

El Kassis E, Cathala N, Rouached H, Fourcroy P, Berthomieu P, Terry N, Davidian JC. 2007. Characterization of a selenate-resistant Arabidopsis mutant. Root growth as a potential target for selenate toxicity. *Plant Physiology* 143: 1231-1241.

Fassel VA. 1978. Quantitative elemental analyses by plasma emission spectroscopy. *Science* 202: 183–191.

Harris J, Schneberg KA, Pilon-Smits EAH. 2014. Sulfur-selenium-molybdenum interactions distinguish selenium hyperaccumulator *Stanleya pinnata* from non-hyperaccumulator *Brassica juncea* (Brassicaceae). *Planta* 239: 479-491.

Murashige T, Skoog F (1962) A revised medium for rapid growth and bioassays with tobacco tissue culture. *Physiologia Plantarum* 15: 437-497.

Prins CN, Hantzis LJ, Quinn CF, Pilon-Smits EAH. 2011. Effects of selenium accumulation on reproductive functions in Brassica juncea and Stanleya pinnata. *Journal of Experimental Biology* 62: 5633-5640.

Schiavon M, Pilon M, Malagoli M, Pilon-Smits EAH. 2015. Exploring the importance of sulfate transporters and ATP sulphurylases for selenium hyperaccumulation—a comparison of *Stanleya pinnata* and *Brassica juncea* (Brassicaceae). *Frontiers in Plant Science* 6: doi: 10.3389.

Zarcinas BA, Cartwright B, Spouncer LR (1987) Nitric acid digestion and multi element analysis of plant material by inductively coupled plasma spectrometry. *Communications in Soil Science and Plant Analysis* 18: 131-146.